ABSTRACT

CHARGE DENSITY ESTIMATIONS FOR PARTICLE BEAMS BASED ON ORTHOGONAL POLYNOMIAL SERIES

Danairis Hernandez, M.S.
Department of Physics
Northern Illinois University, 2012
Bela Erdelyi, Director

A beam's charge density, treated as a smooth and continuous function, can be approximated using polynomial orthogonal series. This will allow a solution of Poisson's equation to be found. Obtaining the most accurate solution to the space-charge potential requires the best approximated charge density. Several beam distributions are approximated using the classic Jacobi polynomials generated by the traditional recursion relations and the moment method. Varying the particle number and the order of the approximation allows us to compare the performance of the different polynomials and to determine if a particular combination of both works best. Although the three polynomials studied give similar results, with Legendre being slightly better, the approximation coefficients should be allowed to converge and taken to high orders for best results.

NORTHERN ILLINOIS UNIVERSITY
DE KALB, ILLINOIS

MAY 2012

CHARGE DENSITY ESTIMATIONS FOR PARTICLE BEAMS BASED ON ORTHOGONAL POLYNOMIAL SERIES

BY

DANAIRIS HERNANDEZ

A THESIS SUBMITTED TO THE GRADUATE SCHOOL

IN PARTIAL FULFILLMENT OF THE REQUIREMENTS

FOR THE DEGREE

MASTER OF SCIENCE

DEPARTMENT OF PHYSICS

Thesis Director:
Bela Erdelyi

DEDICATION

To my family and those whom I love

TABLE OF CONTENTS

LIST OF TABLES

LIST OF FIGURES

Figure Page

Figure Page

Figure Page

Figure Page

Figure Page

Figure Page

Figure Page

Figure Page

Figure Page

Figure Page

Figure Page

Figure Page

Figure Page

Figure Page

Figure Page

Figure Page

Figure Page

Figure Page

Figure Page

Figure Page

CHAPTER 1

INTRODUCTION

The use of particle beams, collections of charged particles traveling with roughly the same speed and in the same direction, has highly evolved since their first applications. In the mid-twentieth century, beams were first used in developing the cathode ray tube, a vacuum tube containing a source of electrons. Now, particle beams are used in every sort of applications, from electronics (television tubes) and appliances (induction cooktops) to science (particle accelerators) and medicine (treatment of cancer patients). With so many applications, it is important to understand what describes and affects the beam, starting with the particle's motion. Defined by the Lorentz force equation, a particle's motion is affected by electromagnetic fields created by the particles in the beam. Since the beam is composed of many particles of the same kind contained in a small volume, these particles tend to interact and repel. In the case where the interactions are due to the particles themselves, like repulsion due to the Coulomb Force, the smooth part is known as space-charge [1], while the case of close range particle collisions is known as intra-beam scattering [5]. The space-charge dominates the dynamics of high intensity beams at low energies, affecting the distributions of beams [6].

In order to be able to obtain the particle's motion, both the external and internal fields are required. Since the external fields are known, it only leaves for the internal fields to be solved for. Poisson's equation, given by (1.1), allows the scalar potential, or space-charge fields $\Phi(\vec{r})$ [7], to be solved for a given smooth charge distribution $\rho(\vec{r})$, where $\vec{r}$ is a three-dimensional vector. Even though beams are composed of

discrete particles, their charge distributions can be treated as smooth if enough particles are concentrated within a small volume. Based on the Weierstrass Theorem, any smooth function can then be approximated by the sum of orthogonal polynomials and their coefficients [1, 2, 3], given by (1.3). Because of the finite number of particles contained in the beam and the computational requirement of a finite series, the coefficients a_i are also approximations truncated at order n.

$$\nabla^2\Phi(\vec{r}) = -\frac{\rho(\vec{r})}{\epsilon_0} \qquad with \qquad \Phi(\infty) = 0 \tag{1.1}$$

$$\Phi(\vec{r'}) = \frac{1}{4\pi}\int \frac{\rho(\vec{r'})}{\left\|\vec{r} - \vec{r'}\right\|} d\vec{r'} \tag{1.2}$$

$$\rho(\vec{r}) = \sum_{i=0}^{n} a_i P_i(\vec{r}) \tag{1.3}$$

Once the charge distribution is approximated with a desired polynomial, the next task is to minimize the error between the approximated charged distribution and the actual one, shown in Figure 1.1. Minimizing the error allows one to find the potential that best corresponds to the charge density. To select the charge density that gives the best result, the error is calculated by the use of norms. In this case, an integral of the absolute value of the differences as in (1.4) was chosen for all error calculations. Once this step is completed, one must go back to Poisson's equation to solve for the potential in (1.1). Once the boundary conditions are applied, in this case that the potential goes to zero as $\vec{r}$ approaches infinity, the solution is given by (1.2). Because the solution to Poisson's equation includes integrating the charge density, the use of orthogonal polynomials simplifies the calculation and reduces

the calculation time and leading to a faster and easier solution of the Lorentz force equation for the particle's motion.

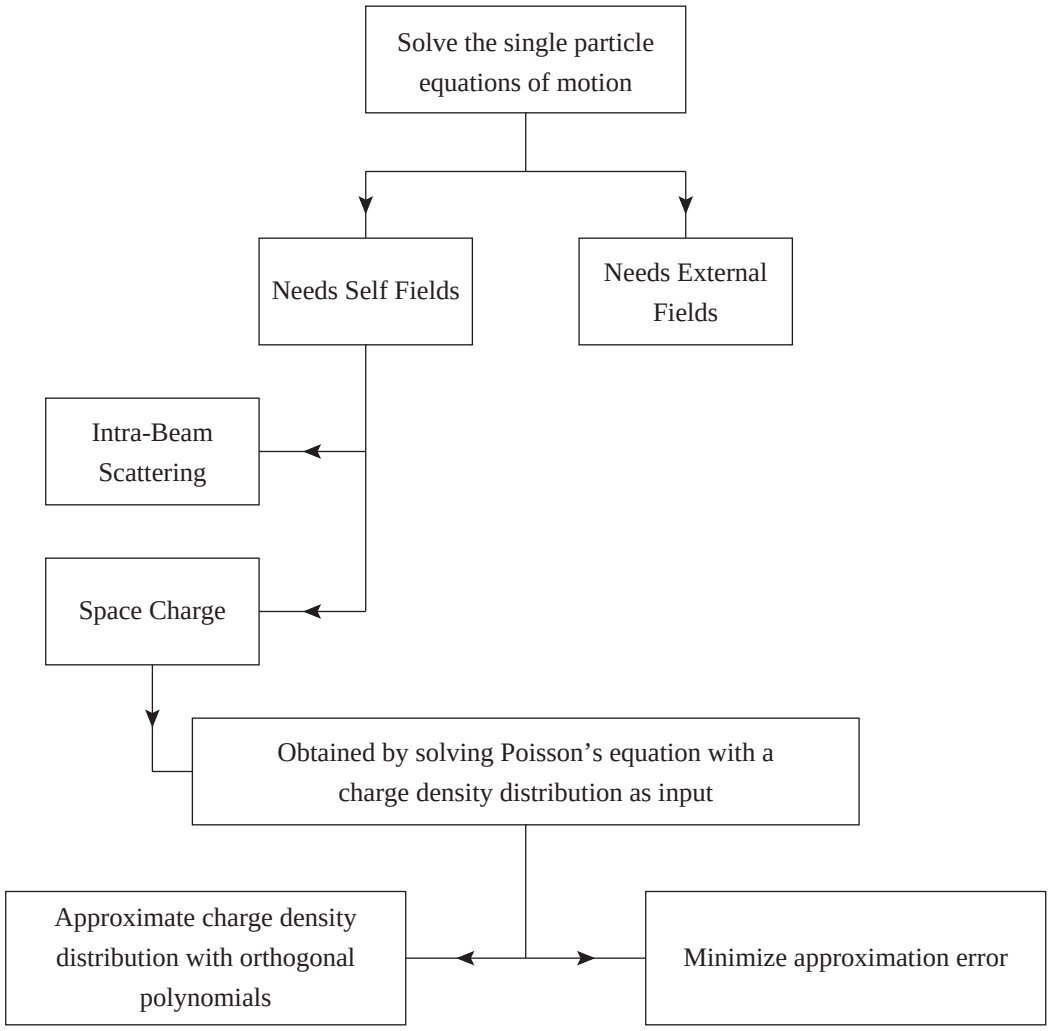

Figure 1.1: Summary of the steps needed to solve for the single particle equation of motion.

$$\epsilon = \int |\rho(\vec{r}) - \rho_a(\vec{r})|\, d\vec{r} \tag{1.4}$$

In order to approximate the density, it is necessary to begin with the theory of orthogonal polynomials, those that will be used throughout the calculations, and those distributions which the approximations will be based on. Once this has been established, the next task is how to approximate the distribution based on the traditional method of using the orthogonal polynomials previously discussed and those generated using distribution moments. The last sections will include samples of the results as well as a discussion of the given errors by the different polynomials. We will finish with a summary of the results and conclusion. It is important to note that previous work on this topic has been done before, with the use of the moment method based on Legendre polynomials, which can be seen in more detail in [4]. Although this work offers good results with the Legendre polynomials at order $n = 16$, we will be focusing on systematic approximations based on orthogonal polynomials, giving us a chance to compare their performance.

CHAPTER 2

ORTHOGONAL POLYNOMIALS

In order to start working on the approximation we will begin by discussing orthogonal polynomials. In more detail, I will explain what is meant by orthogonal, how these polynomials can be derived, and their characteristics. In addition to the traditional method of generating polynomials, I will discuss a second method which generates orthogonal polynomials based on moments.

Any two functions, $F_n(x)$ and $F_m(x)$, that are part of a set on the real interval $[a, b]$, are said to be orthogonal to each other if

$$< F_n(x), F_m(x) >= \int_a^b W(x)F_n(x)F_m(x)dx = 0 \quad for \quad n \neq m \tag{2.1}$$

where $W(x)$ defines a weight function particular to a polynomial, [8]. For the case where $n \equiv m$, the integral becomes the square of the norm. If this value is one, the polynomial is said to be normalized.

$$||F_m(x)||^2 = \int_a^b W(x)F_m^2(x)dx \tag{2.2}$$

Although there are many polynomials with different intervals of orthogonality, we can pick a simple interval between $[-\infty, \infty]$ and just contain the beam within any finite region and scale appropriately. Based on this, the interval chosen is $[-1, 1]$. In order to perform the approximations, we need to use polynomials that are orthogonal on this region, known as the Jacobi polynomials.

2.1 Jacobi polynomials

By taking $[-1, 1]$ as our interval of interest, the Jacobi polynomials can be generated from a homogeneous second order differential equation of the form

$$Q(x)f'' + L(x)f' + \lambda f = 0 \tag{2.3}$$

from which the Jacobi Differential Equation follows [9].

$$\begin{aligned} (1-x^2)f'' &+ [\beta - \alpha - (\alpha + \beta + 2)x]f' + \lambda f = 0 \\ \lambda &= n(1 + n + \alpha + \beta) \\ \alpha, \beta &> -1 \end{aligned} \tag{2.4}$$

The solutions to equation (2.4) are known as Jacobi polynomials and are the classical orthogonal polynomials, where n is the order of the polynomial and α and β are the coefficients to be specified.

$$P_n^{(\alpha,\beta)}(x) = \frac{(-1)^n}{2^n n!}(1-x)^{\alpha}(1+x)^{-\beta}\frac{d^n}{dx^n}[(1-x)^{\alpha+n}(1+x)^{\beta+n}] \tag{2.5}$$

$$P_0^{(\alpha,\beta)}(x) = 1 \tag{2.6}$$

$$P_1^{(\alpha,\beta)}(x) = \frac{1}{2}[2(\alpha+1)+(\alpha+\beta+2)(x-1)] \tag{2.7}$$

$$\begin{aligned} P_2^{(\alpha,\beta)}(x) = {} & \frac{1}{8}[4(\alpha+1)(\alpha+2)+4(\alpha+\beta+3)(\alpha+2)(x-1)+ \\ & (\alpha+\beta+3)(\alpha+\beta+4)(x-1)^2] \end{aligned} \tag{2.8}$$

$$\begin{aligned} P_3^{(\alpha,\beta)}(x) = {} & \frac{1}{48}[8(1+\alpha)(2+\alpha)(3+\alpha)- \\ & 12(2+\alpha)(3+\alpha)(4+\alpha+\beta)(1-x)+ \\ & 6(3+\alpha)(4+\alpha+\beta)(5+\alpha+\beta)(1-x)^2- \\ & (4+\alpha+\beta)(5+\alpha+\beta)(6+\alpha+\beta)(1-x)^3] \end{aligned} \tag{2.9}$$

With and orthogonality relation given by (2.10), Jacobi polynomials form a complete orthonormal basis for the interval $[-1,1]$ with respect to the weight function in (2.11). In the case where $\alpha = \beta$, Jacobi polynomials can be divided into four special cases known as Gegenbauer, Legendre and Chebyshev (type one and two) polynomials [9].

$$\begin{aligned} & \int_{-1}^{1} P_m^{(\alpha,\beta)}(x)P_n^{(\alpha,\beta)}(x)(1-x)^{\alpha}(1+x)^{\beta}dx = \\ & \frac{2^{\alpha+\beta+1}}{2n+\alpha+\beta+1}\frac{\Gamma(n+\alpha+1)\Gamma(n+\beta+1)}{n!\Gamma(n+\alpha+\beta+1)}\delta_{mn} \end{aligned} \tag{2.10}$$

$$W(x) = (1-x)^{\alpha}(1+x)^{\beta} \tag{2.11}$$

2.1.1 Gegenbauer polynomials

Represented by $C_n^{(\lambda)}$, Gegenbauer polynomials are the first special case of Jacobi polynomials . Identified by $\alpha = \beta = \lambda - \frac{1}{2}$, these polynomials have a generating function that is related to Jacobi polynomials [9].

$$C_n^{(\lambda)}(x) = \frac{\Gamma(\lambda+\frac{1}{2})}{\Gamma(2\lambda)}\frac{\Gamma(n+2\lambda)}{\Gamma(n+\lambda+\frac{1}{2})}P_n^{(\lambda-\frac{1}{2},\lambda-\frac{1}{2})}(x) \qquad \lambda > -\frac{1}{2} \tag{2.12}$$

$$C_0^{(\lambda)}(x) = 1 \tag{2.13}$$

$$C_1^{(\lambda)}(x) = 2\lambda x \tag{2.14}$$

$$C_2^{(\lambda)}(x) = -2\lambda + 2\lambda(1+\lambda)x^2 \tag{2.15}$$

$$C_3^{(\lambda)}(x) = -2\lambda(1+\lambda)x + \frac{4}{3}\lambda(1+\lambda)(2+\lambda)x^3 \tag{2.16}$$

As a case of Jacobi polynomials, Gegenbauer polynomials only form an orthogonal set on the $[-1, 1]$ interval, with the orthogonality relation given by (2.17) and weight function by (2.18).

$$\int_{-1}^{1} C_m^(\lambda)(x)C_n^(\lambda)(x)(1-x^2)^{\lambda-\frac{1}{2}}dx = 2^{1-2\lambda}\pi\frac{\Gamma(n+2\lambda)}{(n+\lambda)\Gamma^2(\lambda)\Gamma(n+1)}\delta_{mn} \tag{2.17}$$

$$W(x) = (1-x^2)^{\lambda-\frac{1}{2}} \tag{2.18}$$

2.1.2 Legendre polynomials

Legendre polynomials, written as $P_n(x)$, are obtained from Jacobi polynomials by setting $\alpha = \beta = 0$ in equation (2.5).

$$P_n(x) = P_n^{(0,0)}(x) \tag{2.19}$$

$$P_0(x) = 1 \tag{2.20}$$

$$P_1(x) = x \tag{2.21}$$

$$P_2(x) = \frac{1}{2}(3x^2 - 1) \tag{2.22}$$

$$P_3(x) = \frac{1}{2}(5x^3 - 3x) \tag{2.23}$$

Like all Jacobi polynomials, the Legendre polynomials also form a complete basis set on the interval $[-1, 1]$ with the orthogonality relation and weight function given in (2.24) and (2.25) respectively.

$$\int_{-1}^{1} P_m(x)P_n(x)dx = \frac{2}{2n+1}\delta_{mn} \tag{2.24}$$

$$W(x) = 1 \tag{2.25}$$

Based on Weierstrass's Theorem, Legendre polynomials are also special for the property of minimizing the Least Square Approximation, given by (2.26). In the equation, $f(x)$ is the function being approximated and $p(x)$ is the approximating function [9].

$$Error = \int_{-1}^{1} [f(x) - p(x)]^2 dx \tag{2.26}$$

2.1.3 Chebyshev polynomials of the first kind

The first kind of Chebyshev polynomials are identified by $T_n(x)$ and can be obtained from Jacobi polynomials by setting $\alpha = \beta = -\frac{1}{2}$ in the general equation given by (2.5).

$$T_n(x) = \frac{P_n^{(-\frac{1}{2},-\frac{1}{2})}(x)}{P_n^{(-\frac{1}{2},-\frac{1}{2})}(1)} \tag{2.27}$$

$$T_0(x) = 1 \tag{2.28}$$

$$T_1(x) = x \tag{2.29}$$

$$T_2(x) = (2x^2 - 1) \tag{2.30}$$

$$T_3(x) = (4x^3 - 3x) \tag{2.31}$$

In the interval $[-1, -1]$, Chebyshev Polynomials of the first kind have an orthogonality condition and weight functions given by (2.32) and (2.33) [10].

$$\int_{-1}^{1} \frac{T_m(x)T_n(x)}{\sqrt{1-x^2}} dx = \begin{cases} \frac{1}{2}\pi\delta_{mn} & \text{for } m \neq 0, n \neq 0 \\ \pi & \text{for } m = n = 0 \end{cases} \tag{2.32}$$

$$W(x) = \frac{1}{\sqrt{1-x^2}} \tag{2.33}$$

Also based on the Weierstrass theorem, Chebyshev of the first kind minimizes a particular error calculation called the Minimax Approximation given in (2.33).

$$Error = max_{a \leq x \leq b} |f(x) - p(x)| \tag{2.34}$$

2.1.4 Chebyshev polynomials of the second kind

The second kind of Chebyshev polynomials are identified by $U_n(x)$ and can be obtained from Jacobi polynomials by setting $\alpha = \beta = \frac{1}{2}$ in the general equation given by (2.5).

$$U_n(x) = (n+1)\frac{P_n^{(\frac{1}{2},\frac{1}{2})}(x)}{P_n^{(\frac{1}{2},\frac{1}{2})}(1)} \tag{2.35}$$

$$U_0(x) = 1 \tag{2.36}$$

$$U_1(x) = 2x \tag{2.37}$$

$$U_2(x) = (4x^2 - 1) \tag{2.38}$$

$$U_3(x) = (8x^3 - 4x) \tag{2.39}$$

Chebyshev Polynomials of the second kind are similar to those of the first kind, and in our desired interval, the orthogonality and weight functions are given in (2.39) and (2.40) [10].

$$\int_{-1}^{1} U_m(x) U_n(x) \sqrt{1 - x^2} dx = \frac{\pi}{2} \delta_{mn} \tag{2.40}$$

$$W(x) = \sqrt{1 - x^2} \tag{2.41}$$

2.2 Moment-Based Polynomials

In addition to generating polynomials from a differential equation, polynomials can be generated using measures and moments. A measured space is a σ-algebra, or set of subsets, defined on a set with a non-negative measure. This measure assigns a positive value to each subset in the σ-algebra and has the properties [11]

- The empty set has measure 0.
- The union of two subsets has the same measure as the sum of the two measures taken individually.

The set in the measured space for orthogonal polynomials is the closed interval $[-1, 1]$, where the σ-algebra is the collection of all possible intervals in the set. In general, the measure μ will assign a positive value to each interval by taking an integral over the interval. The simplest way to do this is by assigning the same value to intervals of the same size, as defined by (2.42).

$$\mu([a, b]) = \int_a^b dx \tag{2.42}$$

In general, the measure will be the integral of a weight function $W(x)$, which assigns different values to the different intervals in the domain.

$$\mu([a, b]) = \int_a^b W(x)dx \equiv \int_a^b d\mu(x) \tag{2.43}$$

The moments of a measure μ_n are defined by modifying (2.43) to include x^n in the integral, becoming (2.44) [12, 13].

$$\mu_n = \int_a^b x^n W(x) dx \equiv \int_a^b x^n d\mu(x) \tag{2.44}$$

These moments can then be used to build a set of polynomials $p_n(x)$ using determinants [14],

$$p_n(x) = \det \begin{pmatrix} \mu_0 & \mu_1 & \dots & \mu_n \\ \mu_1 & \mu_2 & \dots & \mu_{n+1} \\ \vdots & \vdots & \ddots & \vdots \\ \mu_{n-1} & \mu_n & \dots & \mu_{2n-1} \\ 1 & x & \dots & x^n \end{pmatrix} \tag{2.45}$$

The polynomials generated by using equation (2.44) can be proven to be orthogonal to all polynomials of order less than n if (2.46) is satisfied.

$$\mu_n = \int_a^b x^k p_n(x) d\mu(x) = 0 \qquad \forall \quad k < n \tag{2.46}$$

The properties of determinants allow the ortogonality of the polynomials generated by (2.45) to be easily proven.

$$\int_a^b x^k p_n(x) \mathrm{d}\mu(x) = \int_a^b x^k \det \begin{pmatrix} \mu_0 & \mu_1 & \dots & \mu_n \\ \vdots & \vdots & \ddots & \vdots \\ \mu_{n-1} & \mu_n & \dots & \mu_{2n-1} \\ 1 & x & \dots & x^n \end{pmatrix} \mathrm{d}\mu(x)$$

$$= \det \begin{pmatrix} \mu_0 & \mu_1 & \cdots & \mu_n \\ \vdots & \vdots & \ddots & \vdots \\ \mu_{n-1} & \mu_n & \cdots & \mu_{2n-1} \\ \int x^k \mathrm{d}\mu(x) & \int x^{k+1}\, \mathrm{d}\mu(x) & \ldots & \int x^{k+n}\, \mathrm{d}\mu(x) \end{pmatrix} \tag{2.47}$$

From (2.46) it is clear that if $k < n$, there will be an identical copy of the last row in one of the previous rows, making the determinant zero; therefore the integral is zero. Because the polynomial $p_n(x)$ is orthogonal to x^k for $k < n$, the polynomial is orthogonal to all polynomials of smaller order. This implies that every polynomial generated using this method is orthogonal to every other polynomial. Because this method requires a weight function to be specified, if the weight associated with a set of polynomials is chosen, the expected polynomials will be generated, although with a different normalization than the one obtained using recursion [13]. Chosing (2.25) will generate Legendre polynomials, while (2.32) and (2.40) will generate the Chebyshev polynomials.

CHAPTER 3

MAIN DISTRIBUTIONS OF BEAM PHYSICS

Typically, the beam's charge density assumes a bell-shaped-like curve. Of course, it also describes the distribution of the particles in the beam. This is due to the Central Limit Theorem. According to the theorem, the cumulative effect of many independent, but unavoidable in practice, small stochastic effects is to transform any initial distribution into the Gaussian distribution if enough time is allowed to pass [15, 16]. However, the beam evolutions are not always long enough on this time scale, and therefore some other distributions are used as well in simulations. As a consequence, beam distributions are represented by one of the following distributions: Gaussian, Uniform, Parabolic, or Waterbag. These distributions include the extremes, starting with uniform on one side and ending with the Gaussian on the other. That is why we study only the Gaussian and the uniform distributions. The different distributions not only describe the shape of the charge distribution, but also describe the nature of the space-charge effects.

3.1 Gaussian Distribution

Also known as a Normal distribution, the Gaussian takes an important role in physics and mathematics because of the previously mentioned Central Limit Theorem. In 4D space the Gaussian distribution takes a form of (3.1) with N as the number of particles; σ is the variance and r and ρ are the radius based on the

standard deviation number n. To project the Gaussian in 2D space, equation (3.1) is integrated over (x', y'), resulting in (3.2). Because the distributions and space-charge affect each other, a Gaussian distribution will generate non-linear space-charge fields that will make the beam evolve over time.

$$f(x, y, x', y') = \frac{N}{4\pi^2\sigma^4} e^{\frac{-\rho^2}{2\sigma^2}} \qquad \rho \leq n\sigma \tag{3.1}$$

$$f(x, y) = \frac{N}{2\pi\sigma^2} e^{\frac{-r^2}{2\sigma^2}} \qquad r = \sqrt{x^2 + y^2} \leq n\sigma \tag{3.2}$$

3.2 Parabolic Distribution

The Parabolic distribution represents a less extreme of the Gaussian distribution and just like it, creates non-linear fields that make the beam change with time. It is also defined over a 4D space by (3.3) and can be projected in the 2D plane by integrating over (x', y'), resulting in (3.4).

$$f(x, y, x', y') = \frac{6N}{\pi^2 a^4}(1 - \frac{\rho^2}{a^2}) \qquad \rho^2 = x^2 + y^2 + x'^2 + y'^2 \leq a^2 \tag{3.3}$$

$$f(x, y) = \frac{3N}{\pi a^2}(1 - \frac{r^2}{a^2})^2 \qquad r^2 = x^2 + y^2 \leq a^2 \tag{3.4}$$

3.3 Waterbag Distribution

The Waterbag distribution varies from the Gaussian distribution even more than the Parabolic, and instead, it gets closer to the next extreme, the K-V Distribution.

Just like the previous two, the Waterbag, defined in the $(x, y, x'y')$ plane by (3.5), can be projected in (x, y) by integrating over the velocities (x', y'), giving us (3.6). It also results in a beam that will evolve over time due to the non-linear fields.

$$f(x, y, x', y') = \frac{2N}{\pi^2 a^4} \qquad \rho^2 = x^2 + y^2 + x'^2 + y'^2 \leq a^2 \tag{3.5}$$

$$f(x, y) = \frac{2N}{\pi a^2}(1 - \frac{r^2}{a^2}) \qquad r^2 = x^2 + y^2 \leq a^2 \tag{3.6}$$

3.4 K-V and Uniform Distributions

Contrary to the previous distributions, the K-V is usually described by linear space-charge fields that create a stationary distribution described by (3.7) in the interval $[a, b, \epsilon_x, \epsilon_y]$. If the 4D K-V distribution in (3.7) is integrated over (x', y') it is then known as the Uniform distribution given by (3.8).

$$f(x, y, x', y') = \frac{N}{\pi^2 ab\epsilon_x\epsilon_y}\delta(\frac{x^2}{a^2} + \frac{y^2}{b^2} + \frac{a^2x'^2}{\epsilon_x^2} + \frac{b^2y'^2}{\epsilon_y^2} - 1) \tag{3.7}$$

$$f(x, y) = \frac{N}{\pi ab} \qquad \frac{x^2}{a^2} + \frac{y^2}{b^2} \leq 1 \tag{3.8}$$

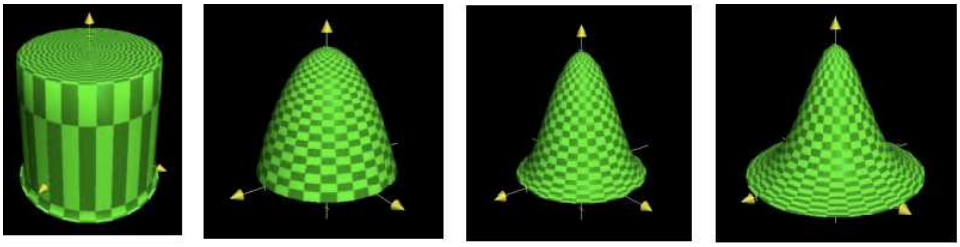

Figure 3.1: From left to right, the K-V, Waterbag, Parabolic and Gaussian Distributions.

.

CHAPTER 4

APPROXIMATIONS OF DISTRIBUTIONS BY ORTHOGONAL POLYNOMIALS

The previous chapters introduced the concept of a charge density of a beam, as well as those distributions that are relevant to the field. The next step is to describe how the charge density is approximated with orthogonal polynomials.

A function composed of a discrete set of points from a known distribution can be written by equation (4.1), where $P_i(x)$ is an orthogonal polynomial and a_i the corresponding coefficient. In order to make the approximation of the distribution, the sum needs to be truncated at a desired order m. Equation (4.1) is now approximated with the truncated sum in equation (4.2).

$$F(x) = \sum_{j}^{N} \delta(x - x_j) \hat{=} \sum_{i}^{\infty} a_i P_i(x) \tag{4.1}$$

$$F(x) \hat{=} \sum_{i}^{\infty} a_i P_i(x) \approx \sum_{i}^{m} a_i P_i(x) \tag{4.2}$$

To begin the approximation, the coefficients a_i need to be solved for. This can be done by taking equation (4.1) and multiplying both sides by $P_n(x)W(x)$ and integrating on the interval $[a, b]$ with respect to x to get (4.3).

$$\sum_{j}^{N} \int_{a}^{b} \delta(x - x_j) P_n(x) W(x) dx = \sum_{i}^{m} \int_{a}^{b} a_i P_i(x) P_n(x) W(x) dx \tag{4.3}$$

$$\int_{-\infty}^{\infty} f(x)\delta(x - x_l)dx = f(x_l) \tag{4.4}$$

Applying orthogonality conditions on the right-hand side and the delta function property given on (4.4), on the left, leads to (4.5) below.

$$\sum_{j}^{N} P_n(x_j)W(x_j) = a_n \int_a^b {P_n}^2(x)W(x)dx \tag{4.5}$$

Equation (4.5) can then be solve for a_n, giving (4.6). This equation will be used with three different polynomials to approximate the charge density based on points from different distributions.

$$a_n = \frac{\sum_j^N P_n(x_j)W(x_j)}{\int_a^b {P_n}^2(x)W(x)dx} \tag{4.6}$$

In the case where instead of a delta function, the function is continuous and given by $g(x)$, equation (4.6) is written as (4.7). These coefficients will serve as a comparison point to the ones calculated by the point approximation.

$$a_n = \frac{\int_a^b g(x)P_n(x)W(x)}{\int_a^b {P_n}^2(x)W(x)dx} \tag{4.7}$$

4.1 Single One-Dimensional Gaussian Distribution

The first distribution used was a single Gaussian (4.8), defined in Mathematica as $NormalDistribution[\mu, \sigma]$ [18], with mean $\mu = 0$ and variance $\sigma^2 = \frac{1}{36}$ to keep the Gaussian function between the interval of orthogonality, $[-1, 1]$ of Legendre and Chebyshev polynomials. To start the approximation, a random set of fifteen million

points indicating the positions of 15 million particles in a beam was created, which followed from the Gaussian curve.

$$g(x) = \frac{1}{\sigma\sqrt{2\pi}} e^{\frac{-(x-\mu)^2}{2\sigma^2}} \tag{4.8}$$

Using equation (4.6) the coefficients up to order $n = 20$ for Legendre and Chevyshev polynomials were approximated for every ten thousand points up to 1 million and for every 1 million up to fifteen million. To have a comparison perspective, equation (4.7) was used to calculate the coefficients to $n = 20$ directly from the Gaussian.

After the coefficients were approximated and calculated, plots were made that showed how the approximated charge distributions resembled the Gaussian curve with changing order and number of particles. The sets of coefficients were also used to show convergence for every order as the number of particles increased. Lastly, the difference between the approximated charge distribution and the actual function was calculated by equation (1.3).

4.1.1 Legendre Polynomials

The first polynomial used to approximate the single Gaussian distribution was Legendre Polynomials. Based on equation (4.6), all $a_n = 0$ if $n = odd$. Figures [4.1] through [4.5] show the convergence of the coefficients from ten thousand to one million points for specific orders.

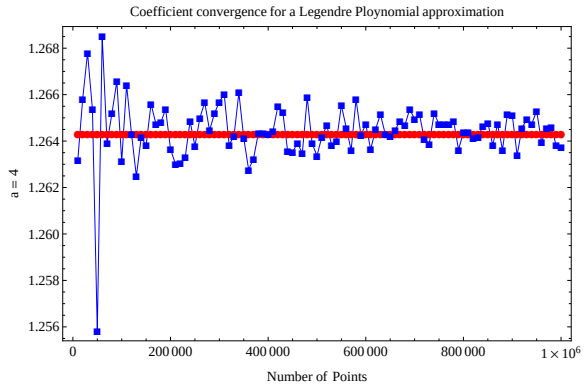

Figure 4.1: Coefficient convergence of a_4 for the Legendre polynomial approximation of a Gaussian distribution.

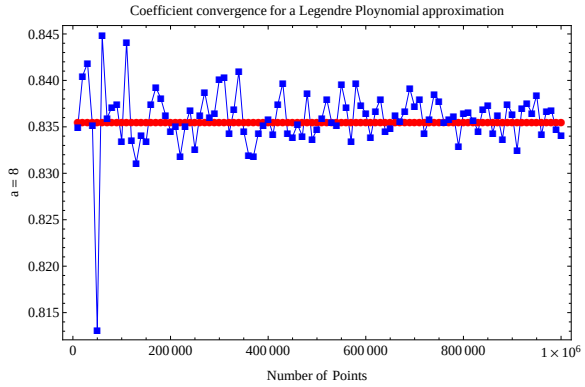

Figure 4.2: Coefficient convergence of a_8 for the Legendre polynomial approximation of a Gaussian distribution.

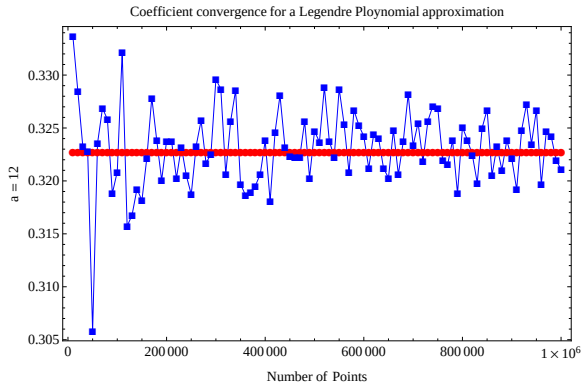

Figure 4.3: Coefficient convergence of a_{12} for the Legendre polynomial approximation of a Gaussian distribution.

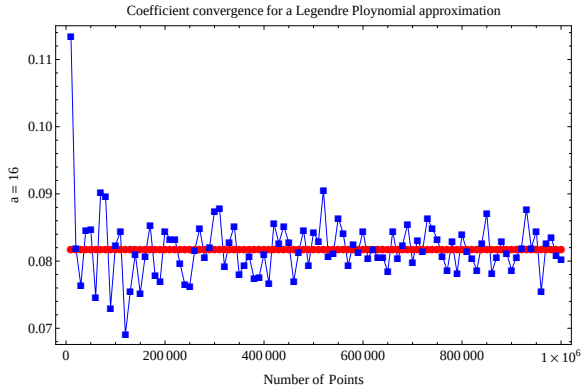

Figure 4.4: Coefficient convergence of a_{16} for the Legendre polynomial approximation of a Gaussian distribution.

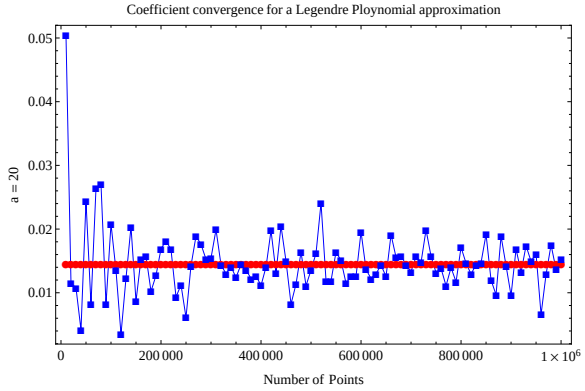

Figure 4.5: Coefficient convergence of a_{20} for the Legendre polynomial approximation of a Gaussian distribution.

Although the scales in the convergence plots are different, by taking the net difference in the range, you see that the lower orders, $n = 8$ and below, converge faster and oscillate closer to the expected coefficient value. To have a visual comparison of the approximated charge distribution, the results of equation (4.2) were plotted overlapping the Gaussian distribution. (See Figures 4.6 to 4.35.)

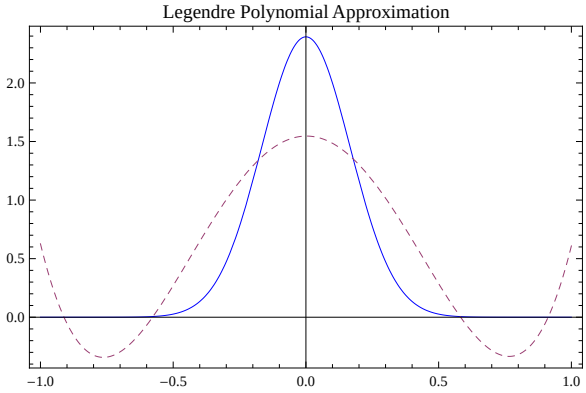

Figure 4.6: Legendre polynomial approximation of the charge density for $n = 4$ and ten thousand points.

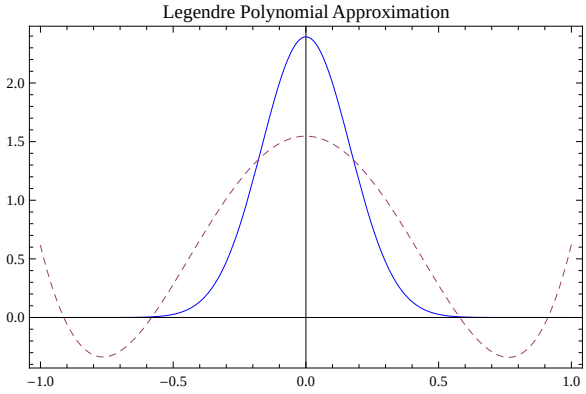

Figure 4.7: Legendre polynomial approximation of the charge density for $n = 4$ and one hundred thousand points.

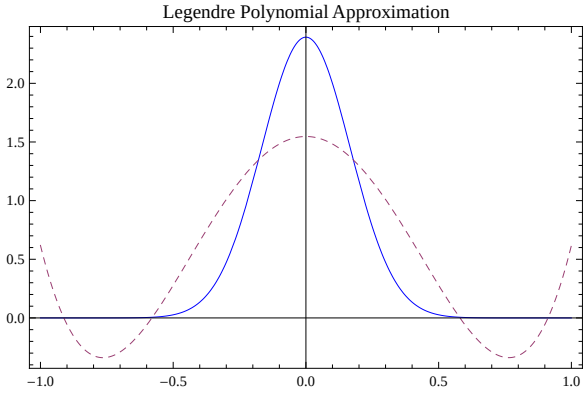

Figure 4.8: Legendre polynomial approximation of the charge density for $n = 4$ and one million points.

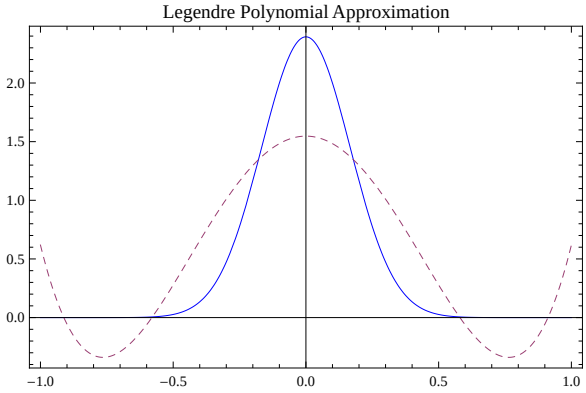

Figure 4.9: Legendre polynomial approximation of the charge density for $n = 4$ and five million points.

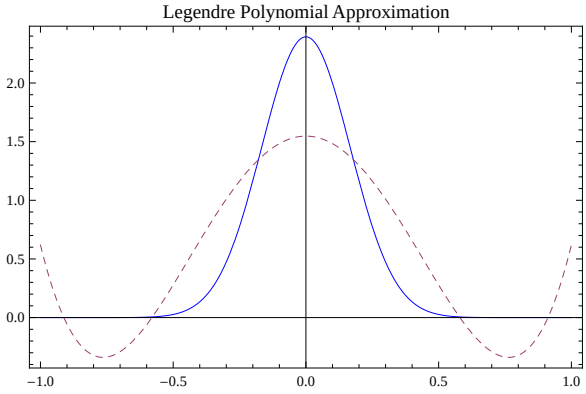

Figure 4.10: Legendre polynomial approximation of the charge density for $n = 4$ and ten million points.

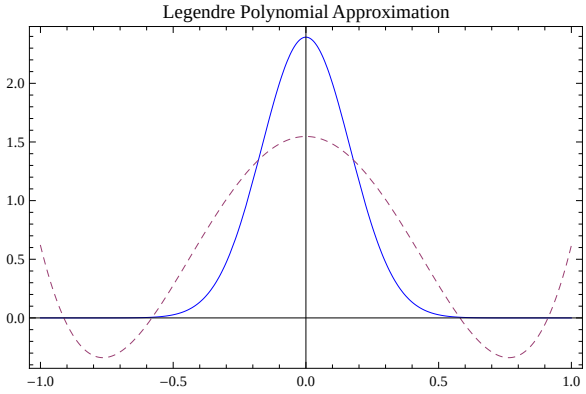

Figure 4.11: Legendre polynomial approximation of the charge density for $n = 4$ and fifteen million points.

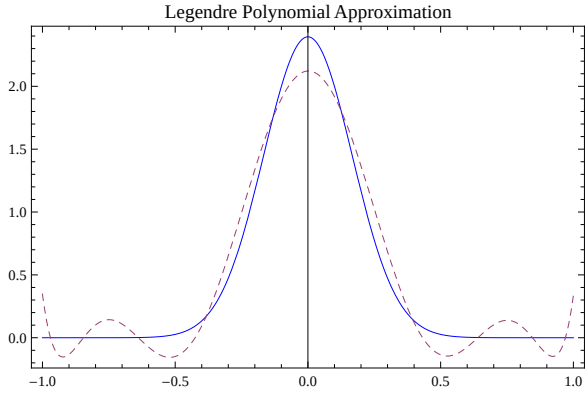

Figure 4.12: Legendre polynomial approximation of the charge density for $n = 8$ and ten thousand points.

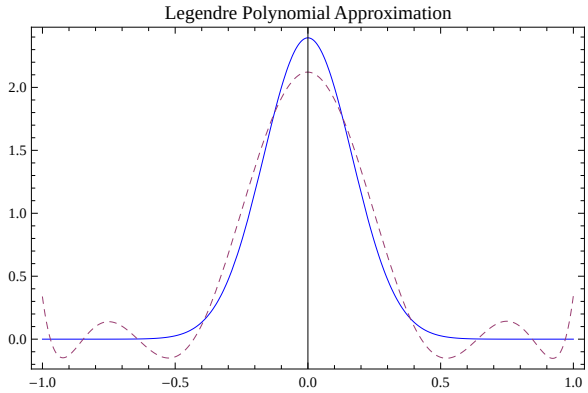

Figure 4.13: Legendre polynomial approximation of the charge density for $n = 8$ and one hundred thousand points.

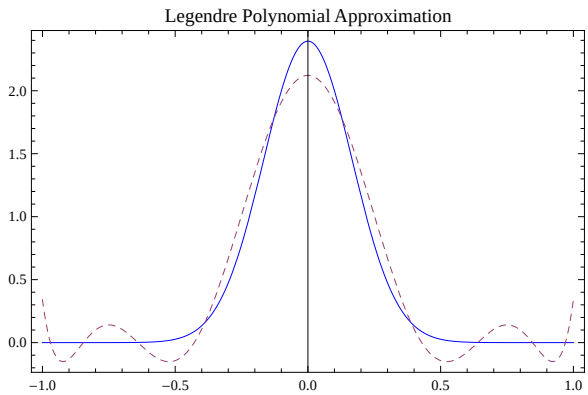

Figure 4.14: Legendre polynomial approximation of the charge density for $n = 8$ and one million points.

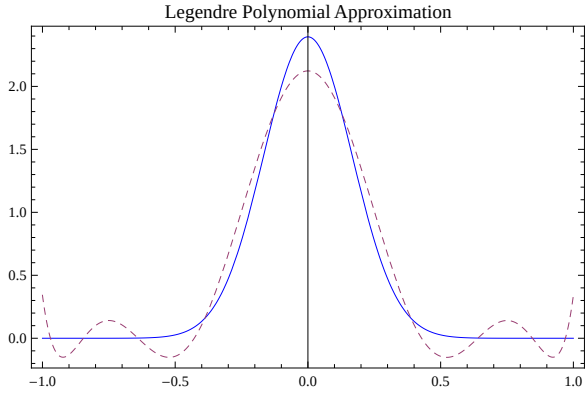

Figure 4.15: Legendre polynomial approximation of the charge density for $n = 8$ and five million points.

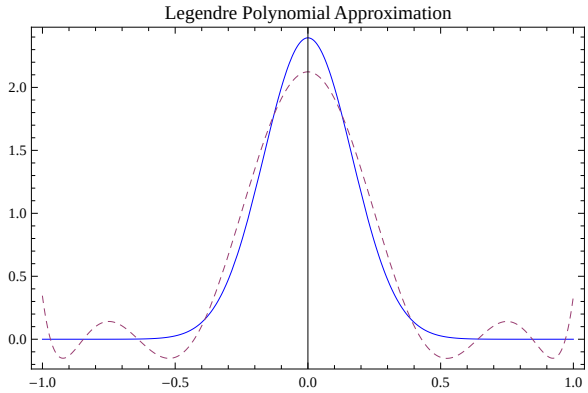

Figure 4.16: Legendre polynomial approximation of the charge density for $n = 8$ and ten million points.

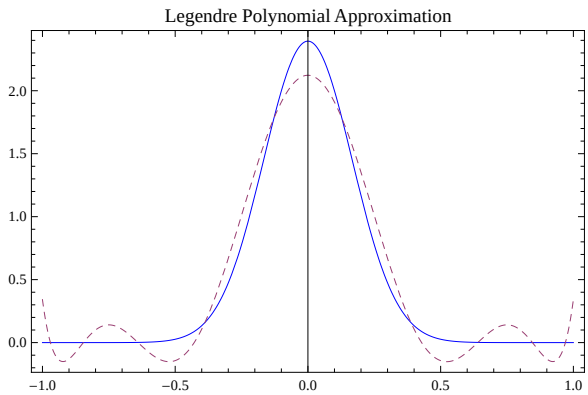

Figure 4.17: Legendre polynomial approximation of the charge density for $n = 8$ and fifteen million points.

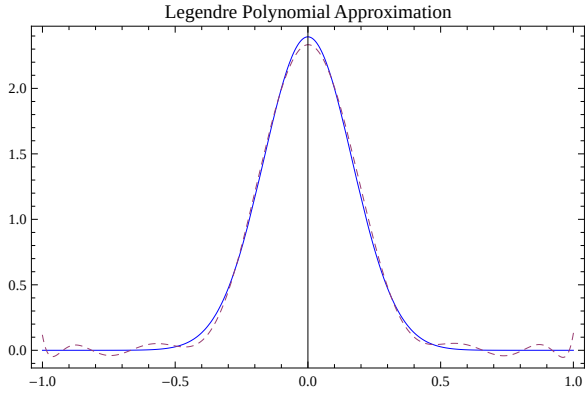

Figure 4.18: Legendre polynomial approximation of the charge density for $n = 12$ and ten thousand points.

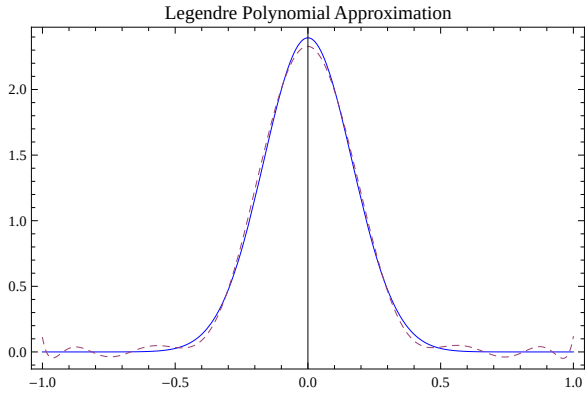

Figure 4.19: Legendre polynomial approximation of the charge density for $n = 12$ and one hundred thousand points.

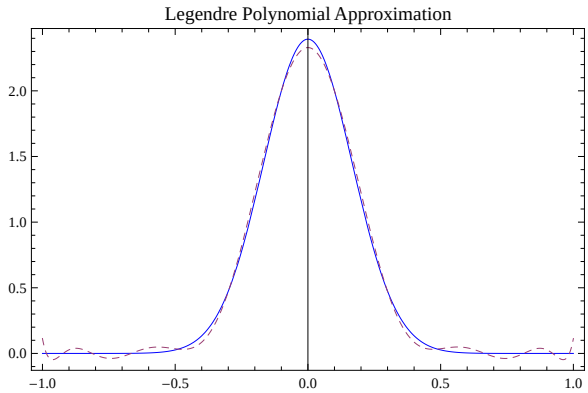

Figure 4.20: Legendre polynomial approximation of the charge density for $n = 12$ and one million points.

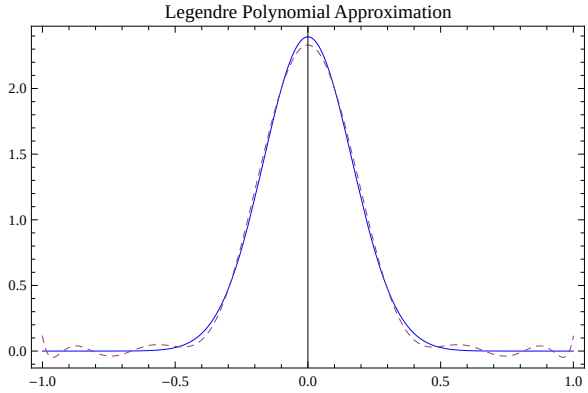

Figure 4.21: Legendre polynomial approximation of the charge density for $n = 12$ and five million points.

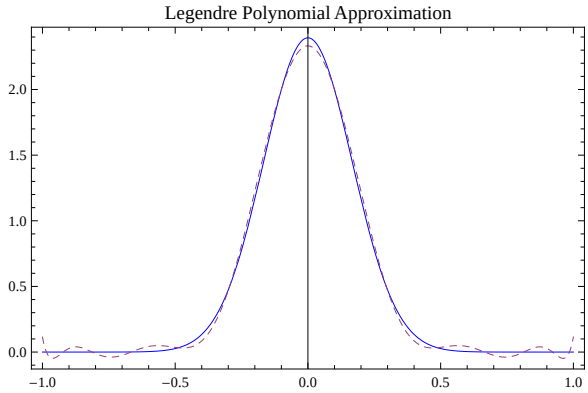

Figure 4.22: Legendre polynomial approximation of the charge density for $n = 12$ and ten million points.

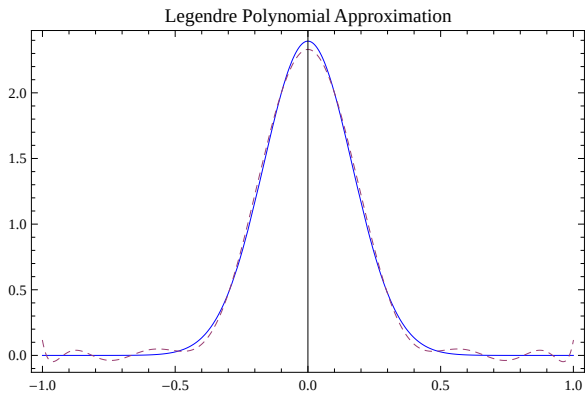

Figure 4.23: Legendre polynomial approximation of the charge density for $n = 12$ and fifteen million points.

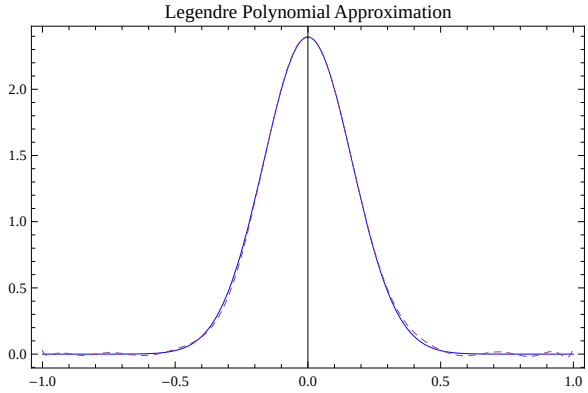

Figure 4.24: Legendre polynomial approximation of the charge density for $n = 16$ and ten thousand points.

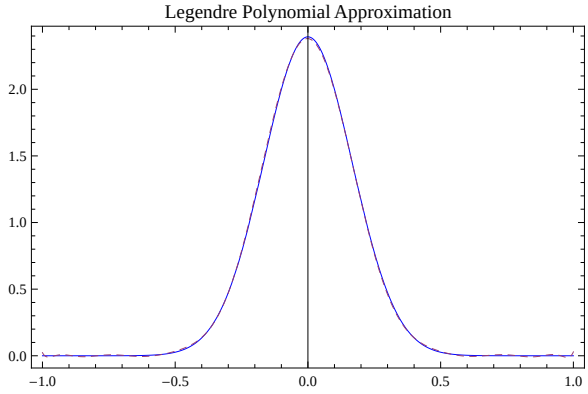

Figure 4.25: Legendre polynomial approximation of the charge density for $n = 16$ and one hundred thousand points.

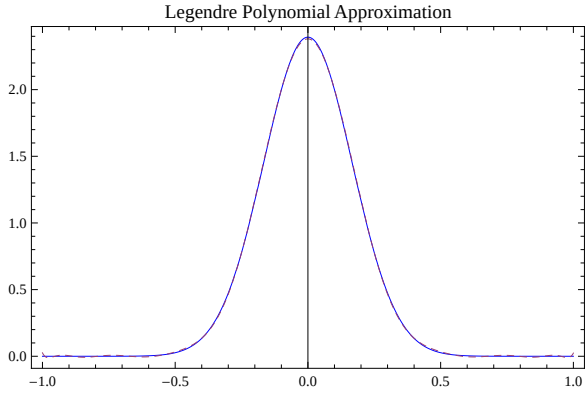

Figure 4.26: Legendre polynomial approximation of the charge density for $n = 16$ and one million points.

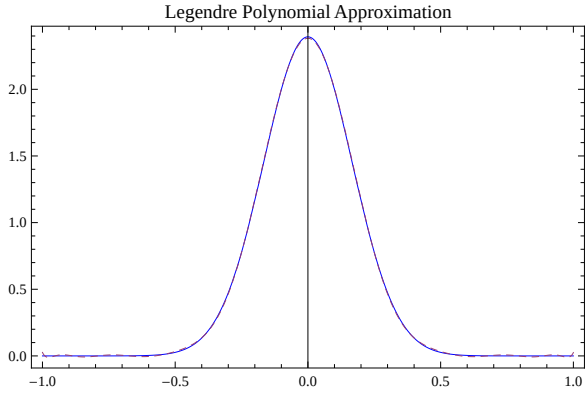

Figure 4.27: Legendre polynomial approximation of the charge density for $n = 16$ and five million points.

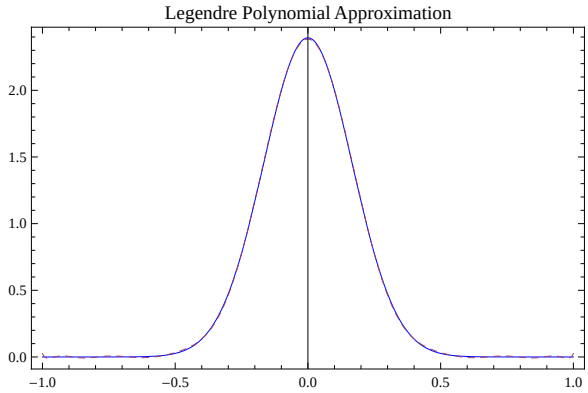

Figure 4.28: Legendre polynomial approximation of the charge density for $n = 16$ and ten million points.

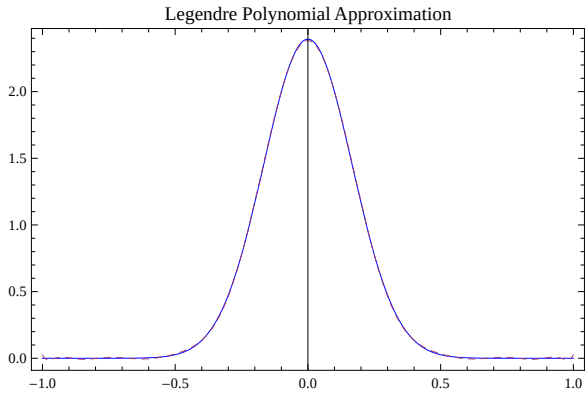

Figure 4.29: Legendre polynomial approximation of the charge density for $n = 16$ and fifteen million points.

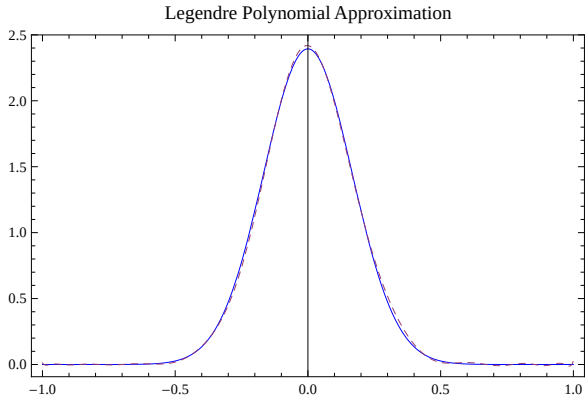

Figure 4.30: Legendre polynomial approximation of the charge density for $n = 20$ and ten thousand points.

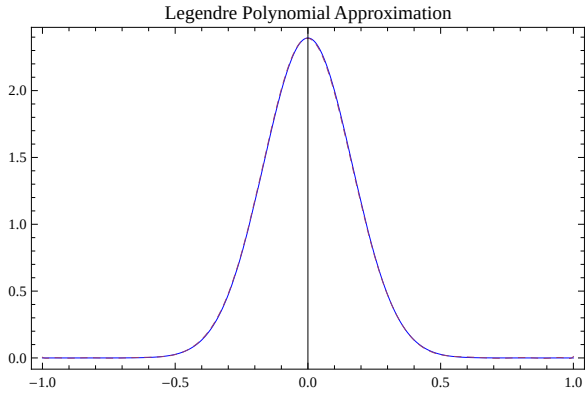

Figure 4.31: Legendre polynomial approximation of the charge density for $n = 20$ and one hundred thousand points.

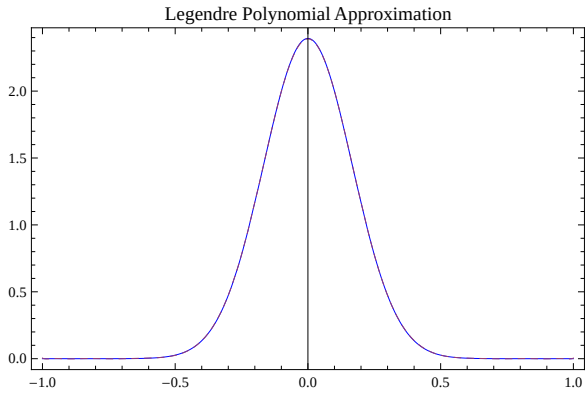

Figure 4.32: Legendre polynomial approximation of the charge density for $n = 20$ and one million points.

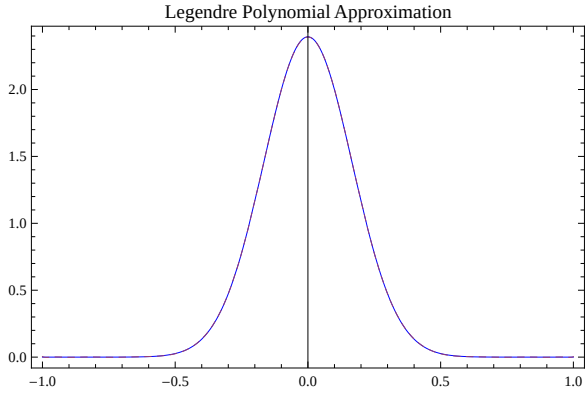

Figure 4.33: Legendre polynomial approximation of the charge density for $n = 20$ and five million points.

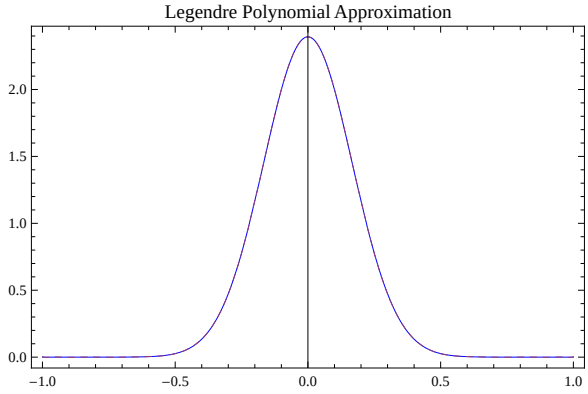

Figure 4.34: Legendre polynomial approximation of the charge density for $n = 20$ and ten million points.

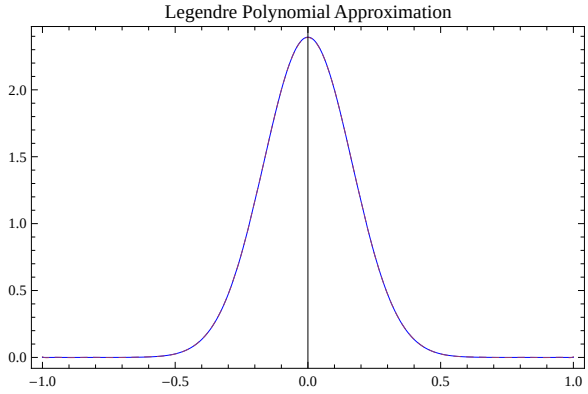

Figure 4.35: Legendre polynomial approximation of the charge density for $n = 20$ and fifteen million points.

From Figures [4.30] to [4.35], you can see that the charge density based on Legendre polynomials does a very nice job at approximating a Gaussian distribution, especially at order 20. Looking at the error difference between the two curves will give a better idea of how good the approximation is. (See Figures 4.36 to 4.40.)

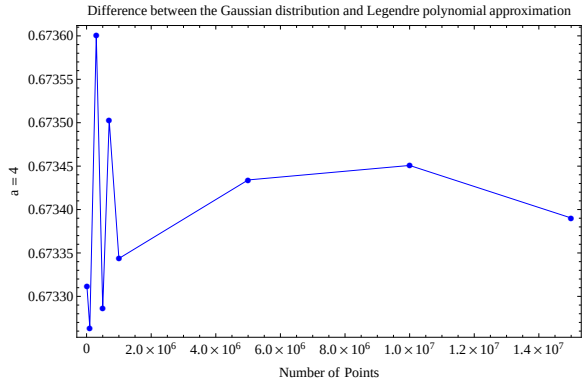

Figure 4.36: Error for a Gaussian Legendre polynomial approximation for $n = 4$.

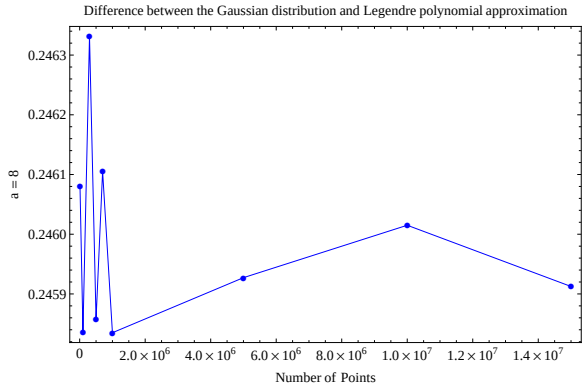

Figure 4.37: Error for a Gaussian Legendre polynomial approximation for $n = 8$.

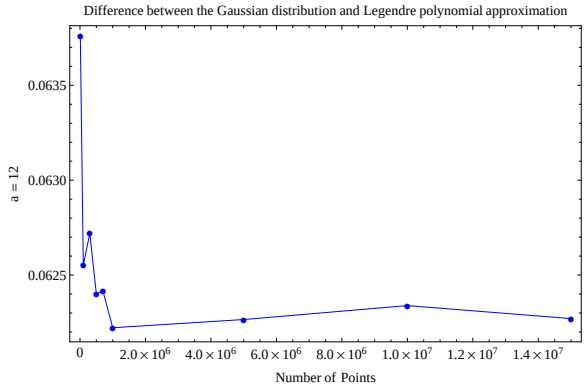

Figure 4.38: Error for a Gaussian Legendre polynomial approximation for $n = 12$.

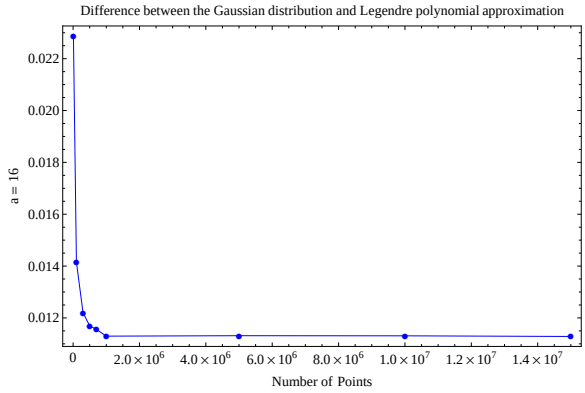

Figure 4.39: Error for a Gaussian Legendre polynomial approximation for $n = 16$.

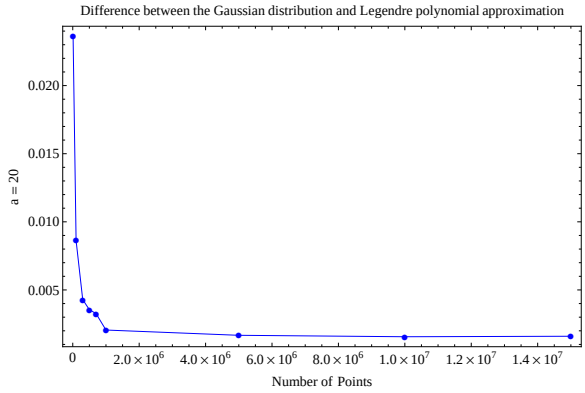

Figure 4.40: Error for a Gaussian Legendre polynomial approximation for $n = 20$.

The error figures 4.36 to 4.40 show a significant increase in the accuracy of the approximation as the order increases. The plots also show that, after around five million particles, there is not much change in the difference of the curves.

4.1.2 Chebyshev Polynomials of the first kind

The second polynomial used to approximate the single Gaussian distribution was Chebyshev polynomials of the first kind. Based the calculations following from equation (4.6), all $a_m = 0$ if $m = odd$. Figures 4.41 trough 4.45 show the convergence of the coefficients from ten thousand to one million points for specific orders.

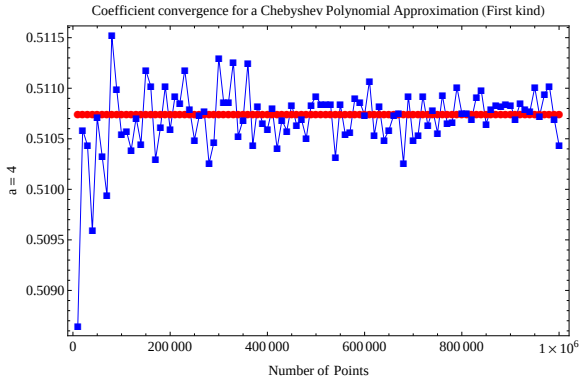

Figure 4.41: Coefficient convergence of a_4 for the first kind Chebyshev polynomial approximation.

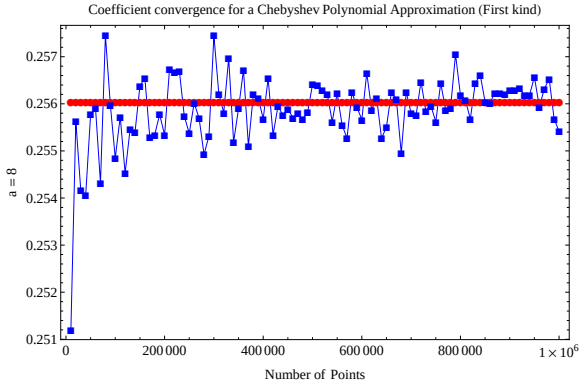

Figure 4.42: Coefficient convergence of a_8 for the first kind Chebyshev polynomial approximation.

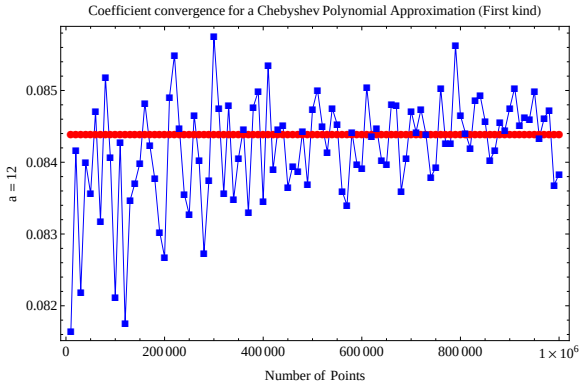

Figure 4.43: Coefficient convergence of a_{12} for the first kind Chebyshev polynomial approximation.

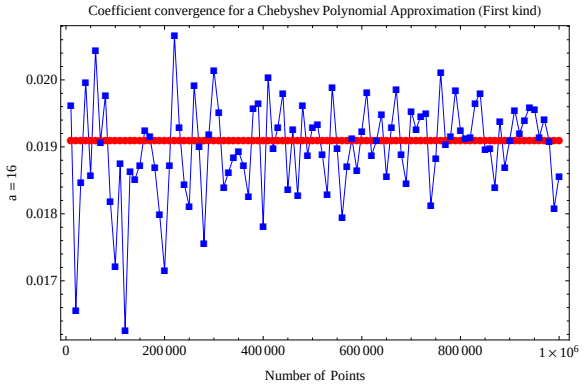

Figure 4.44: Coefficient convergence of a_{16} for the first kind Chebyshev polynomial approximation.

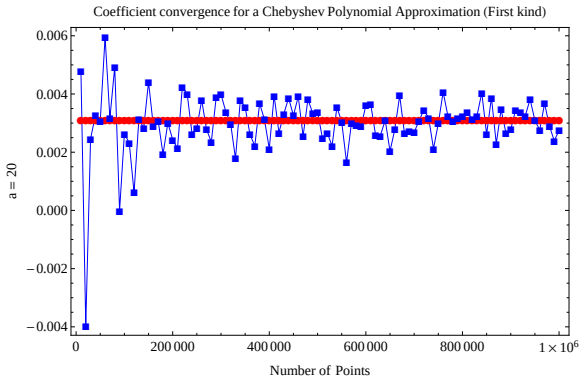

Figure 4.45: Coefficient convergence of a_{20} for the first kind Chebyshev polynomial approximation.

Just like with Legendre polynomials, the Chebyshev approximation of the first kind seems to converge faster in the lower orders. To have a visual comparison of the approximated charge distribution, the results of equation (4.2) were plotted overlapping the Gaussian distribution. (See Figures 4.46 to 4.75.)

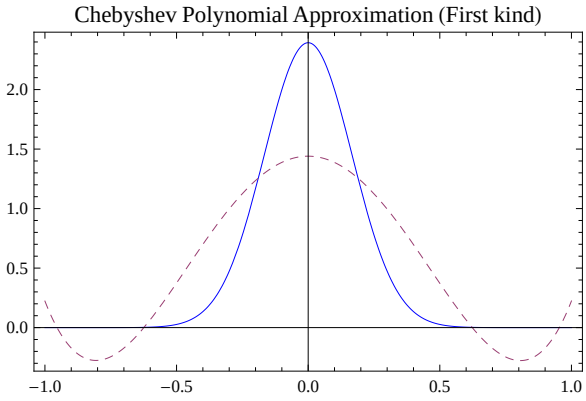

Figure 4.46: Chebyshev polynomial (first kind) approximation of the charge density for $n = 4$ and ten thousand points.

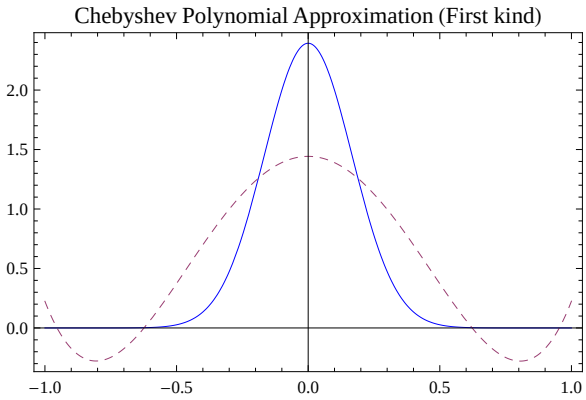

Figure 4.47: Chebyshev polynomial (first kind) approximation of the charge density for $n = 4$ and one hundred thousand points.

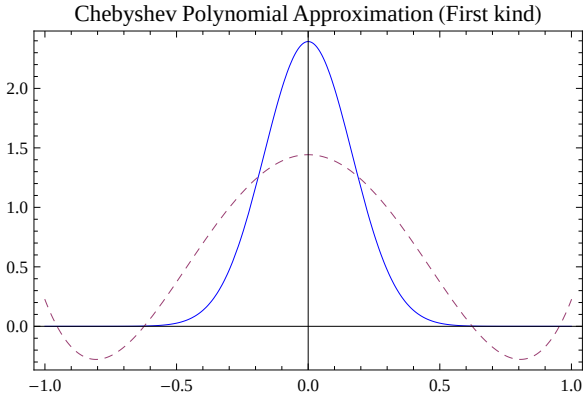

Figure 4.48: Chebyshev polynomial (first kind) approximation of the charge density for $n = 4$ and one million points.

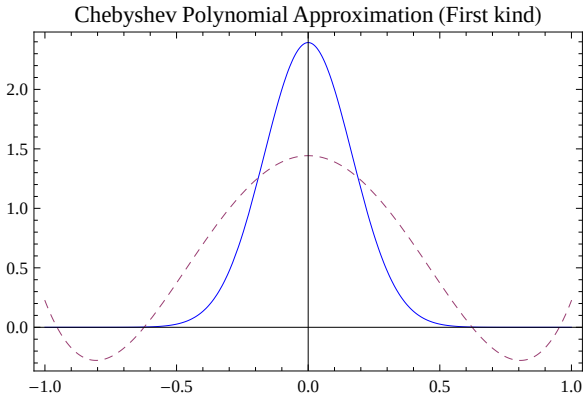

Figure 4.49: Chebyshev polynomial (first kind) approximation of the charge density for $n = 4$ and five million points.

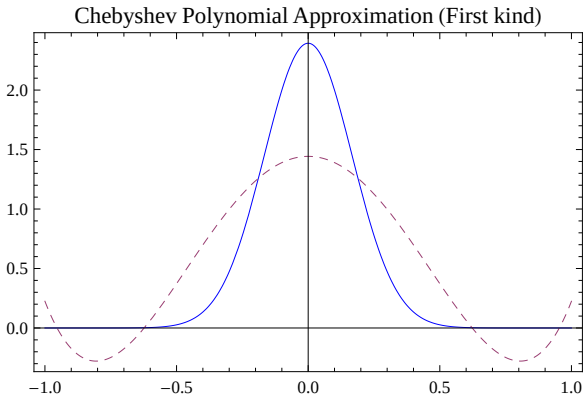

Figure 4.50: Chebyshev polynomial (first kind) approximation of the charge density for $n = 4$ and ten million points.

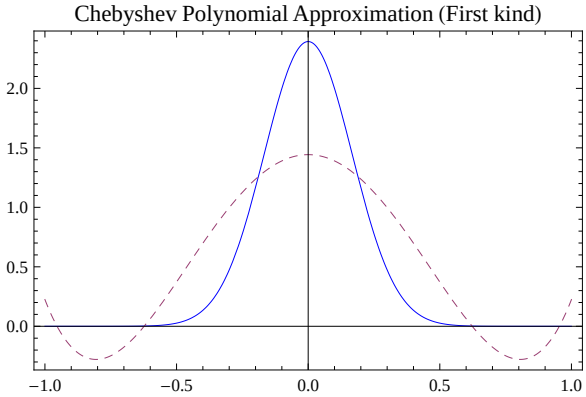

Figure 4.51: Chebyshev polynomial (first kind) approximation of the charge density for $n = 4$ and fifteen million points.

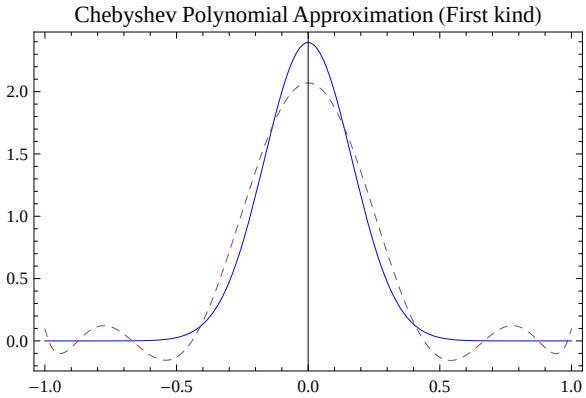

Figure 4.52: Chebyshev polynomial (first kind) approximation of the charge density for $n = 8$ and ten thousand points.

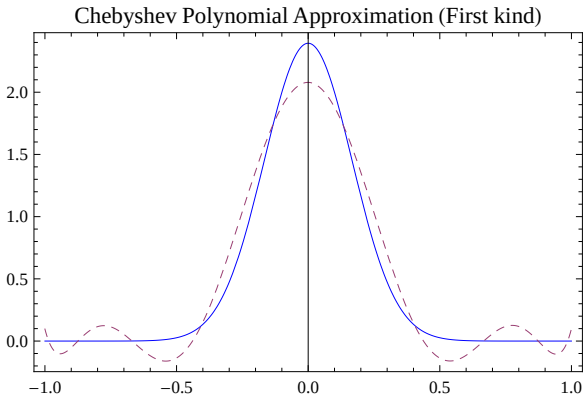

Figure 4.53: Chebyshev polynomial (first kind) approximation of the charge density for $n = 8$ and one hundred thousand points.

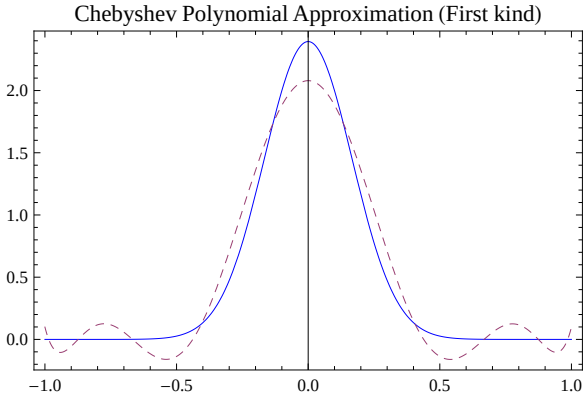

Figure 4.54: Chebyshev polynomial (first kind) approximation of the charge density for $n = 8$ and one million points.

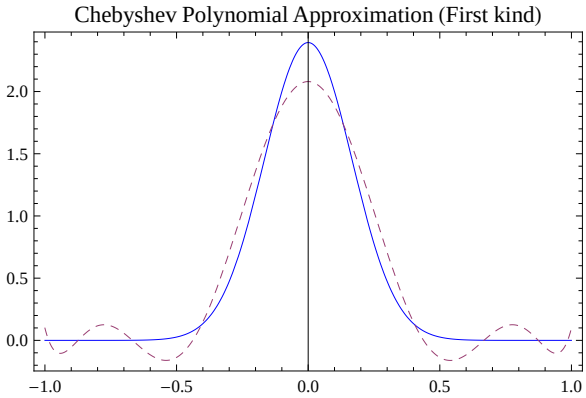

Figure 4.55: Chebyshev polynomial (first kind) approximation of the charge density for $n = 8$ and five million points.

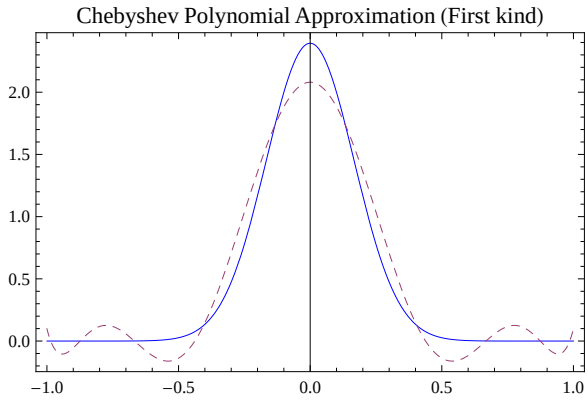

Figure 4.56: Chebyshev polynomial (first kind) approximation of the charge density for $n = 8$ and ten million points.

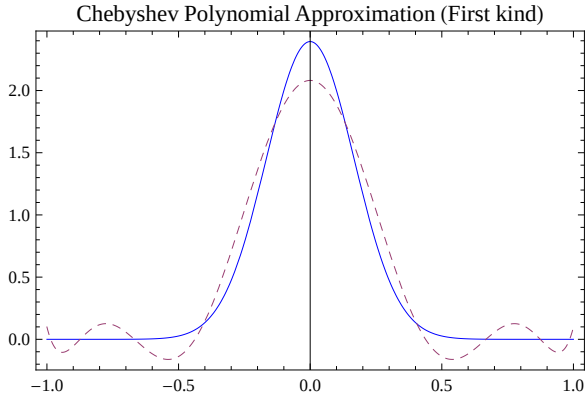

Figure 4.57: Chebyshev polynomial (first kind) approximation of the charge density for $n = 8$ and fifteen million points.

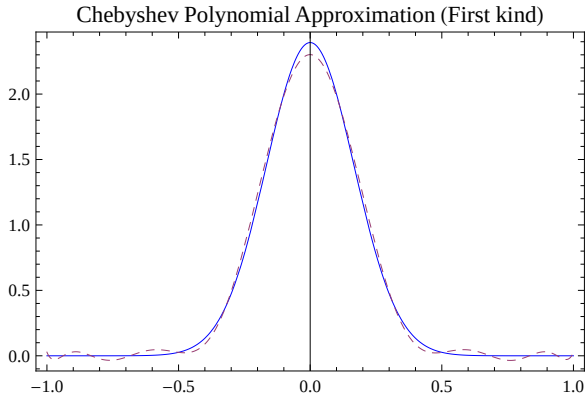

Figure 4.58: Chebyshev polynomial (first kind) approximation of the charge density for $n = 12$ and ten thousand points.

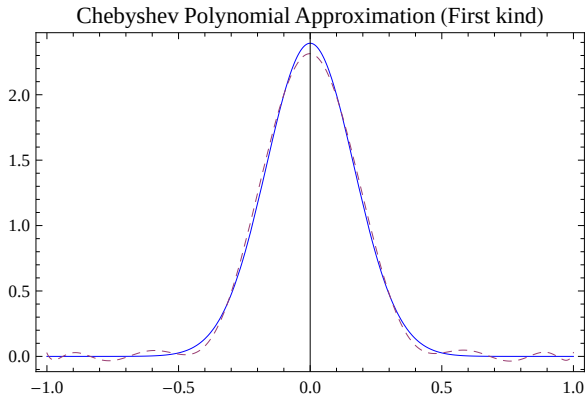

Figure 4.59: Chebyshev polynomial (first kind) approximation of the charge density for $n = 12$ and one hundred thousand points.

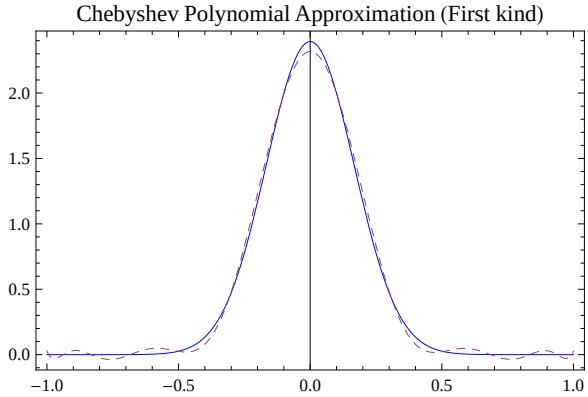

Figure 4.60: Chebyshev polynomial (first kind) approximation of the charge density for $n = 12$ and one million points.

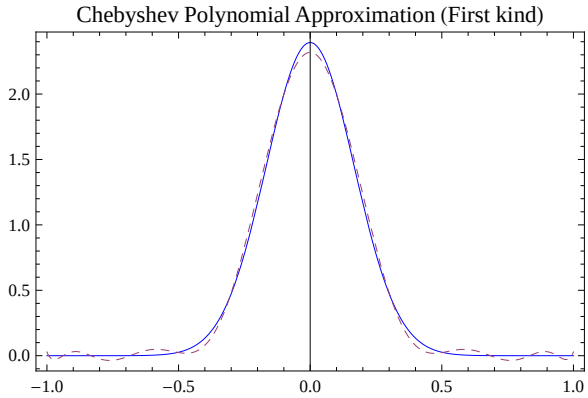

Figure 4.61: Chebyshev polynomial (first kind) approximation of the charge density for $n = 12$ and five million points.

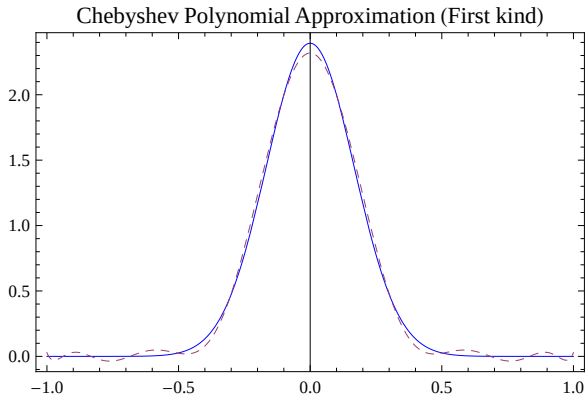

Figure 4.62: Chebyshev polynomial (first kind) approximation of the charge density for $n = 12$ and ten million points.

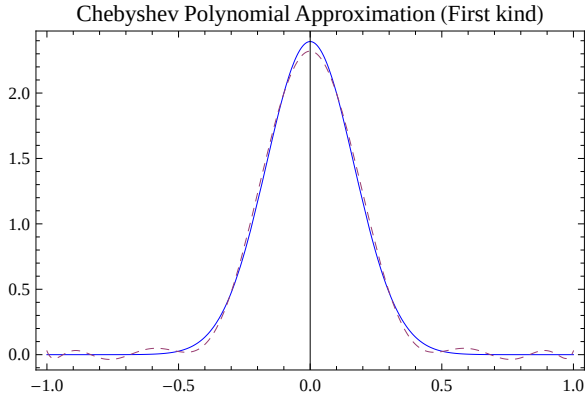

Figure 4.63: Chebyshev polynomial (first kind) approximation of the charge density for $n = 12$ and fifteen million points.

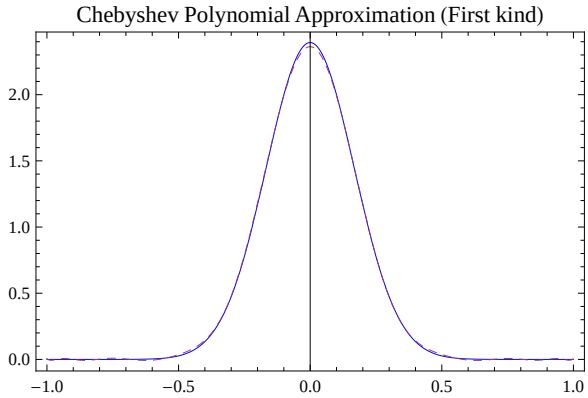

Figure 4.64: Chebyshev polynomial (first kind) approximation of the charge density for $n = 16$ and ten thousand points.

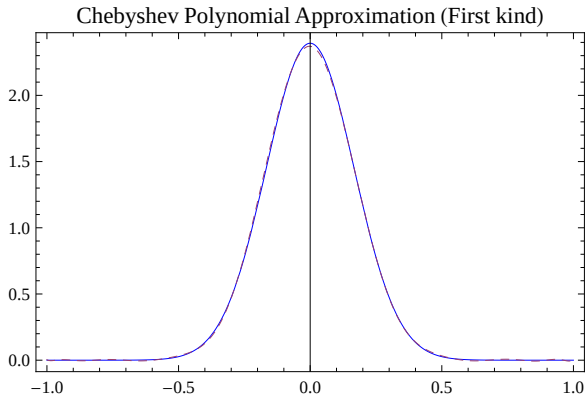

Figure 4.65: Chebyshev polynomial (first kind) approximation of the charge density for $n = 16$ and one hundred thousand points.

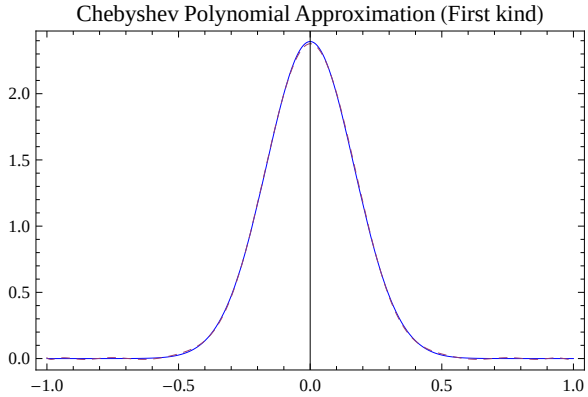

Figure 4.66: Chebyshev polynomial (first kind) approximation of the charge density for $n = 16$ and one million points.

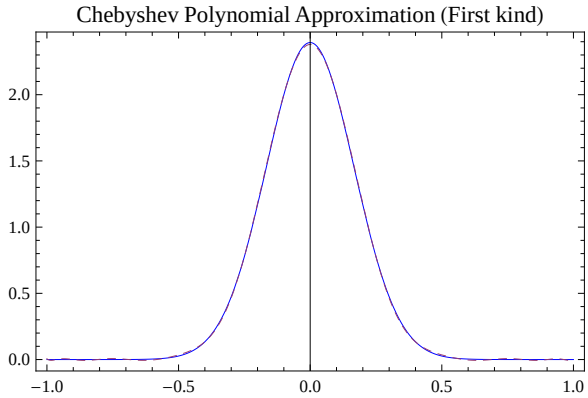

Figure 4.67: Chebyshev polynomial (first kind) approximation of the charge density for $n = 16$ and five million points.

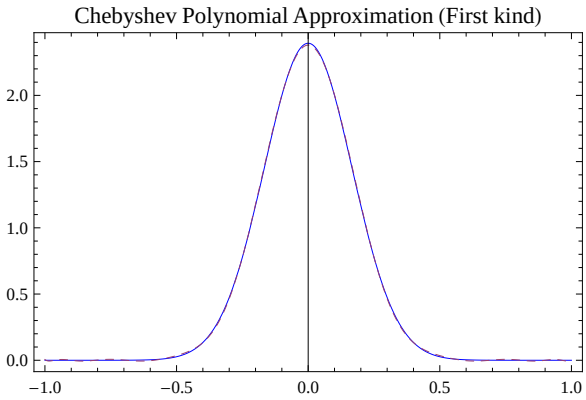

Figure 4.68: Chebyshev polynomial (first kind) approximation of the charge density for $n = 16$ and ten million points.

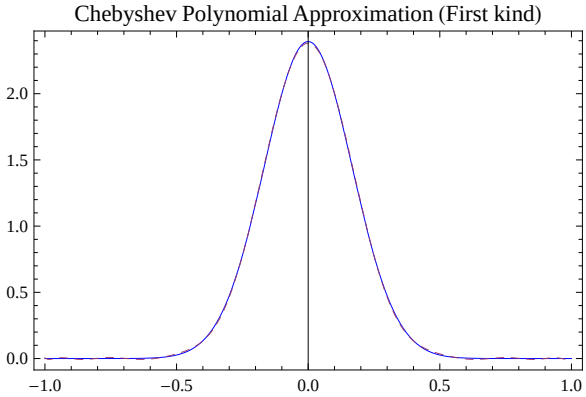

Figure 4.69: Chebyshev polynomial (first kind) approximation of the charge density for $n = 16$ and fifteen million points.

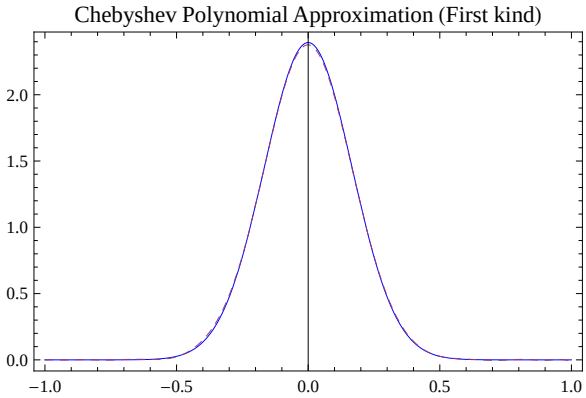

Figure 4.70: Chebyshev polynomial (first kind) approximation of the charge density for $n = 20$ and ten thousand points.

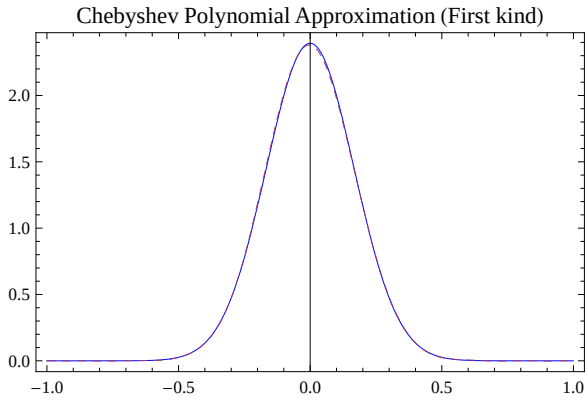

Figure 4.71: Chebyshev polynomial (first kind) approximation of the charge density for $n = 20$ and one hundred thousand points.

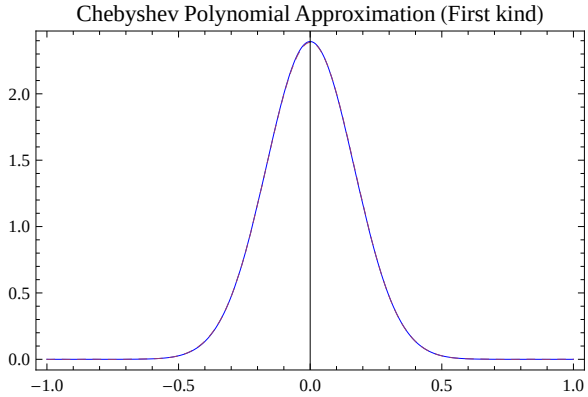

Figure 4.72: Chebyshev polynomial (first kind) approximation of the charge density for $n = 20$ and one million points.

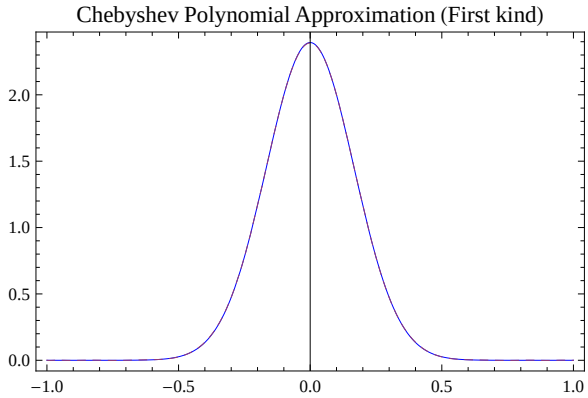

Figure 4.73: Chebyshev polynomial (first kind) approximation of the charge density for $n = 20$ and five million points.

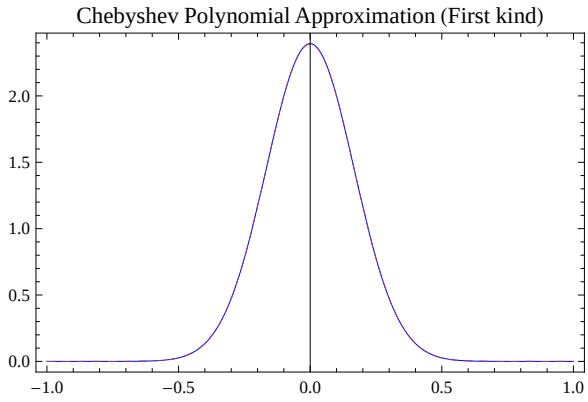

Figure 4.74: Chebyshev polynomial (first kind) approximation of the charge density for $n = 20$ and ten million points.

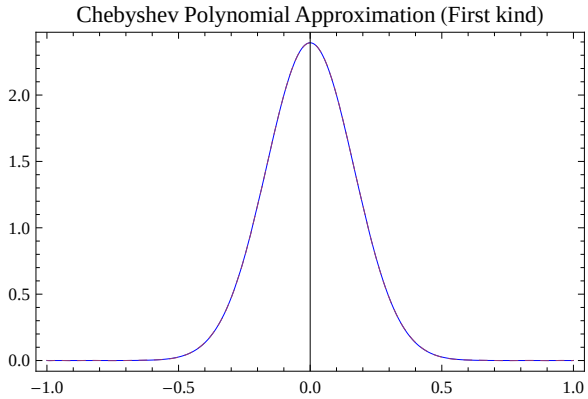

Figure 4.75: Chebyshev polynomial (first kind) approximation of the charge density for $n = 20$ and fifteen million points.

From Figures 4.71 to 4.75, it is clear that the charge density based on Chebyshev polynomials (first kind) does a very nice job at approximating a Gaussian distribution at $n = 20$, just the like Legendre polynomials. The numerical difference between the curves will give a better answer to what order and/or number of particles gives a better approximation. (See Figures 4.76 to 4.80.)

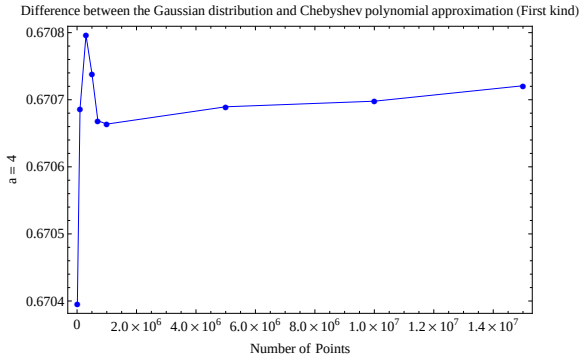

Figure 4.76: Error for a Gaussian Chebyshev polynomial approximation (First kind) for $n = 4$.

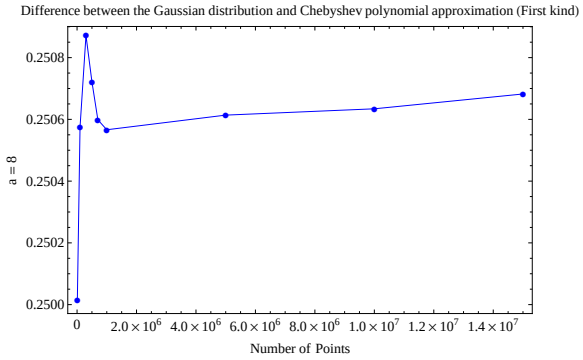

Figure 4.77: Error for a Gaussian Chebyshev polynomial approximation (First kind) for $n = 8$.

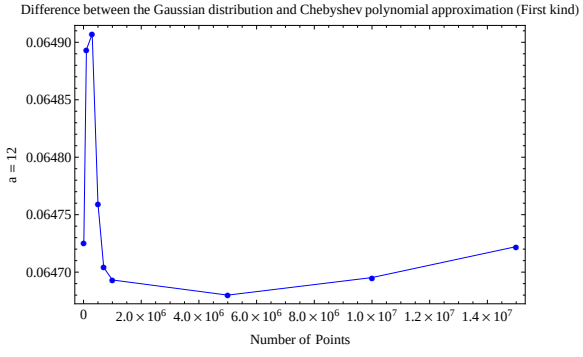

Figure 4.78: Error for a Gaussian Chebyshev polynomial approximation (First kind) for $n = 12$.

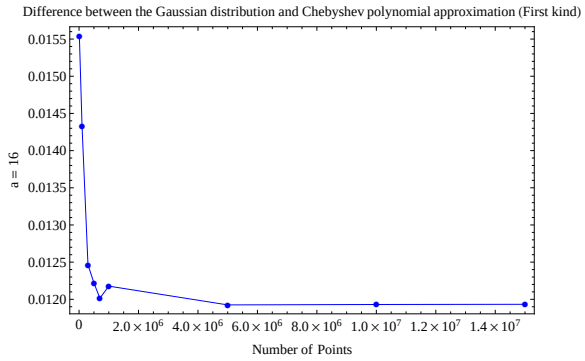

Figure 4.79: Error for a Gaussian Chebyshev polynomial approximation (First kind) for $n = 16$.

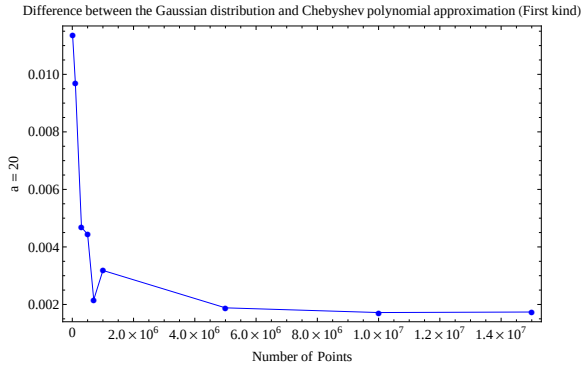

Figure 4.80: Error for a Gaussian Chebyshev polynomial approximation (First kind) for $n = 20$.

Similar to the Legendre polynomials, the Chebyshev of the first kind show very significant changes in the difference between the curves as the order increases. Once the number of particles reaches five million, the change on the error slows down to almost no change.

4.1.3 Chebyshev Polynomials of the second kind

The third and last polynomial used to approximate the single Gaussian distribution was Chebyshev polynomials of the second kind. Based on the calculations following from equation (4.6), all $a_m = 0$ if $m = odd$. Figures 4.81 trough 4.85 show the convergence of the coefficients from ten thousand to one million points for specific orders.

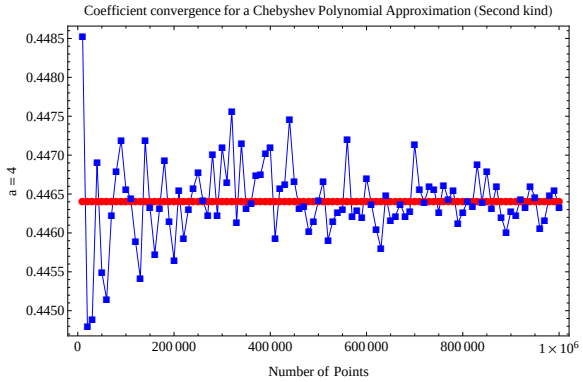

Figure 4.81: Coefficient convergence of a_4 for the second kind Chebyshev polynomial approximation.

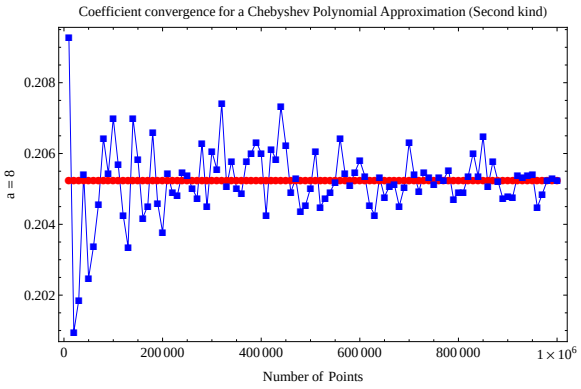

Figure 4.82: Coefficient convergence of a_8 for the second kind Chebyshev polynomial approximation.

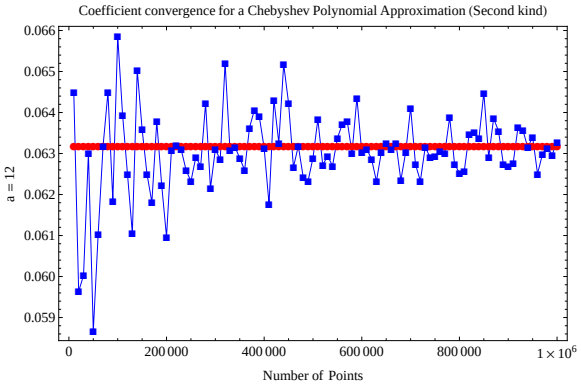

Figure 4.83: Coefficient convergence of a_{12} for the second kind Chebyshev polynomial approximation.

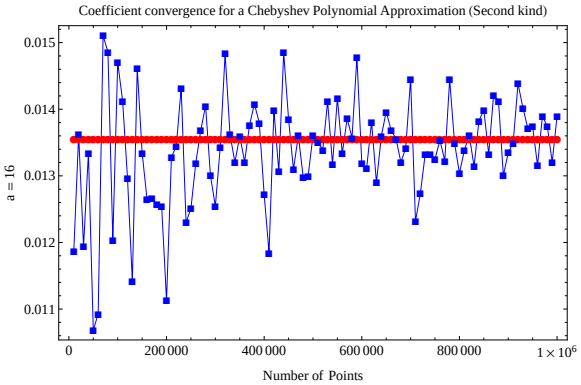

Figure 4.84: Coefficient convergence of a_{16} for the second kind Chebyshev polynomial approximation.

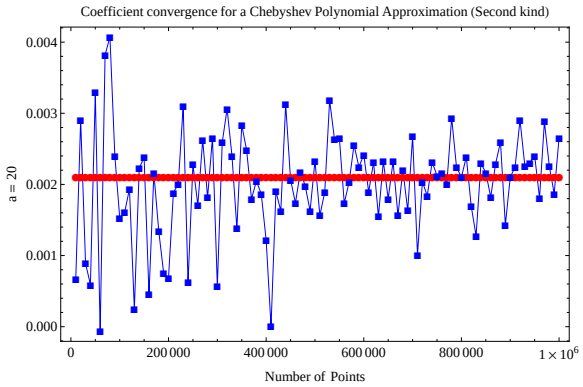

Figure 4.85: Coefficient convergence of a_{20} for the second kind Chebyshev polynomial approximation.

Comparing figures 4.81 to 4.85 to those of Legendre and Chebyshev of the first kind, it seems easier to notice the difference of the ranges in the graphs. Just like the previous two approximations, the lower orders converge much faster that those higher. To visually compare the approximated charge distribution, the results of equations (4.6) and (4.7) were plotted overlapping the Gaussian distribution. (See Figures 4.86 to 4.115.)

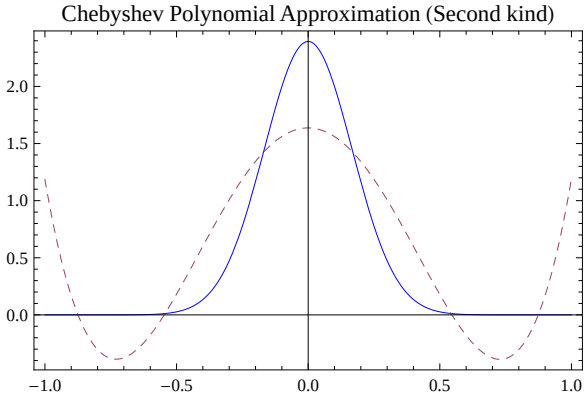

Figure 4.86: Chebyshev polynomial (second kind) approximation of the charge density for $n = 4$ and ten thousand points.

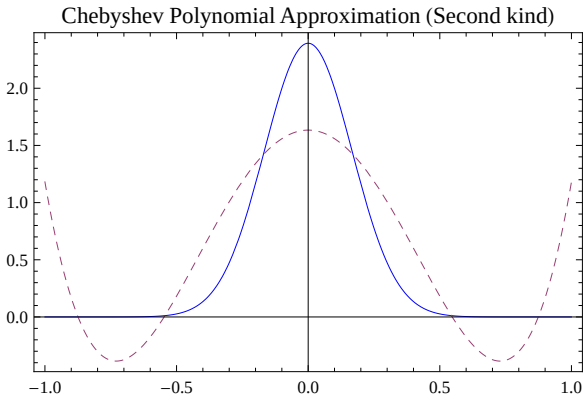

Figure 4.87: Chebyshev polynomial (second kind) approximation of the charge density for $n = 4$ and one hundred thousand points.

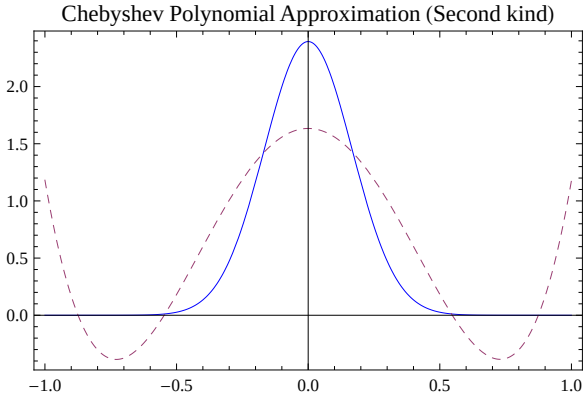

Figure 4.88: Chebyshev polynomial (second kind) approximation of the charge density for $n = 4$ and one million points.

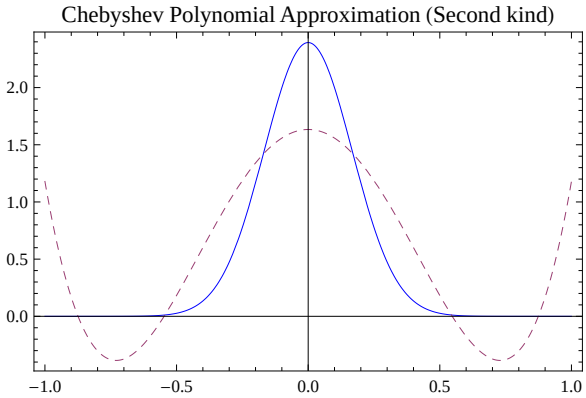

Figure 4.89: Chebyshev polynomial (second kind) approximation of the charge density for $n = 4$ and five million points.

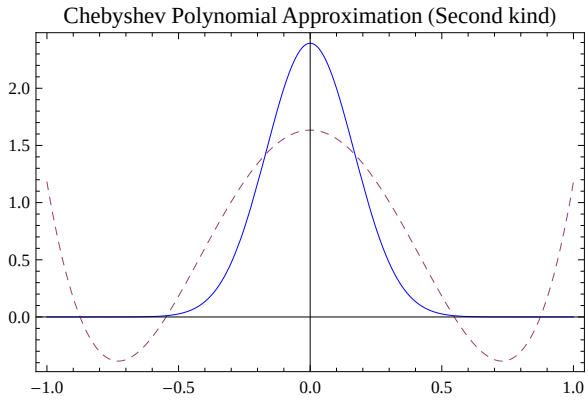

Figure 4.90: Chebyshev polynomial (second kind) approximation of the charge density for $n = 4$ and ten million points.

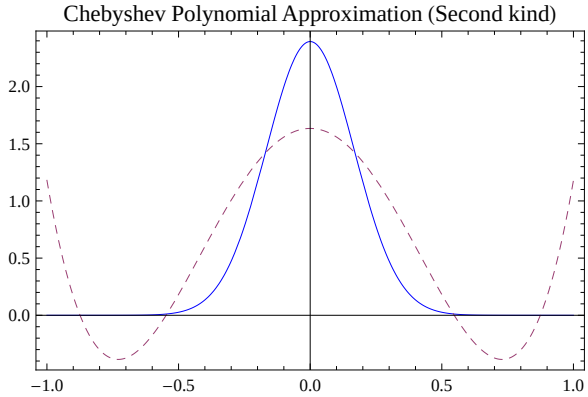

Figure 4.91: Chebyshev polynomial (second kind) approximation of the charge density for $n = 4$ and fifteen million points.

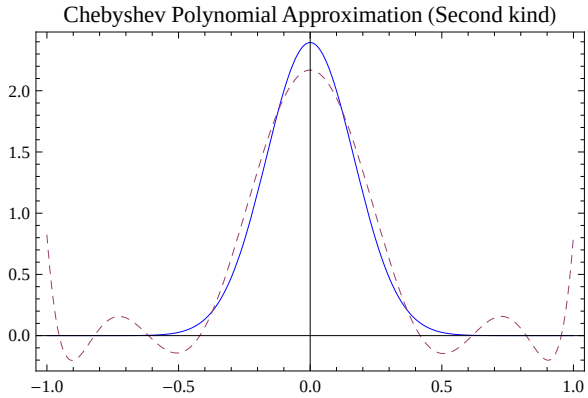

Figure 4.92: Chebyshev polynomial (second kind) approximation of the charge density for $n = 8$ and ten thousand points.

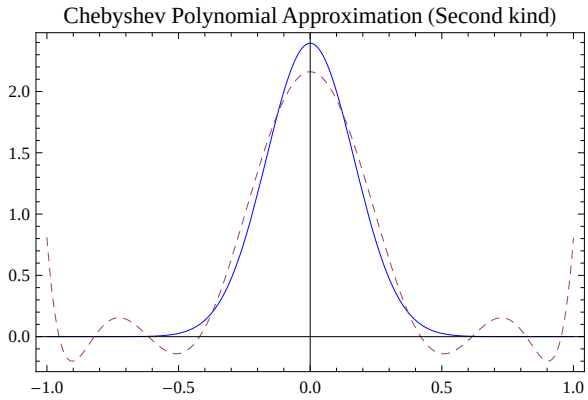

Figure 4.93: Chebyshev polynomial (second kind) approximation of the charge density for $n = 8$ and one hundred thousand points.

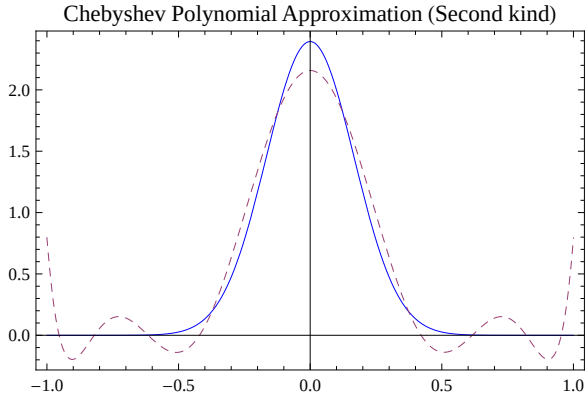

Figure 4.94: Chebyshev polynomial (second kind) approximation of the charge density for $n = 8$ and one million points.

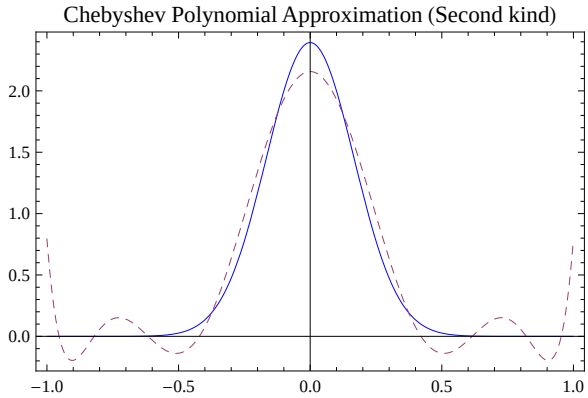

Figure 4.95: Chebyshev polynomial (second kind) approximation of the charge density for $n = 8$ and five million points.

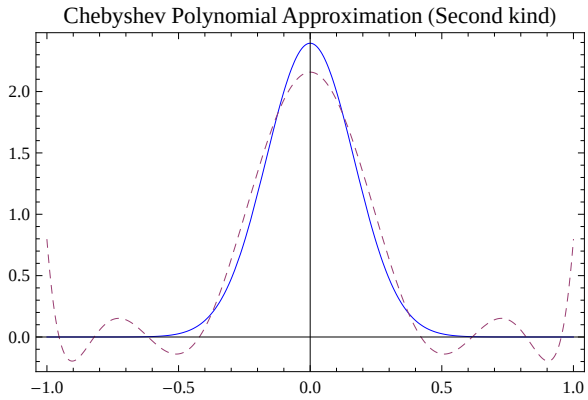

Figure 4.96: Chebyshev polynomial (second kind) approximation of the charge density for $n = 8$ and ten million points.

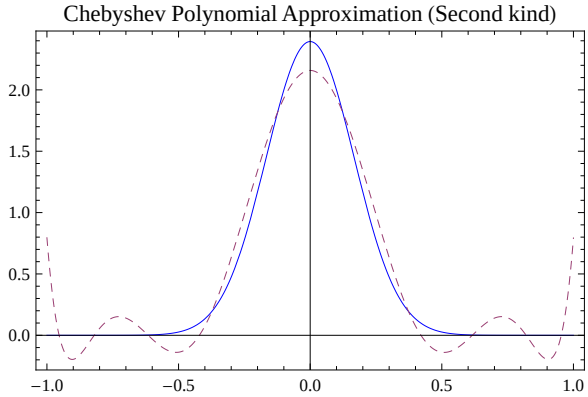

Figure 4.97: Chebyshev polynomial (second kind) approximation of the charge density for $n = 8$ and fifteen million points.

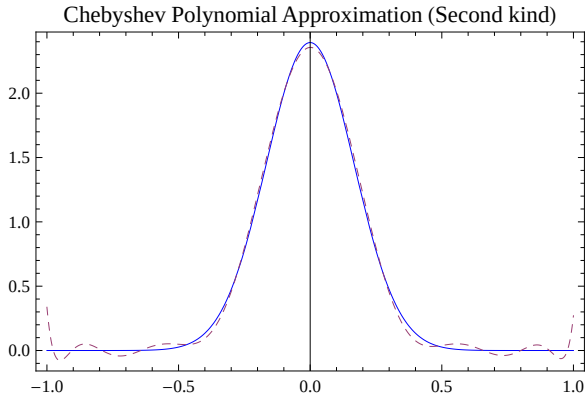

Figure 4.98: Chebyshev polynomial (second kind) approximation of the charge density for $n = 12$ and ten thousand points.

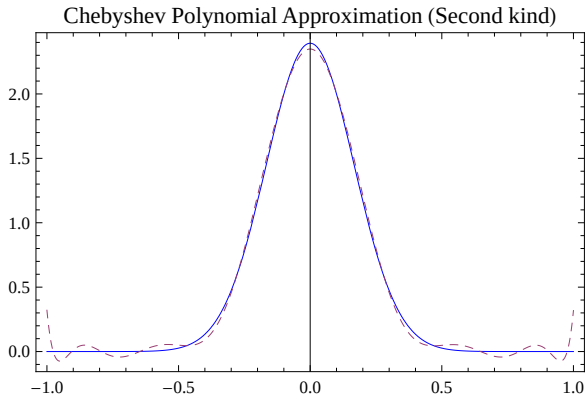

Figure 4.99: Chebyshev polynomial (second kind) approximation of the charge density for $n = 12$ and one hundred thousand points.

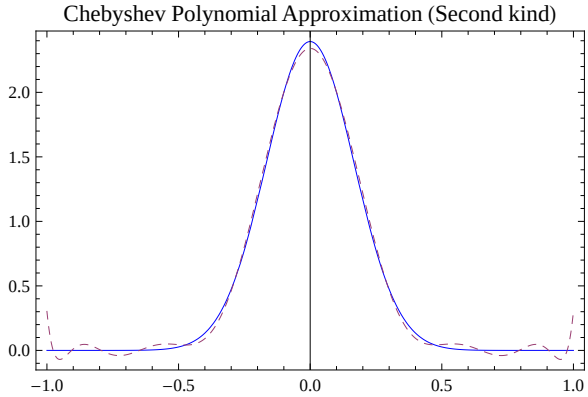

Figure 4.100: Chebyshev polynomial (second kind) approximation of the charge density for $n = 12$ and one million points.

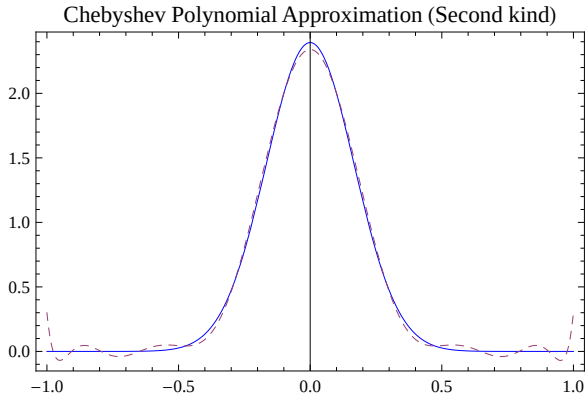

Figure 4.101: Chebyshev polynomial (second kind) approximation of the charge density for $n = 12$ and five million points.

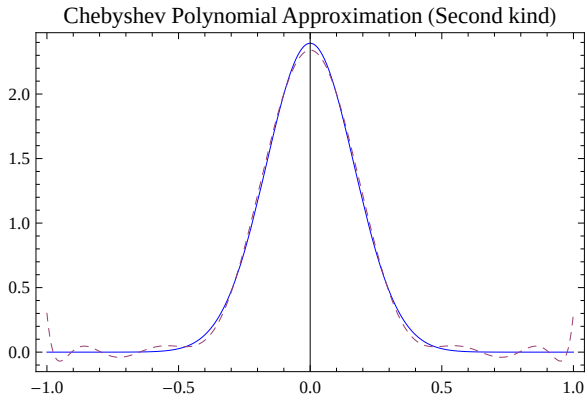

Figure 4.102: Chebyshev polynomial (second kind) approximation of the charge density for $n = 12$ and ten million points.

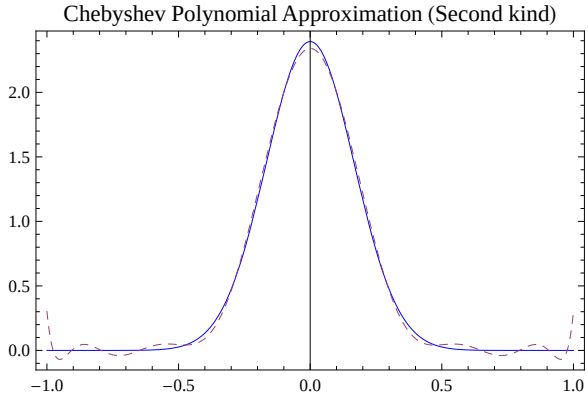

Figure 4.103: Chebyshev polynomial (second kind) approximation of the charge density for $n = 12$ and fifteen million points.

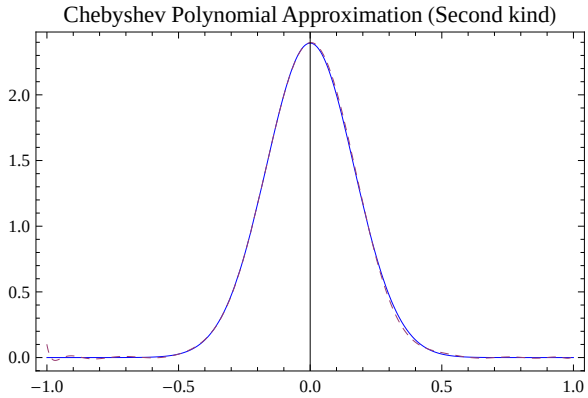

Figure 4.104: Chebyshev polynomial (second kind) approximation of the charge density for $n = 16$ and ten thousand points.

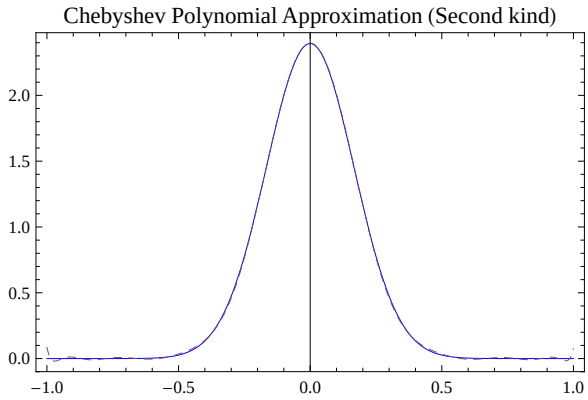

Figure 4.105: Chebyshev polynomial (second kind) approximation of the charge density for $n = 16$ and one hundred thousand points.

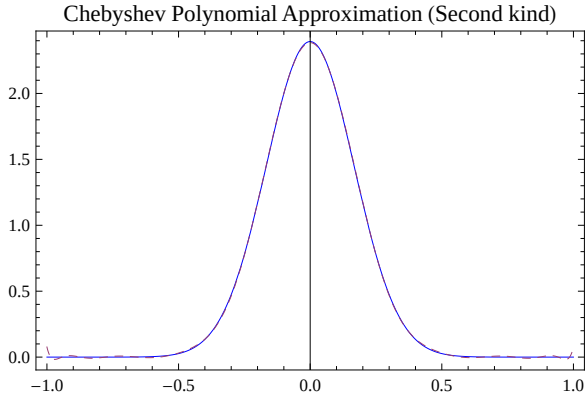

Figure 4.106: Chebyshev polynomial (second kind) approximation of the charge density for $n = 16$ and one million points.

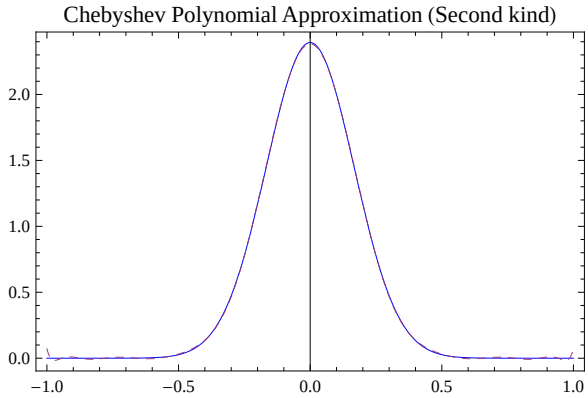

Figure 4.107: Chebyshev polynomial (second kind) approximation of the charge density for $n = 16$ and five million points.

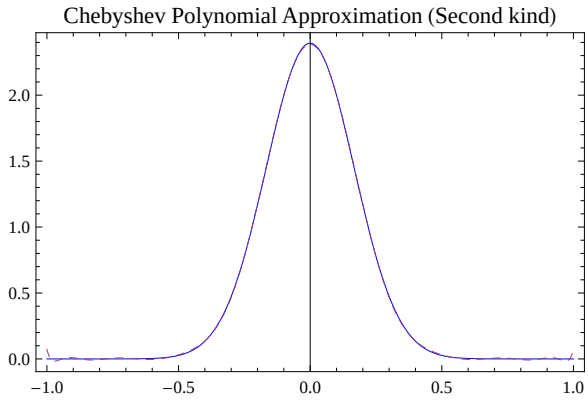

Figure 4.108: Chebyshev polynomial (second kind) approximation of the charge density for $n = 16$ and ten million points.

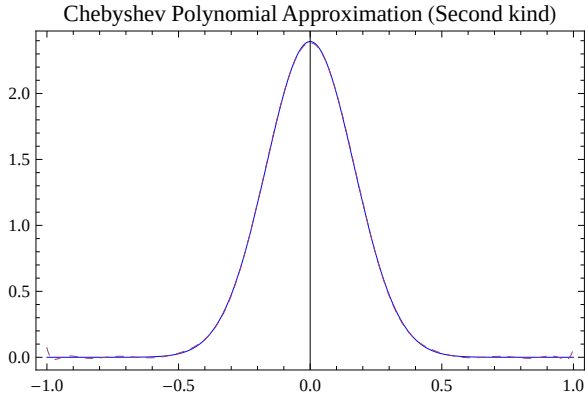

Figure 4.109: Chebyshev polynomial (second kind) approximation of the charge density for $n = 16$ and fifteen million points.

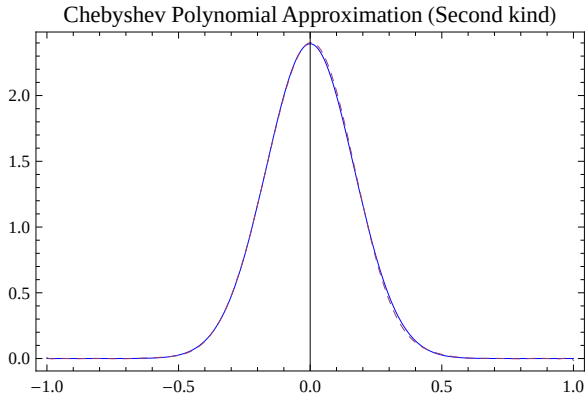

Figure 4.110: Chebyshev polynomial (second kind) approximation of the charge density for $n = 20$ and ten thousand points.

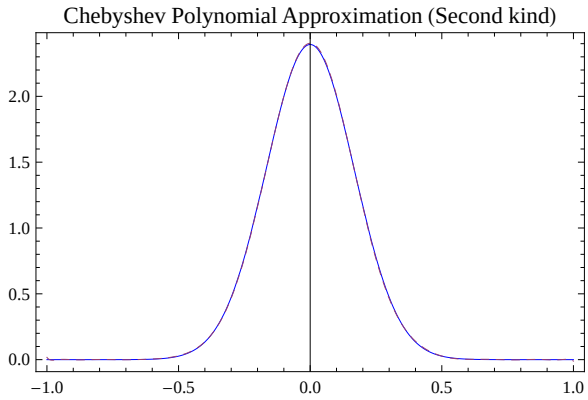

Figure 4.111: Chebyshev polynomial (second kind) approximation of the charge density for $n = 20$ and one hundred thousand points.

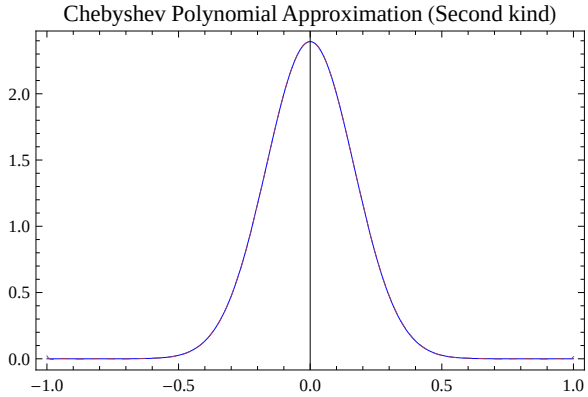

Figure 4.112: Chebyshev polynomial (second kind) approximation of the charge density for $n = 20$ and one million points.

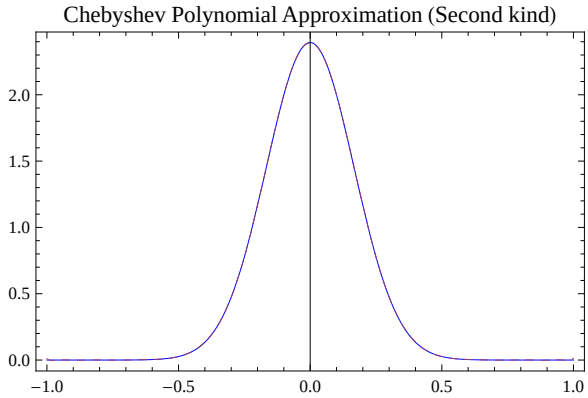

Figure 4.113: Chebyshev polynomial (second kind) approximation of the charge density for $n = 20$ and five million points.

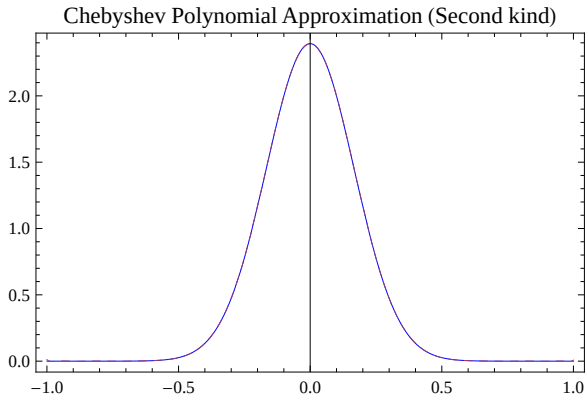

Figure 4.114: Chebyshev polynomial (second kind) approximation of the charge density for $n = 20$ and ten million points.

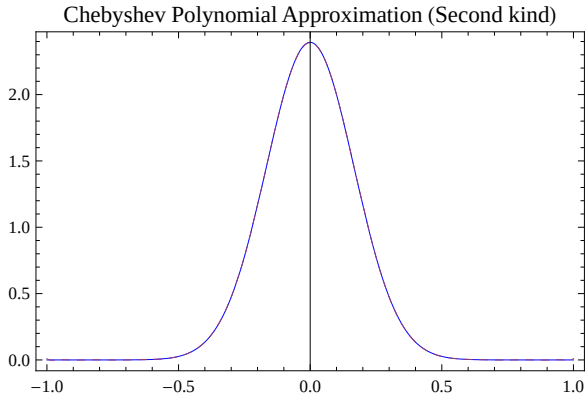

Figure 4.115: Chebyshev polynomial (second kind) approximation of the charge density for $n = 20$ and fifteen million points.

From Figures 4.110 to 4.115, Chebyshev polynomials (second kind) do a very nice job at approximating a Gaussian distribution, just the like Legendre polynomials and the first kind of Chebyshev polynomials. The numerical difference between the curves will give a better answer to what order and/or number of particles gives a better approximation. (See Figures 4.116 to 4.120.)

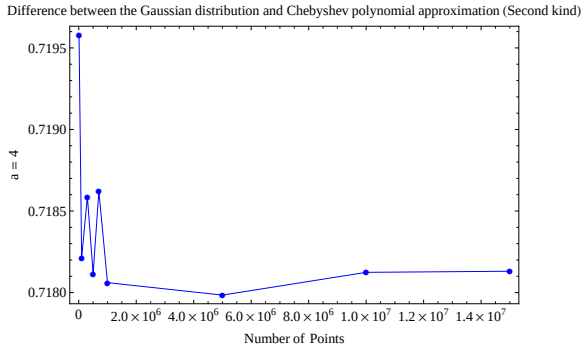

Figure 4.116: Error for a Gaussian Chebyshev polynomial approximation (Second kind) for $n = 4$.

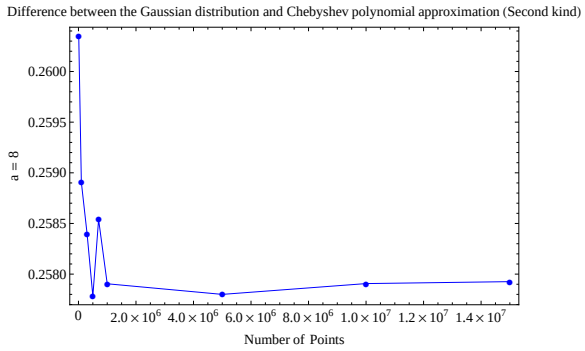

Figure 4.117: Error for a Gaussian Chebyshev polynomial approximation (Second kind) for $n = 8$.

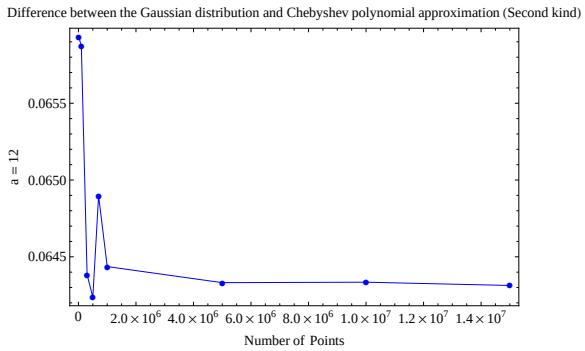

Figure 4.118: Error for a Gaussian Chebyshev polynomial approximation (Second kind) for $n = 12$.

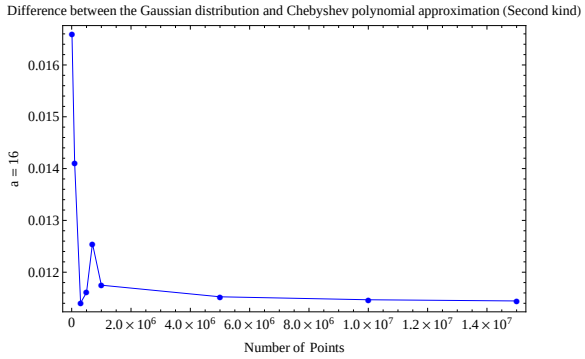

Figure 4.119: Error for a Gaussian Chebyshev polynomial approximation (Second kind) for $n = 16$.

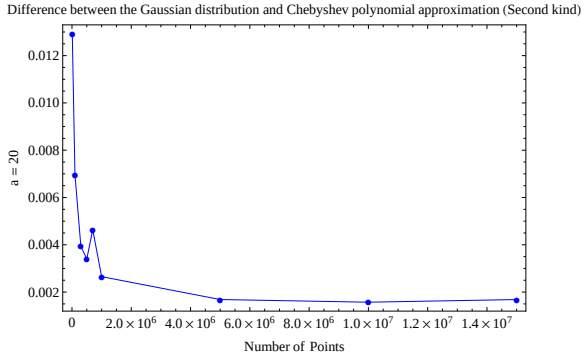

Figure 4.120: Error for a Gaussian Chebyshev polynomial approximation (Second kind) for $n = 20$.

The second kind of Chebyshev polynomials also give a difference pattern that is consistent with the other polynomials. It shows major decreases as n increases and stability after five million particles.

4.2 Uniform Distribution

With a constant probability, the uniform distribution is described by equation (4.9) with H as the Heavyside step function and in Mathematica by the $UniformDistribution[a, b]$ command .

$$P(x) = \frac{H(x-a) - H(x-b)}{b-a} \tag{4.9}$$

To keep the distribution with a maximum of $P(x) = 1$, the coefficients a and b were set to -0.5 and 0.5 respectively. To keep with consistency, the coefficients were calculated up to $n = 20$ with a number of particles ranging from ten thousand to one-million in ten thousand increments and from one million to fifteen million in one million increments. The next sections, containing Figures 4.121 to 4.243, illustrate these calculations.

4.2.1 Legendre Polynomials

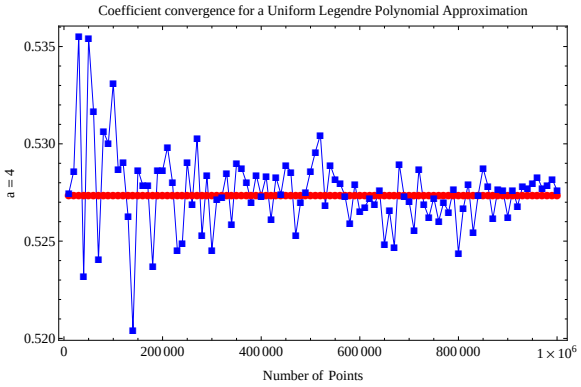

Figure 4.121: Convergence for a Uniform Legendre polynomial approximation for $n = 4$.

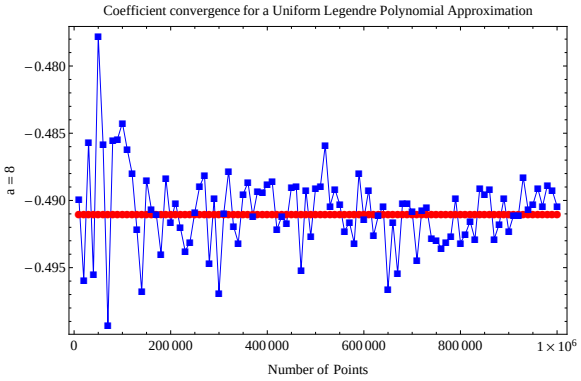

Figure 4.122: Convergence for a Uniform Legendre polynomial approximation for $n = 8$.

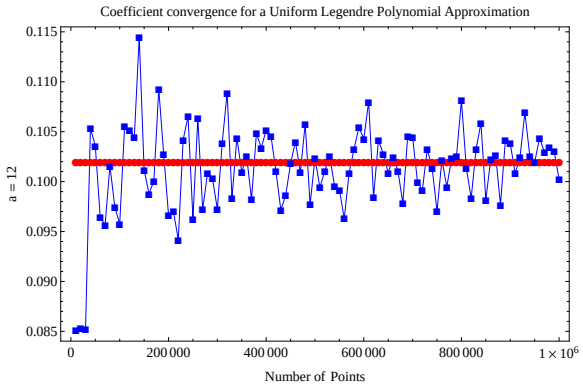

Figure 4.123: Convergence for a Uniform Legendre polynomial approximation for $n = 12$.

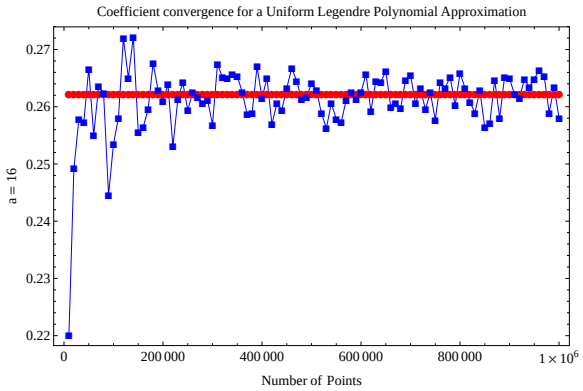

Figure 4.124: Convergence for a Uniform Legendre polynomial approximation for $n = 16$.

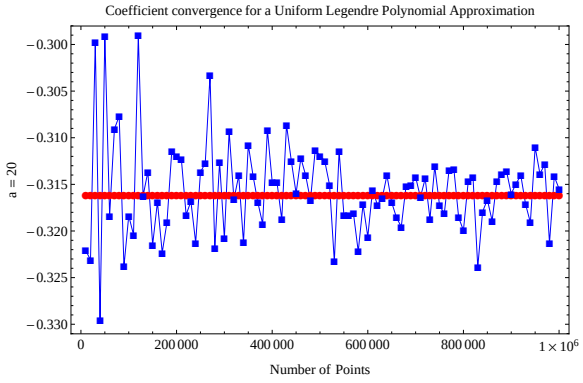

Figure 4.125: Convergence for a Uniform Legendre polynomial approximation for $n = 20$.

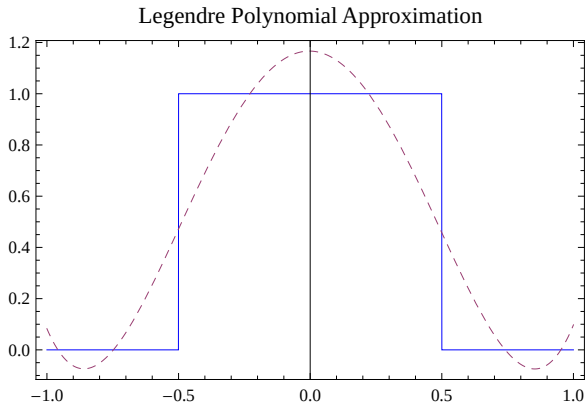

Figure 4.126: Uniform Legendre polynomial approximation for $n = 4$ and ten thousand particles.

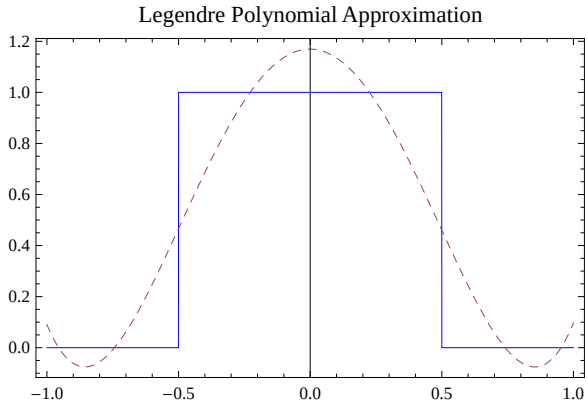

Figure 4.127: Uniform Legendre polynomial approximation for $n = 4$ and one hundred thousand particles.

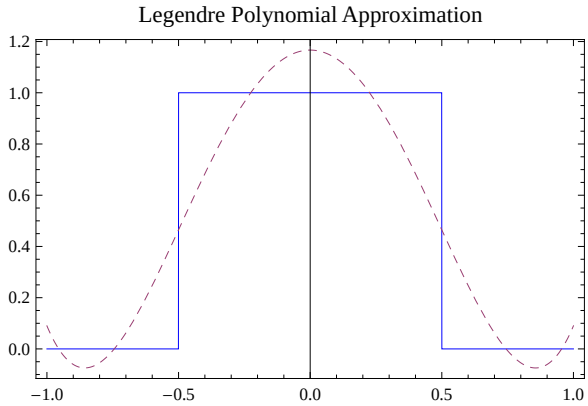

Figure 4.128: Uniform Legendre polynomial approximation for $n = 4$ and one million particles.

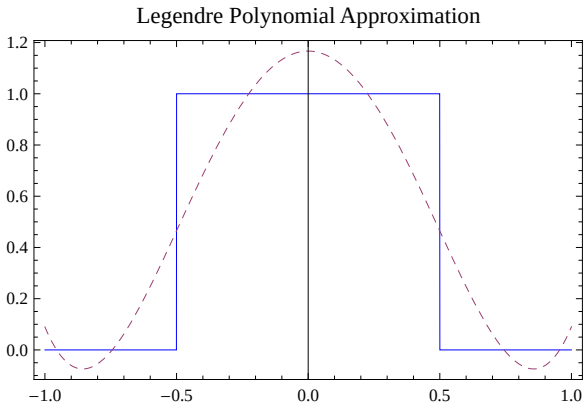

Figure 4.129: Uniform Legendre polynomial approximation for $n = 4$ and five million particles.

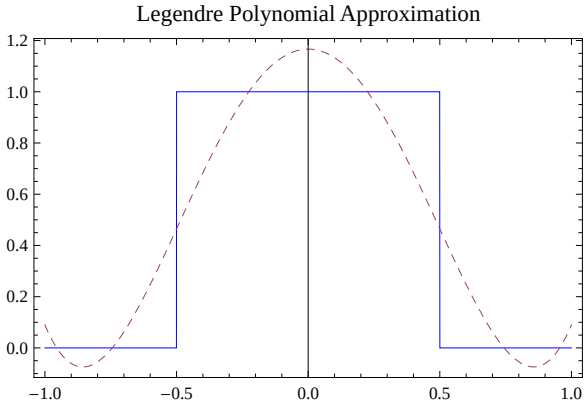

Figure 4.130: Uniform Legendre polynomial approximation for $n = 4$ and ten million particles.

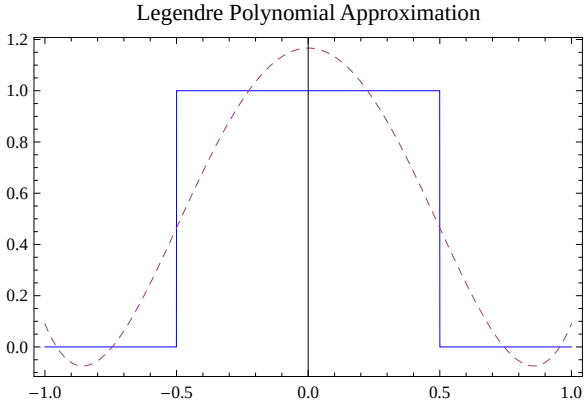

Figure 4.131: Uniform Legendre polynomial approximation for $n = 4$ and fifteen million particles.

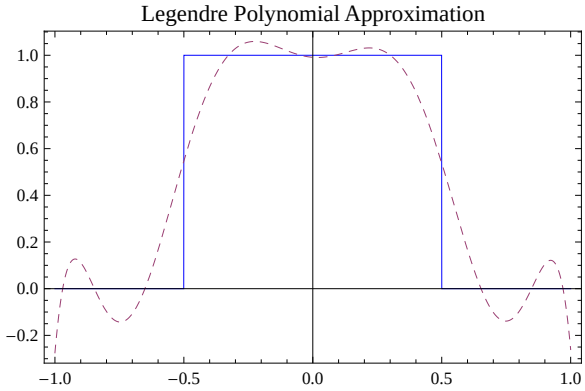

Figure 4.132: Uniform Legendre polynomial approximation for $n = 8$ and ten thousand particles.

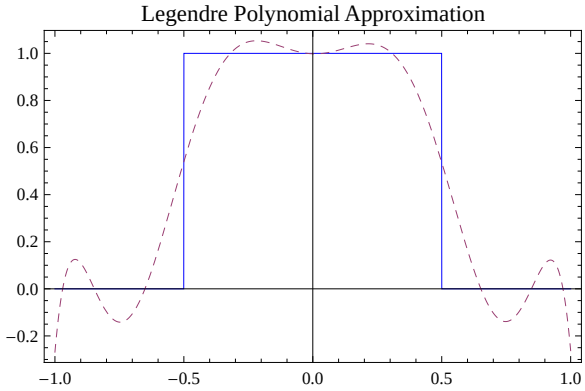

Figure 4.133: Uniform Legendre polynomial approximation for $n = 8$ and one hundred thousand particles.

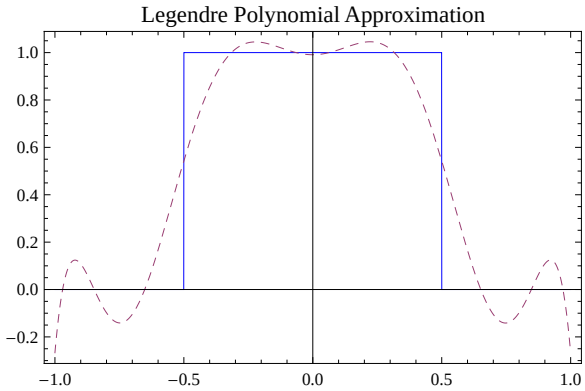

Figure 4.134: Uniform Legendre polynomial approximation for $n = 8$ and one million particles.

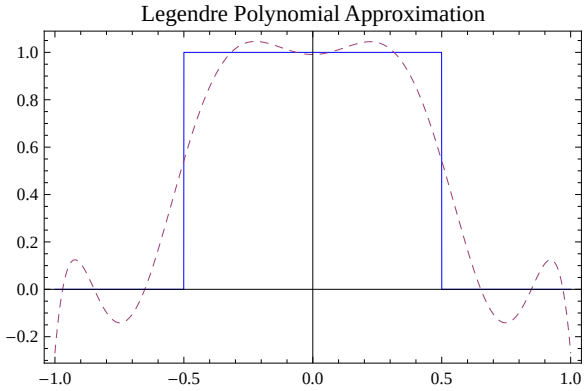

Figure 4.135: Uniform Legendre polynomial approximation for $n = 8$ and five million particles.

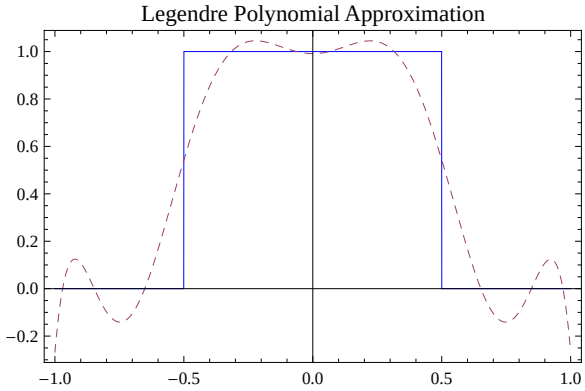

Figure 4.136: Uniform Legendre polynomial approximation for $n = 8$ and ten million particles.

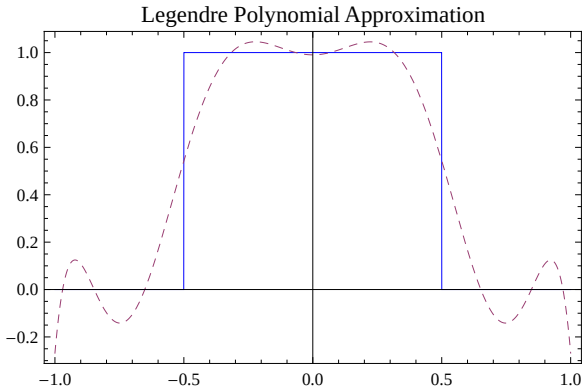

Figure 4.137: Uniform Legendre polynomial approximation for $n = 8$ and fifteen million particles.

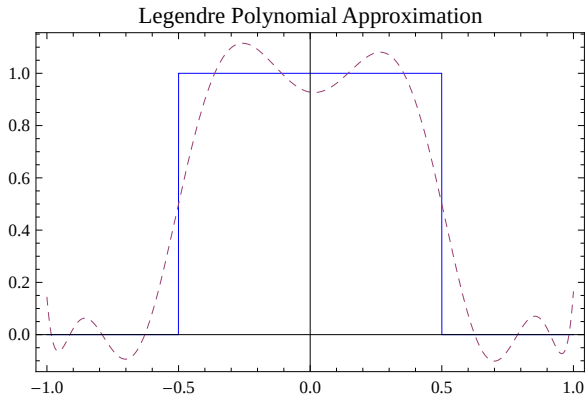

Figure 4.138: Uniform Legendre polynomial approximation for $n = 12$ and ten thousand particles.

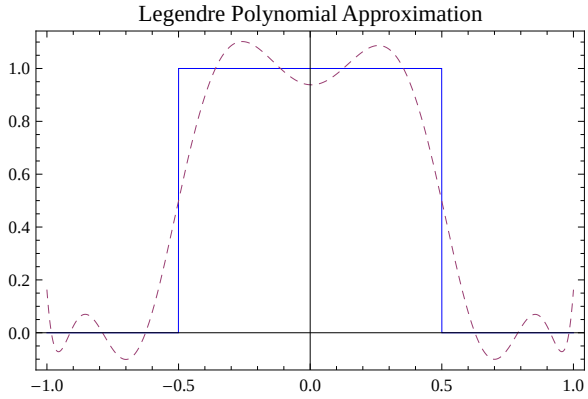

Figure 4.139: Uniform Legendre polynomial approximation for $n = 12$ and one hundred thousand particles.

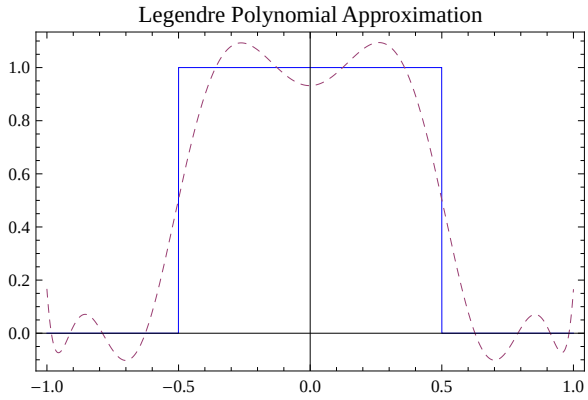

Figure 4.140: Uniform Legendre polynomial approximation for $n = 12$ and one million particles.

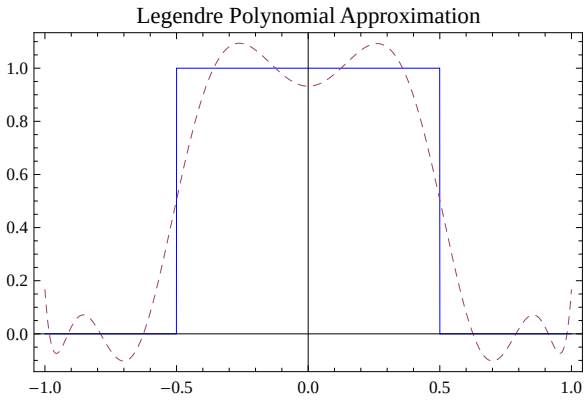

Figure 4.141: Uniform Legendre polynomial approximation for $n = 12$ and five million particles.

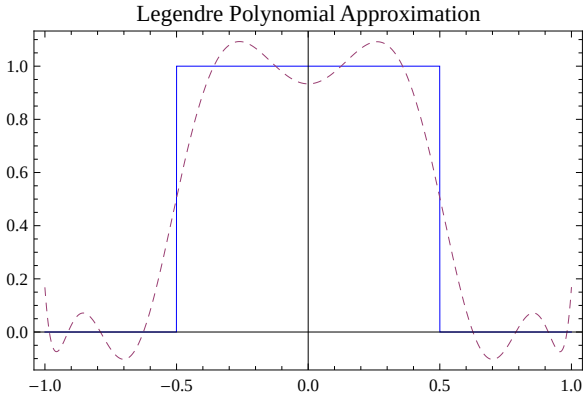

Figure 4.142: Uniform Legendre polynomial approximation for $n = 12$ and ten million particles.

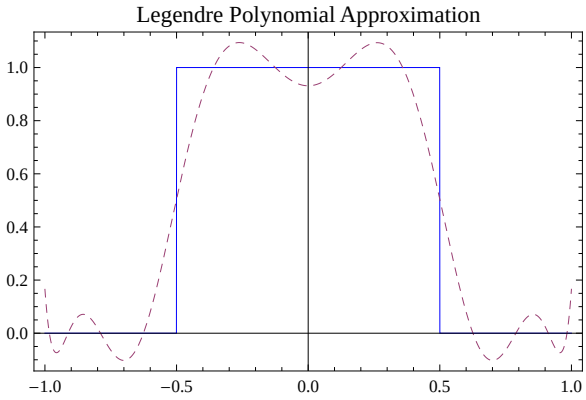

Figure 4.143: Uniform Legendre polynomial approximation for $n = 12$ and fifteen million particles.

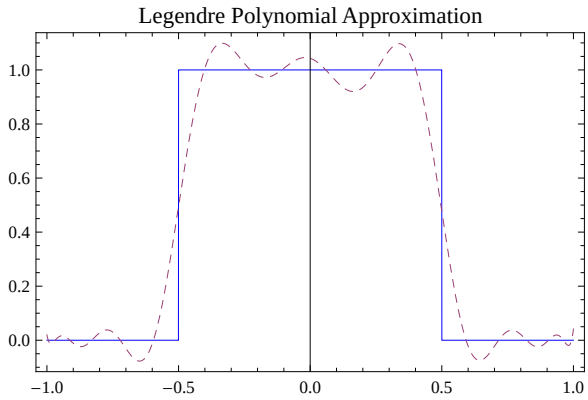

Figure 4.144: Uniform Legendre polynomial approximation for $n = 16$ and ten thousand particles.

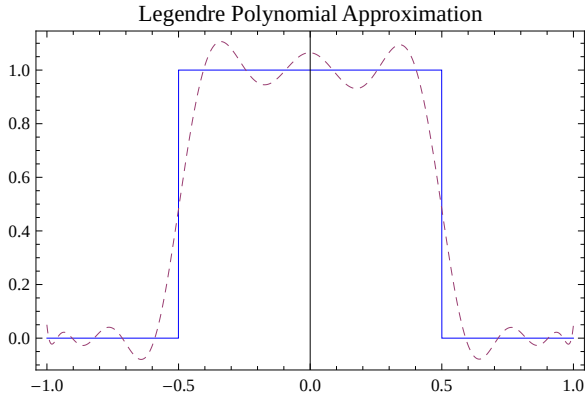

Figure 4.145: Uniform Legendre polynomial approximation for $n = 16$ and one hundred thousand particles.

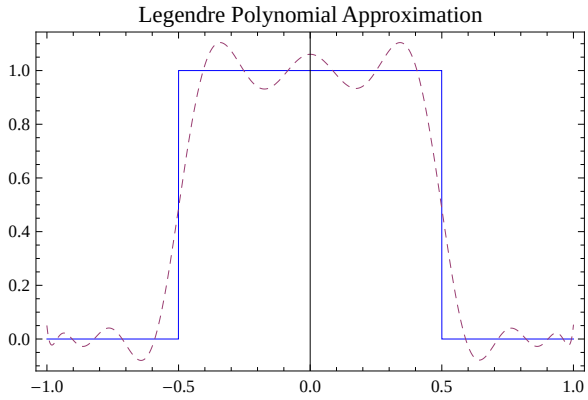

Figure 4.146: Uniform Legendre polynomial approximation for $n = 16$ and one million particles.

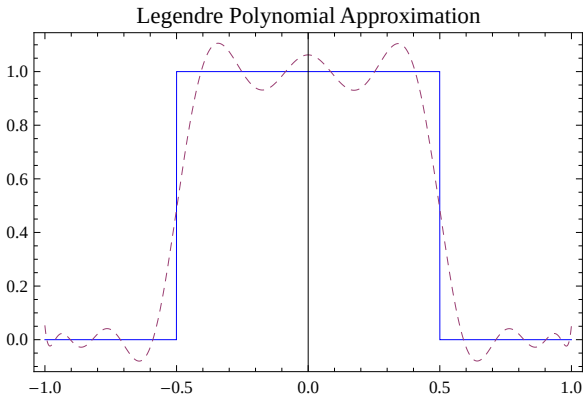

Figure 4.147: Uniform Legendre polynomial approximation for $n = 16$ and five million particles.

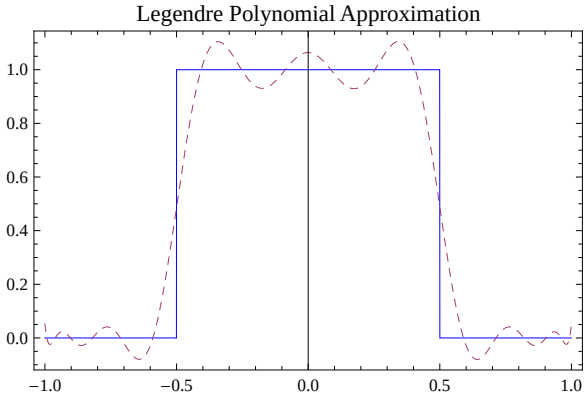

Figure 4.148: Uniform Legendre polynomial approximation for $n = 16$ and ten million particles.

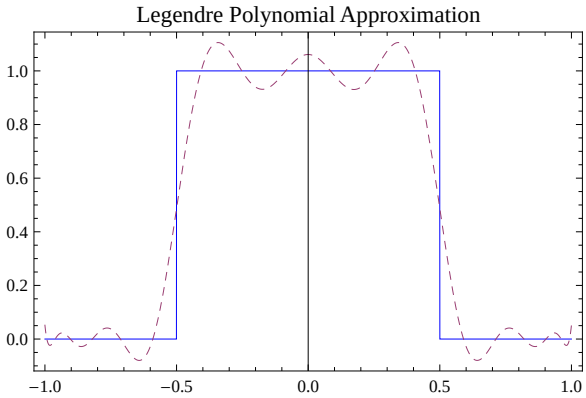

Figure 4.149: Uniform Legendre polynomial approximation for $n = 16$ and fifteen million particles.

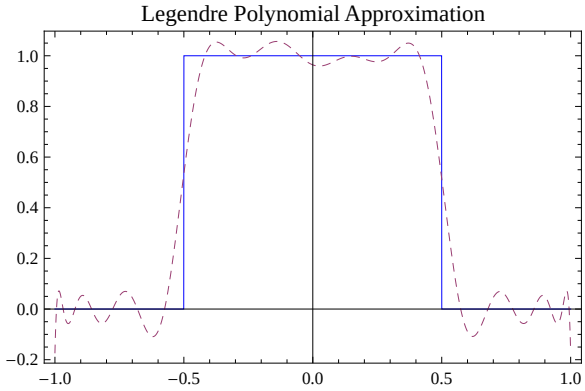

Figure 4.150: Uniform Legendre polynomial approximation for $n = 20$ and ten thousand particles.

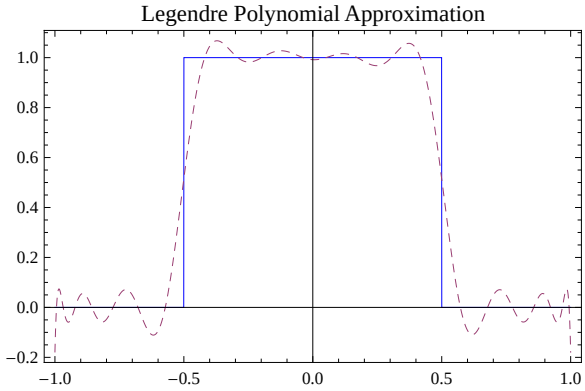

Figure 4.151: Uniform Legendre polynomial approximation for $n = 20$ and one hundred thousand particles.

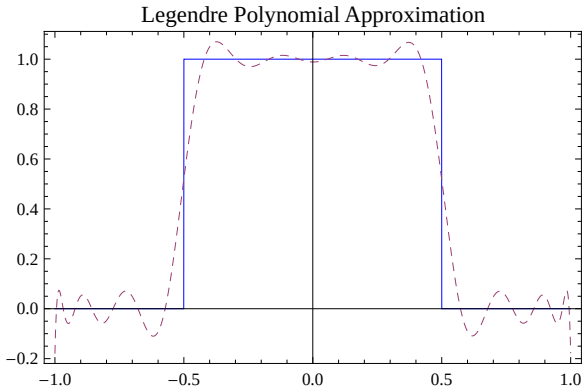

Figure 4.152: Uniform Legendre polynomial approximation for $n = 20$ and one million particles.

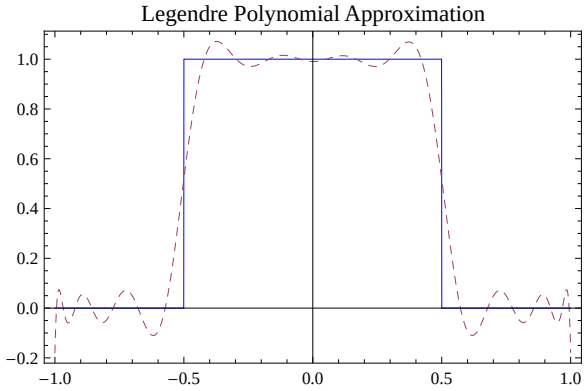

Figure 4.153: Uniform Legendre polynomial approximation for $n = 20$ and five million particles.

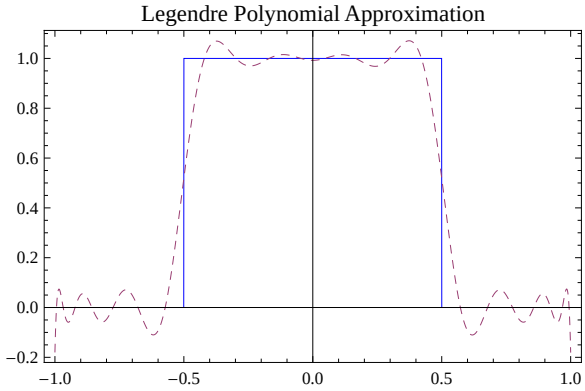

Figure 4.154: Uniform Legendre polynomial approximation for $n = 20$ and ten million particles.

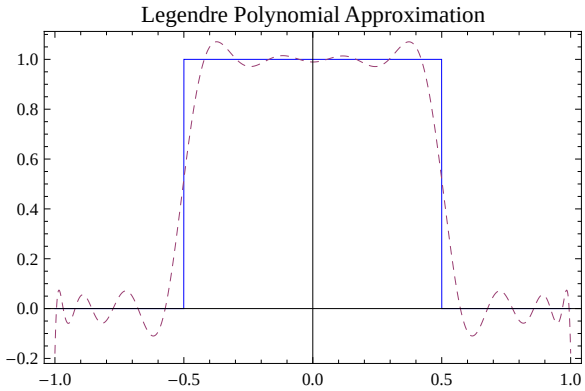

Figure 4.155: Uniform Legendre polynomial approximation for $n = 20$ and fifteen million particles.

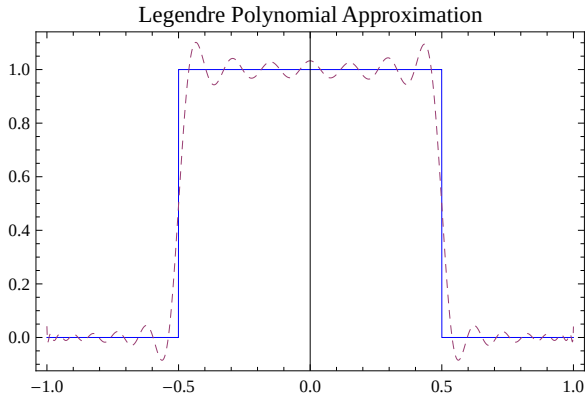

Figure 4.156: Uniform Legendre polynomial approximation for $n = 40$ and one million particles.

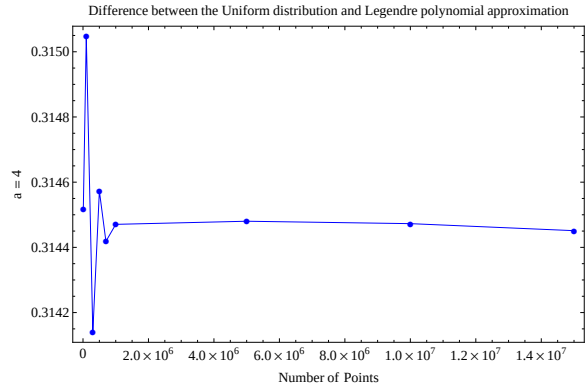

Figure 4.157: Difference between the Uniform distribution and the Legendre polynomial approximation for $n = 4$.

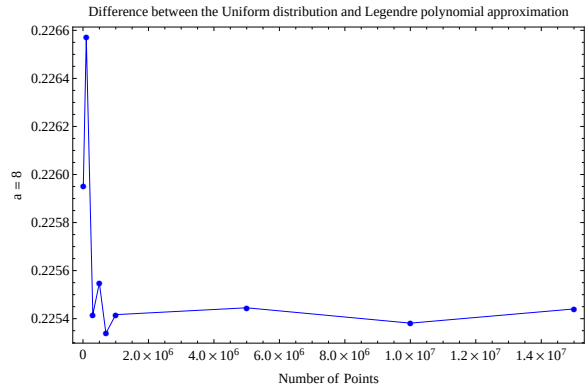

Figure 4.158: Difference between the Uniform distribution and the Legendre polynomial approximation for $n = 8$.

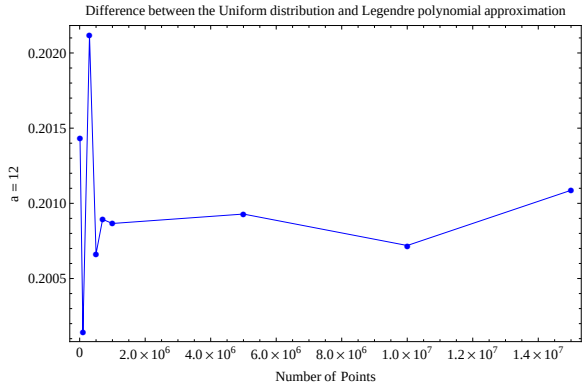

Figure 4.159: Difference between the Uniform distribution and the Legendre polynomial approximation for $n = 12$.

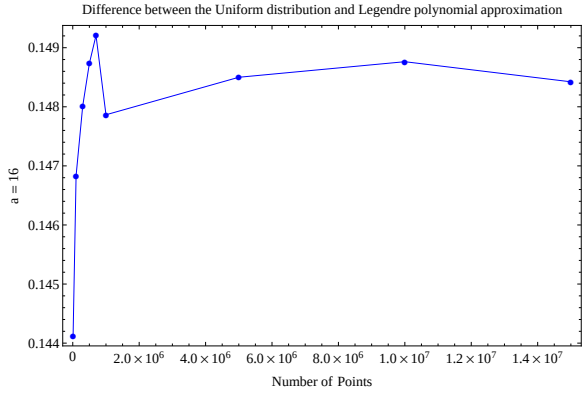

Figure 4.160: Difference between the Uniform distribution and the Legendre polynomial approximation for $n = 16$.

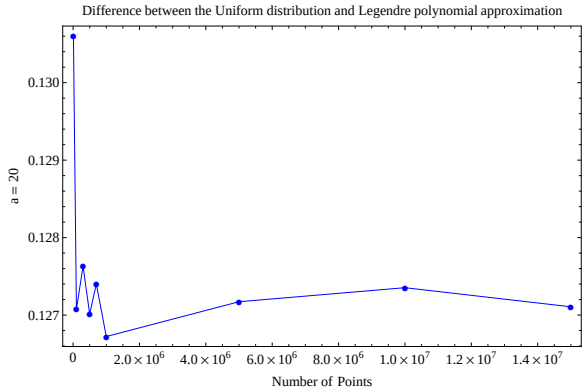

Figure 4.161: Difference between the Uniform distribution and the Legendre polynomial approximation for $n = 20$.

4.2.2 Chebyshev Polynomials of the first kind

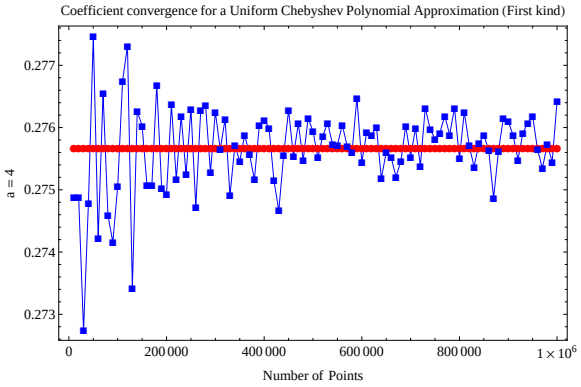

Figure 4.162: Convergence for a Uniform Chebyshev polynomial (first kind) approximation for $n = 4$.

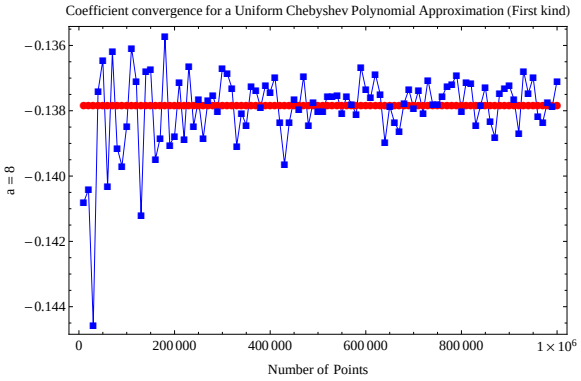

Figure 4.163: Convergence for a Uniform Chebyshev polynomial (first kind) approximation for $n = 8$.

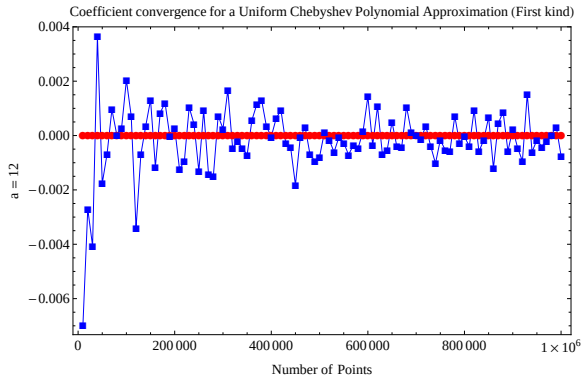

Figure 4.164: Convergence for a Uniform Chebyshev polynomial (first kind) approximation for $n = 12$.

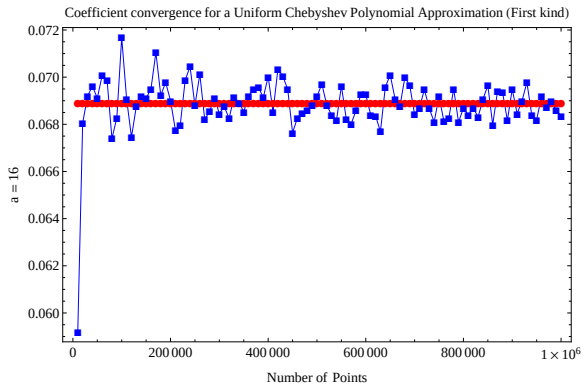

Figure 4.165: Convergence for a Uniform Chebyshev polynomial (first kind) approximation for $n = 16$.

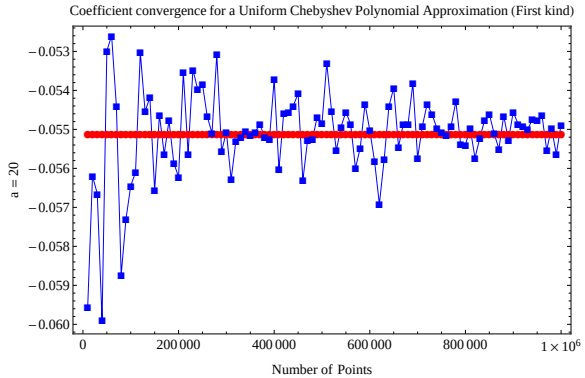

Figure 4.166: Convergence for a Uniform Chebyshev polynomial (first kind) approximation for $n = 20$.

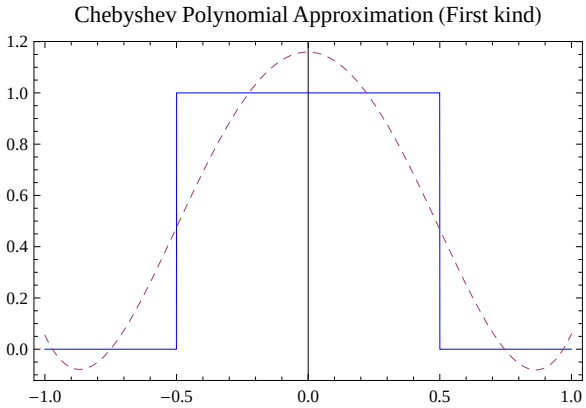

Figure 4.167: Uniform Chebyshev polynomial (first kind) approximation for $n = 4$ and ten thousand particles.

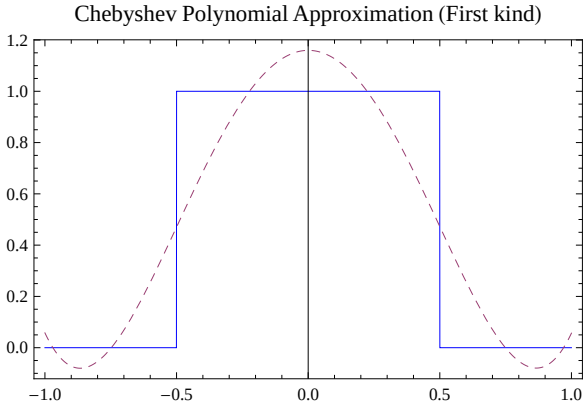

Figure 4.168: Uniform Chebyshev polynomial (first kind) approximation for $n = 4$ and one hundred thousand particles.

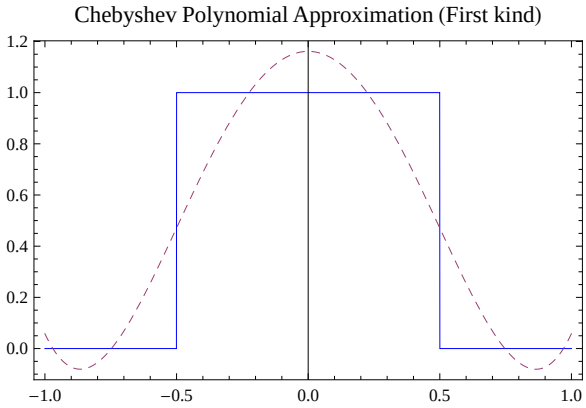

Figure 4.169: Uniform Chebyshev polynomial (first kind) approximation for $n = 4$ and one million particles.

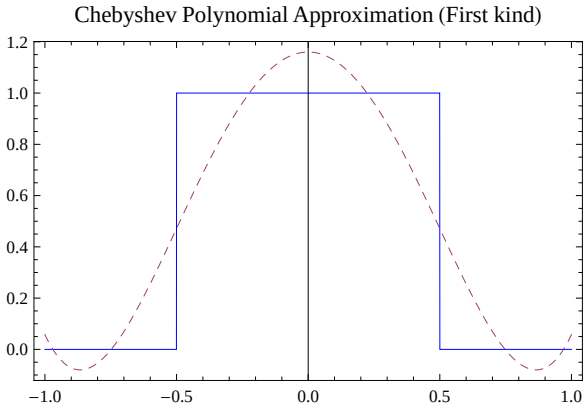

Figure 4.170: Uniform Chebyshev polynomial (first kind) approximation for $n = 4$ and five million particles.

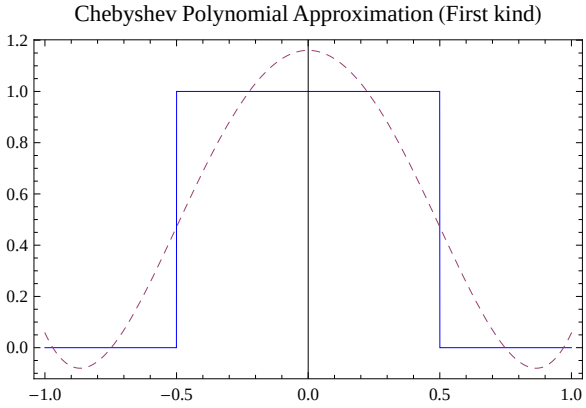

Figure 4.171: Uniform Chebyshev polynomial (first kind) approximation for $n = 4$ and ten million particles.

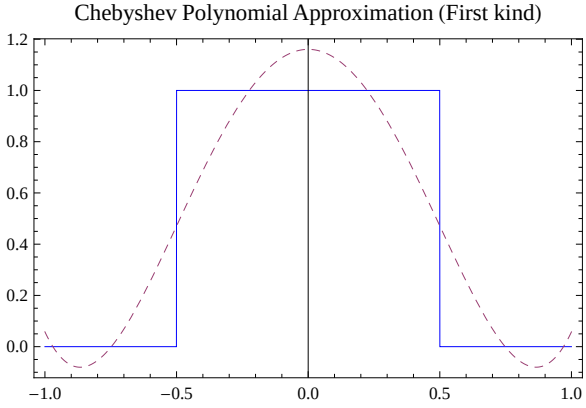

Figure 4.172: Uniform Chebyshev polynomial (first kind) approximation for $n = 4$ and fifteen million particles.

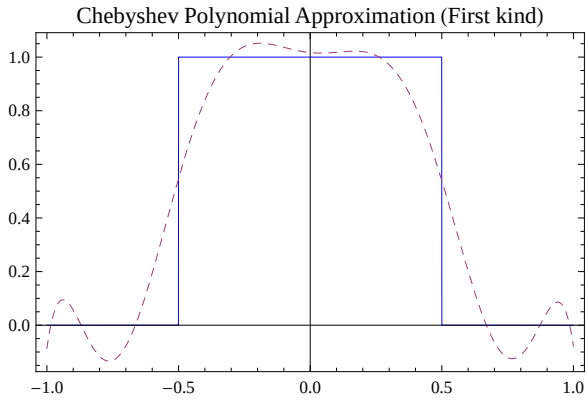

Figure 4.173: Uniform Chebyshev polynomial (first kind) approximation for $n = 8$ and ten thousand particles.

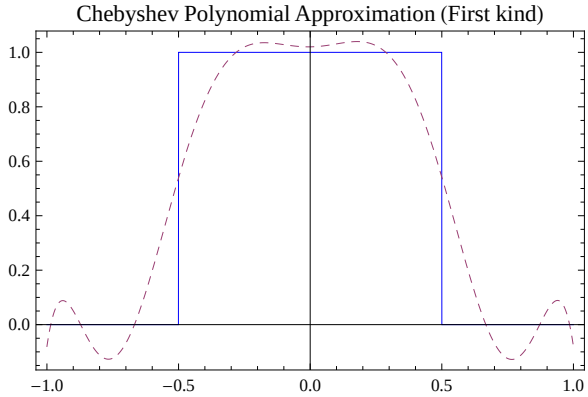

Figure 4.174: Uniform Chebyshev polynomial (first kind) approximation for $n = 8$ and one hundred thousand particles.

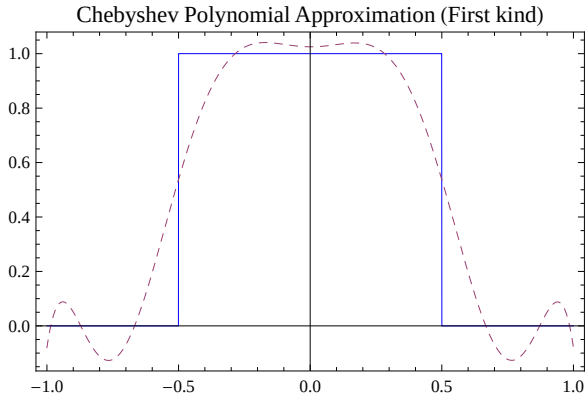

Figure 4.175: Uniform Chebyshev polynomial (first kind) approximation for $n = 8$ and one million particles.

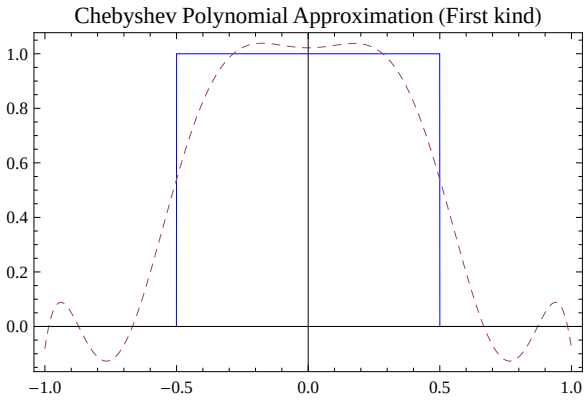

Figure 4.176: Uniform Chebyshev polynomial (first kind) approximation for $n = 8$ and five million particles.

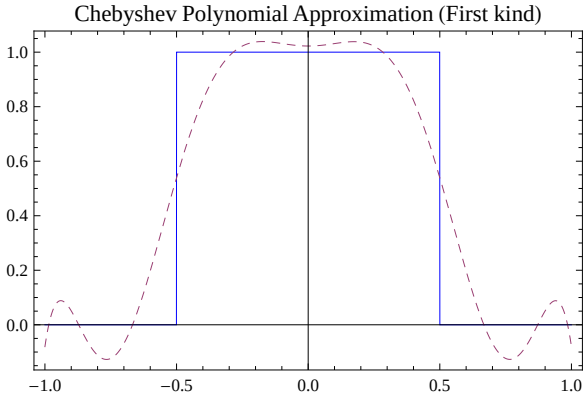

Figure 4.177: Uniform Chebyshev polynomial (first kind) approximation for $n = 8$ and ten million particles.

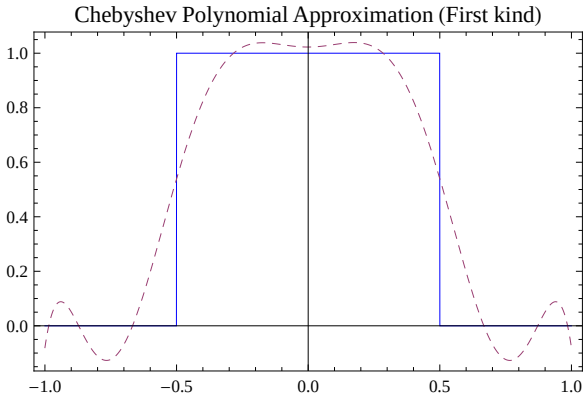

Figure 4.178: Uniform Chebyshev polynomial (first kind) approximation for $n = 8$ and fifteen million particles.

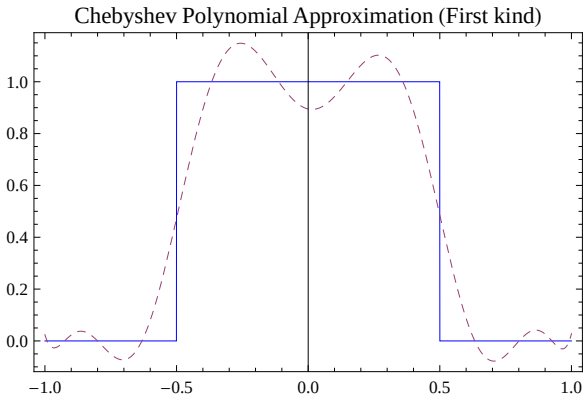

Figure 4.179: Uniform Chebyshev polynomial (first kind) approximation for $n = 12$ and ten thousand particles.

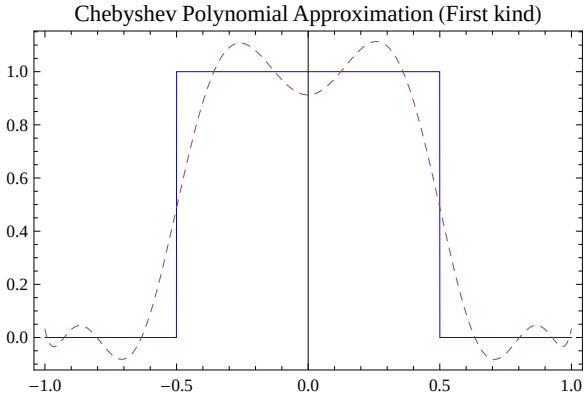

Figure 4.180: Uniform Chebyshev polynomial (first kind) approximation for $n = 12$ and one hundred thousand particles.

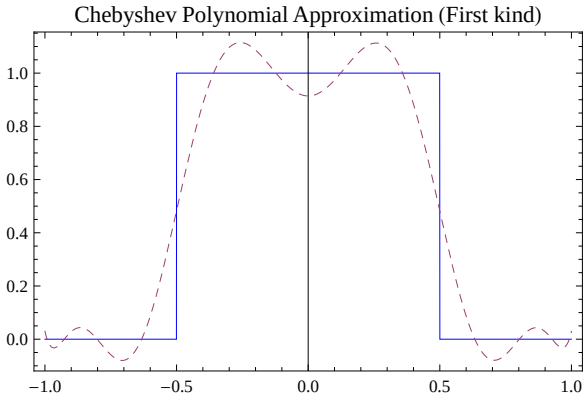

Figure 4.181: Uniform Chebyshev polynomial (first kind) approximation for $n = 12$ and one million particles.

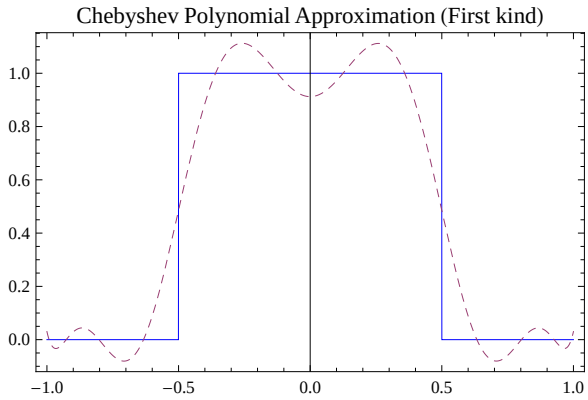

Figure 4.182: Uniform Chebyshev polynomial (first kind) approximation for $n = 12$ and five million particles.

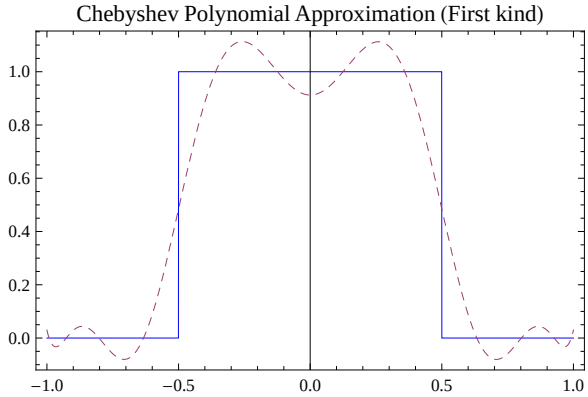

Figure 4.183: Uniform Chebyshev polynomial (first kind) approximation for $n = 12$ and ten million particles.

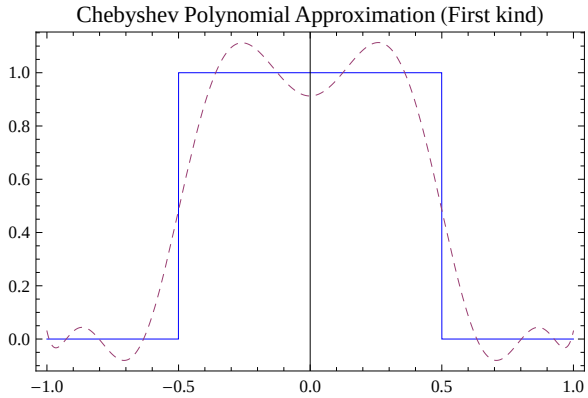

Figure 4.184: Uniform Chebyshev polynomial (first kind) approximation for $n = 12$ and fifteen million particles.

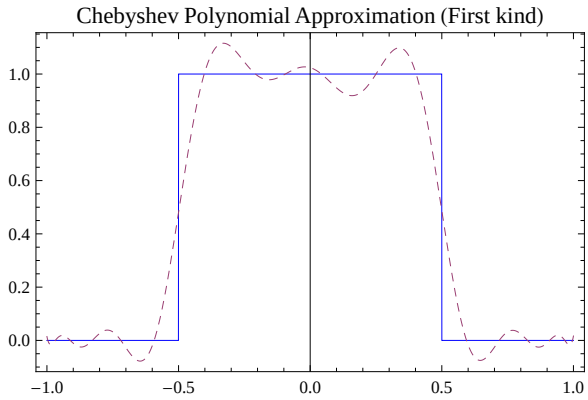

Figure 4.185: Uniform Chebyshev polynomial (first kind) approximation for $n = 16$ and ten thousand particles.

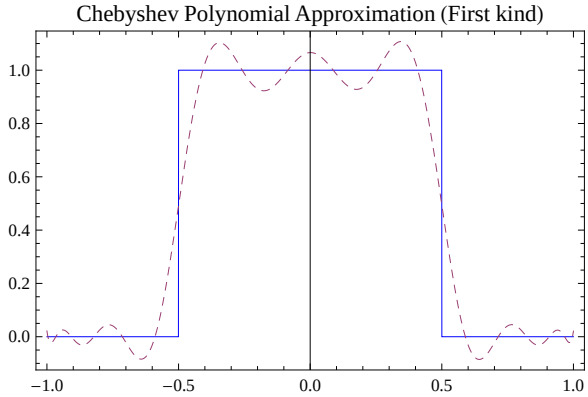

Figure 4.186: Uniform Chebyshev polynomial (first kind) approximation for $n = 16$ and one hundred thousand particles.

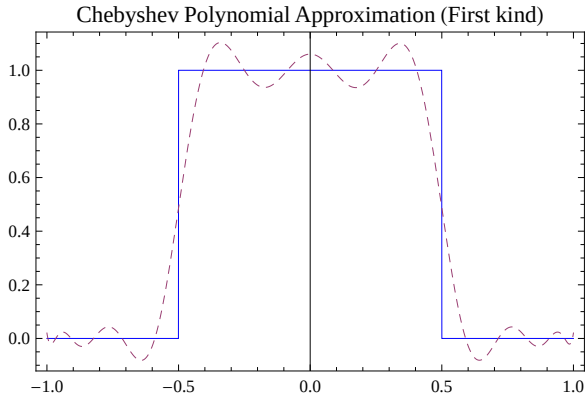

Figure 4.187: Uniform Chebyshev polynomial (first kind) approximation for $n = 16$ and one million particles.

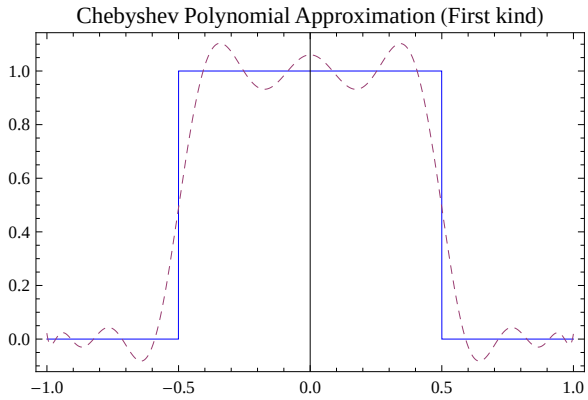

Figure 4.188: Uniform Chebyshev polynomial (first kind) approximation for $n = 16$ and five million particles.

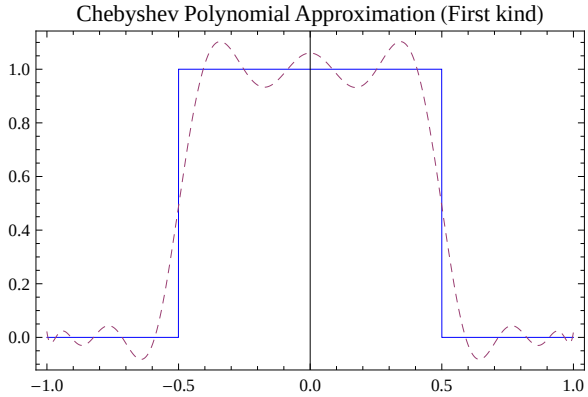

Figure 4.189: Uniform Chebyshev polynomial (first kind) approximation for $n = 16$ and ten million particles.

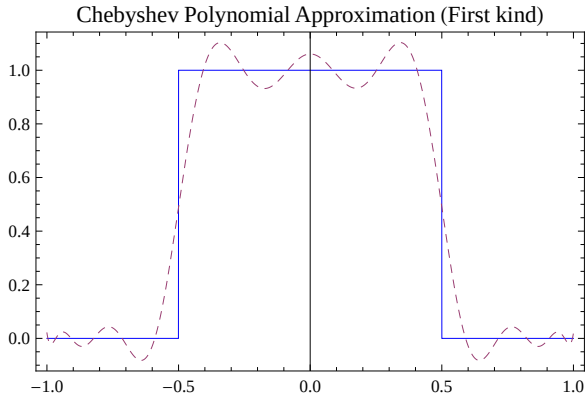

Figure 4.190: Uniform Chebyshev polynomial (first kind) approximation for $n = 16$ and fifteen million particles.

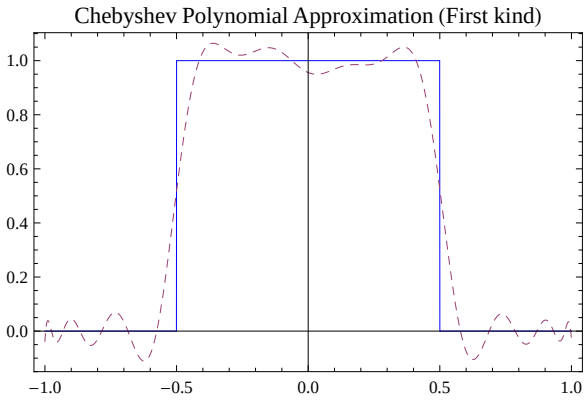

Figure 4.191: Uniform Chebyshev polynomial (first kind) approximation for $n = 20$ and ten thousand particles.

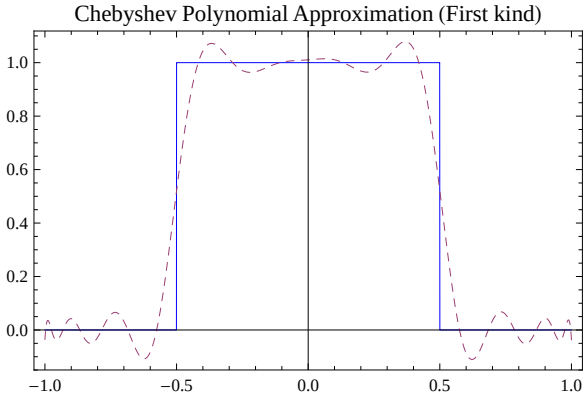

Figure 4.192: Uniform Chebyshev polynomial (first kind) approximation for $n = 20$ and one hundred thousand particles.

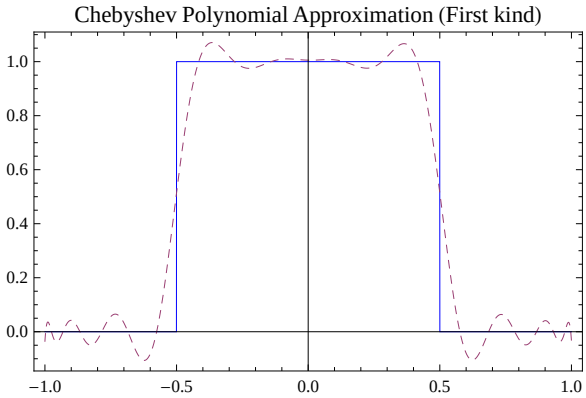

Figure 4.193: Uniform Chebyshev polynomial (first kind) approximation for $n = 20$ and one million particles.

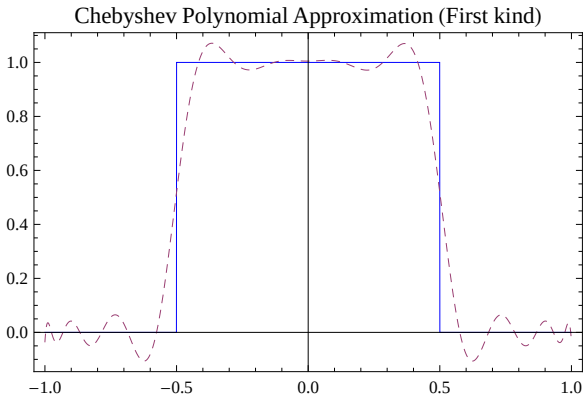

Figure 4.194: Uniform Chebyshev polynomial (first kind) approximation for $n = 20$ and five million particles.

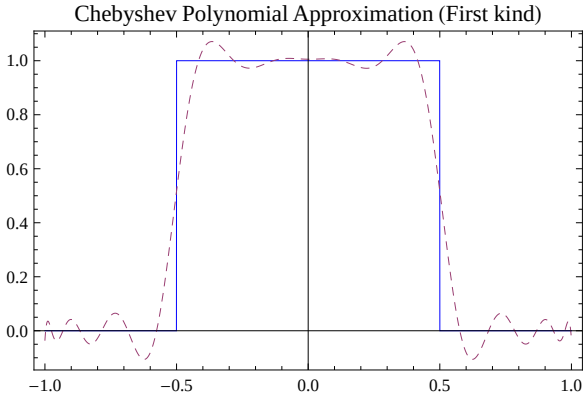

Figure 4.195: Uniform Chebyshev polynomial (first kind) approximation for $n = 20$ and ten million particles.

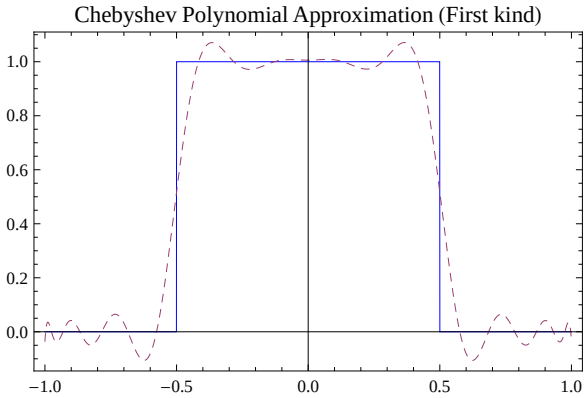

Figure 4.196: Uniform Chebyshev polynomial (first kind) approximation for $n = 20$ and fifteen million particles.

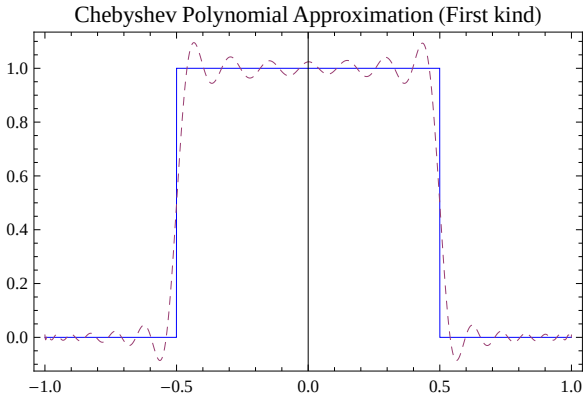

Figure 4.197: Uniform Chebyshev polynomial (first kind) approximation for $n = 40$ and fifteen million particles.

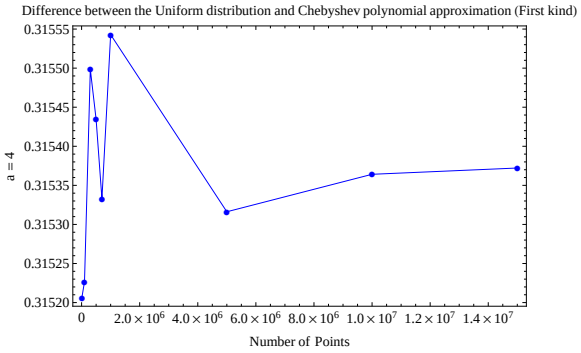

Figure 4.198: Difference between the Uniform distribution and the Chebyshev polynomial (first kind) approximation for $n = 4$.

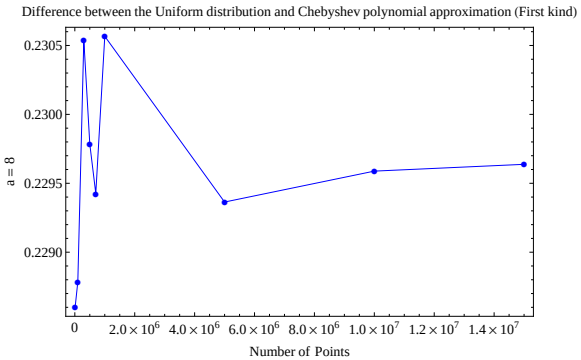

Figure 4.199: Difference between the Uniform distribution and the Chebyshev polynomial (first kind) approximation for $n = 8$.

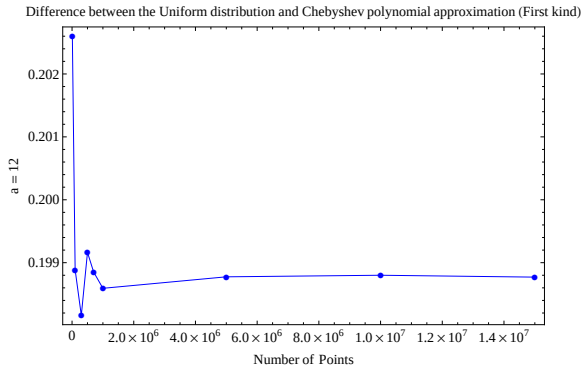

Figure 4.200: Difference between the Uniform distribution and the Chebyshev polynomial (first kind) approximation for $n = 12$.

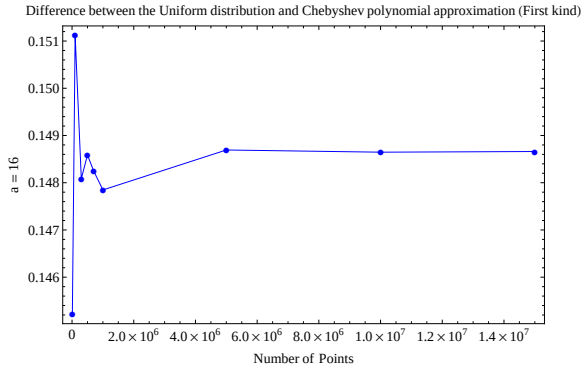

Figure 4.201: Difference between the Uniform distribution and the Chebyshev polynomial (first kind) approximation for $n = 16$.

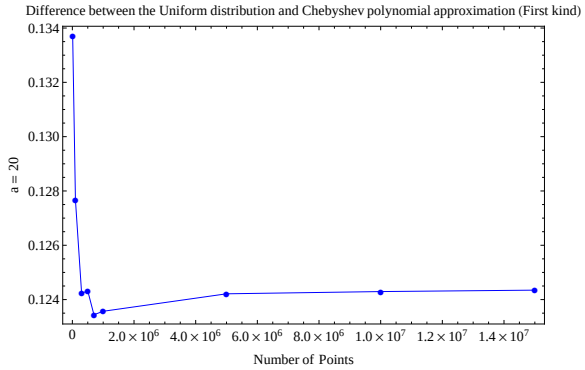

Figure 4.202: Difference between the Uniform distribution and the Chebyshev polynomial (first kind) approximation for $n = 20$.

4.2.3 Chebyshev Polynomials of the second kind

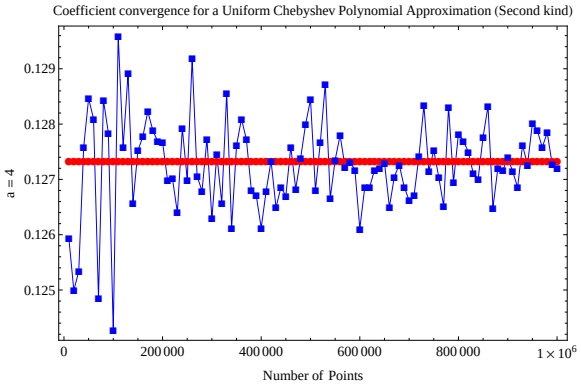

Figure 4.203: Convergence for a Uniform Chebyshev polynomial (second kind) approximation for $n = 4$.

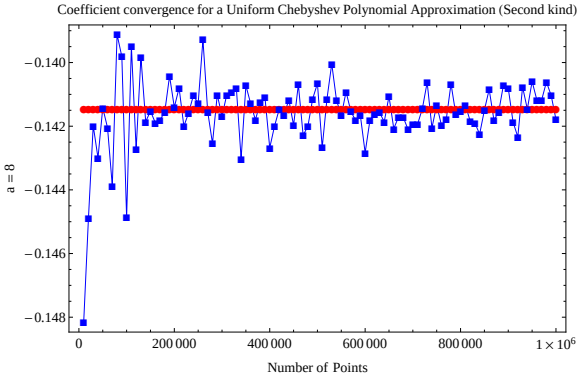

Figure 4.204: Convergence for a Uniform Chebyshev polynomial (second kind) approximation for $n = 8$.

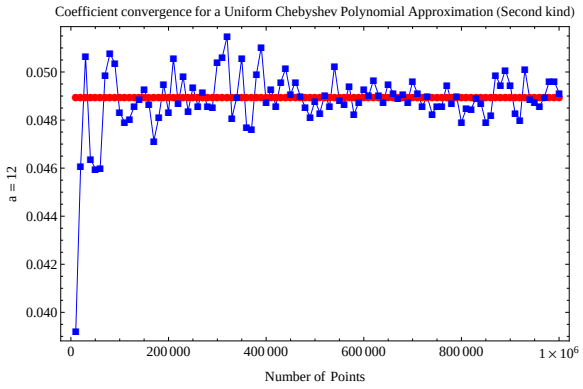

Figure 4.205: Convergence for a Uniform Chebyshev polynomial (second kind) approximation for $n = 12$.

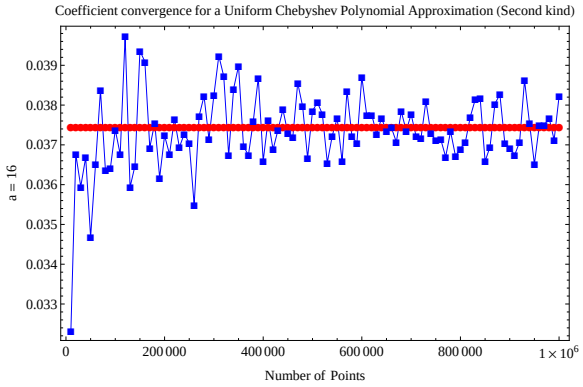

Figure 4.206: Convergence for a Uniform Chebyshev polynomial (second kind) approximation for $n = 16$.

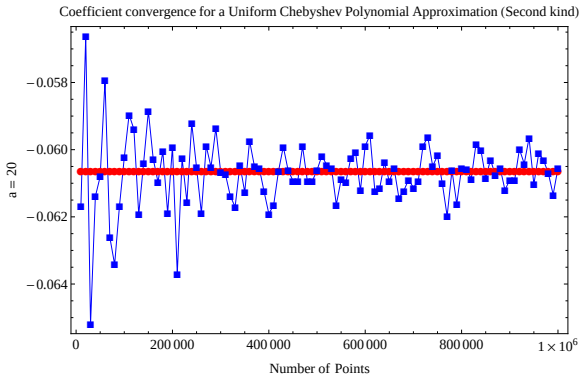

Figure 4.207: Convergence for a Uniform Chebyshev polynomial (second kind) approximation for $n = 20$.

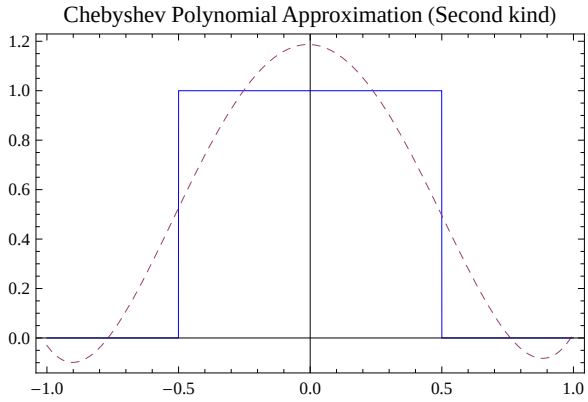

Figure 4.208: Uniform Chebyshev polynomial (second kind) approximation for $n = 4$ and ten thousand particles.

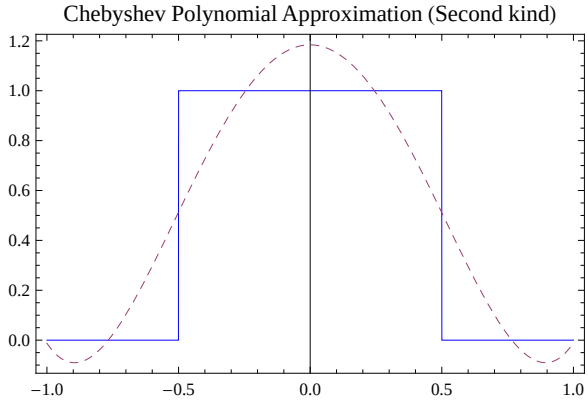

Figure 4.209: Uniform Chebyshev polynomial (second kind) approximation for $n = 4$ and one hundred thousand particles.

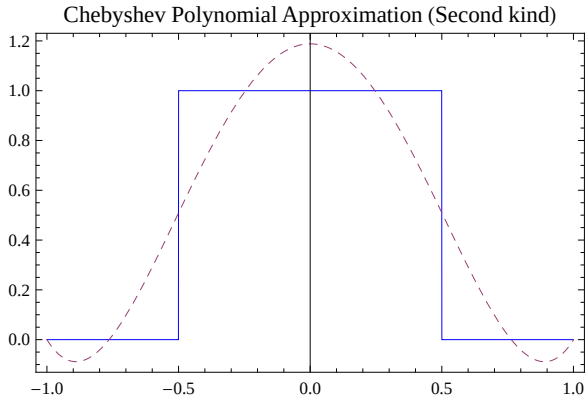

Figure 4.210: Uniform Chebyshev polynomial (second kind) approximation for $n = 4$ and one million particles.

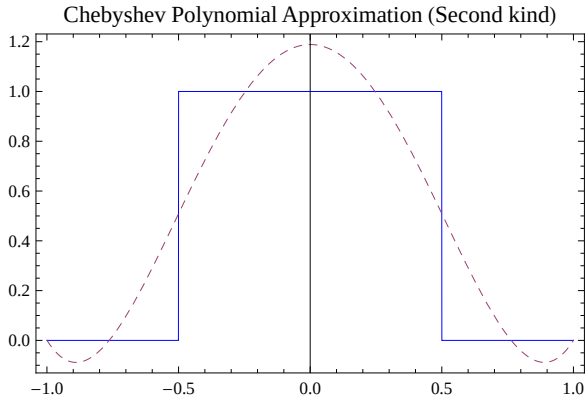

Figure 4.211: Uniform Chebyshev polynomial (second kind) approximation for $n = 4$ and five million particles.

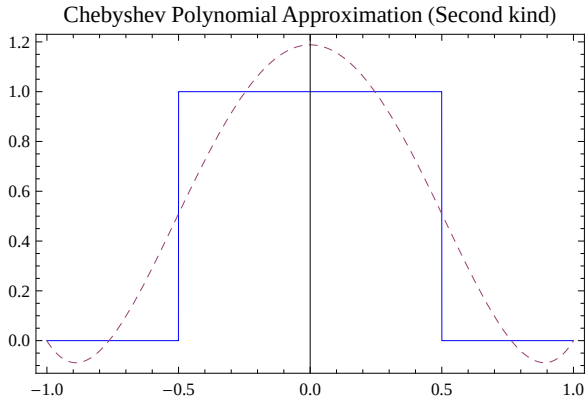

Figure 4.212: Uniform Chebyshev polynomial (second kind) approximation for $n = 4$ and ten million particles.

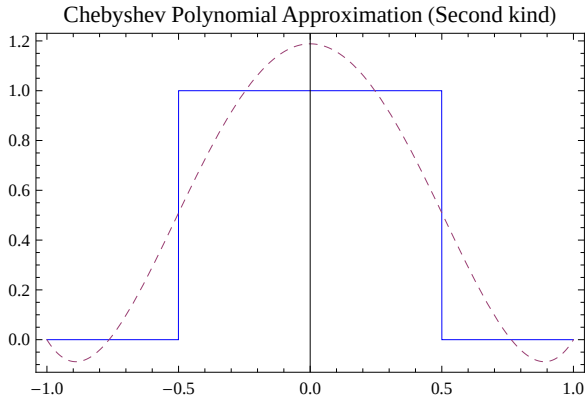

Figure 4.213: Uniform Chebyshev polynomial (second kind) approximation for $n = 4$ and fifteen million particles.

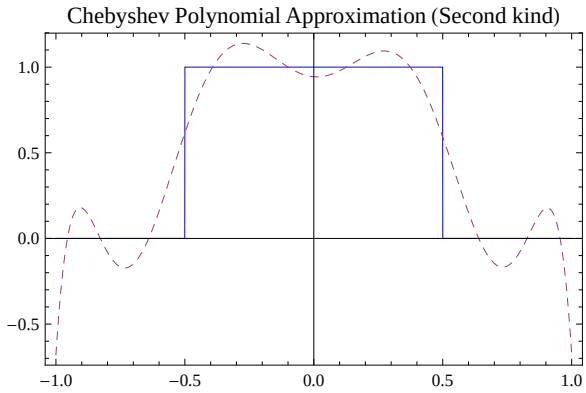

Figure 4.214: Uniform Chebyshev polynomial (second kind) approximation for $n = 8$ and ten thousand particles.

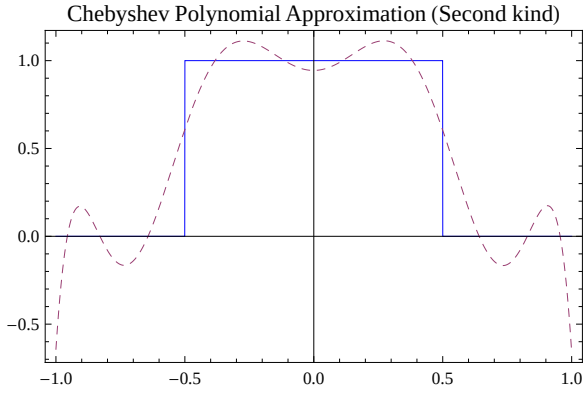

Figure 4.215: Uniform Chebyshev polynomial (second kind) approximation for $n = 8$ and one hundred thousand particles.

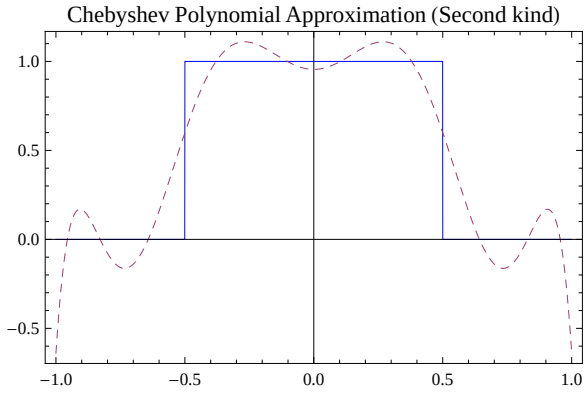

Figure 4.216: Uniform Chebyshev polynomial (second kind) approximation for $n = 8$ and one million particles.

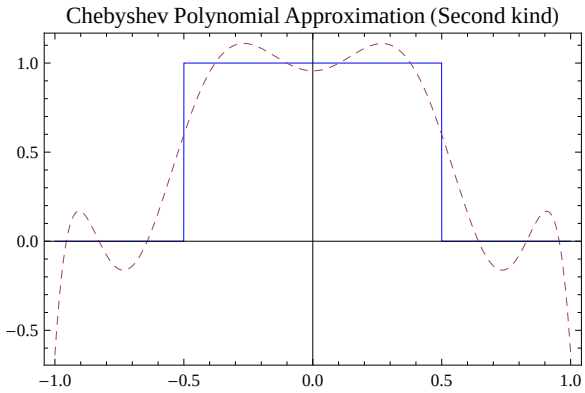

Figure 4.217: Uniform Chebyshev polynomial (second kind) approximation for $n = 8$ and five million particles.

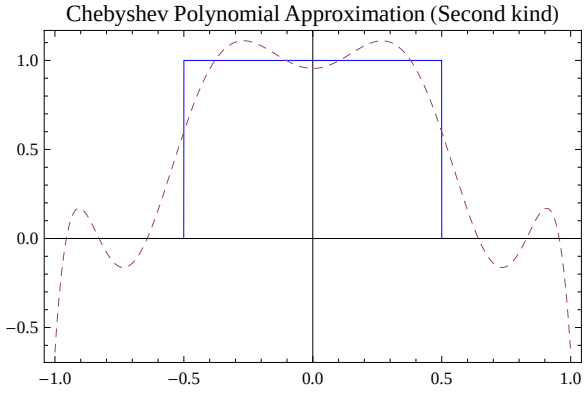

Figure 4.218: Uniform Chebyshev polynomial (second kind) approximation for $n = 8$ and ten million particles.

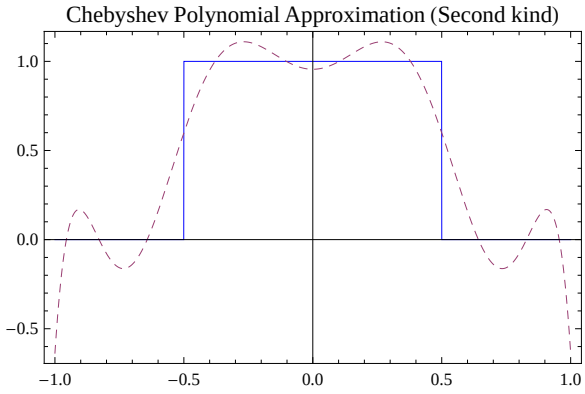

Figure 4.219: Uniform Chebyshev polynomial (second kind) approximation for $n = 8$ and fifteen million particles.

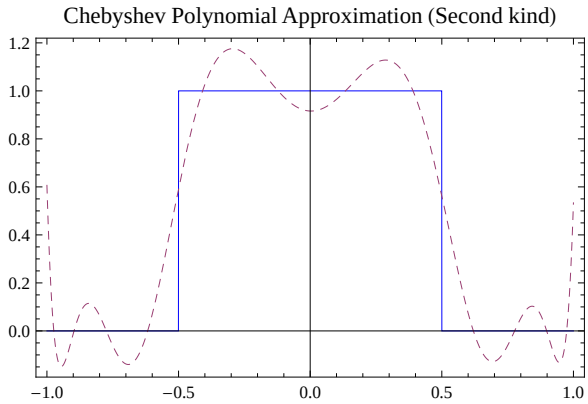

Figure 4.220: Uniform Chebyshev polynomial (second kind) approximation for $n = 12$ and ten thousand particles.

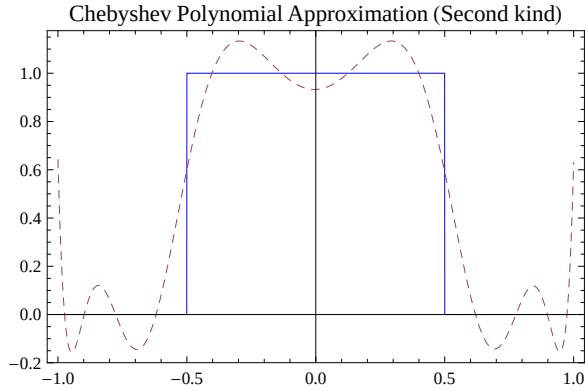

Figure 4.221: Uniform Chebyshev polynomial (second kind) approximation for $n = 12$ and one hundred thousand particles.

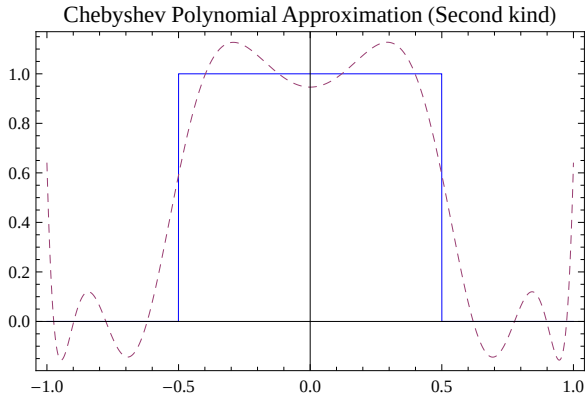

Figure 4.222: Uniform Chebyshev polynomial (second kind) approximation for $n = 12$ and one million particles.

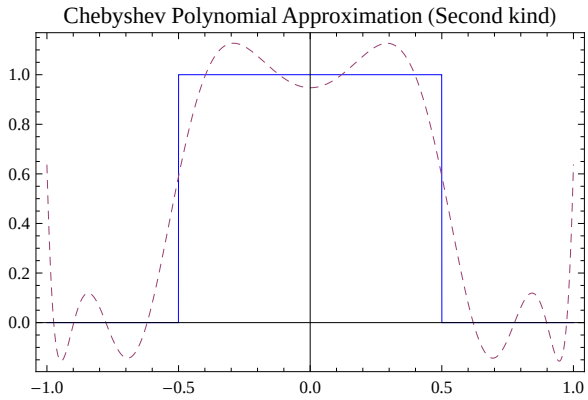

Figure 4.223: Uniform Chebyshev polynomial (second kind) approximation for $n = 12$ and five million particles.

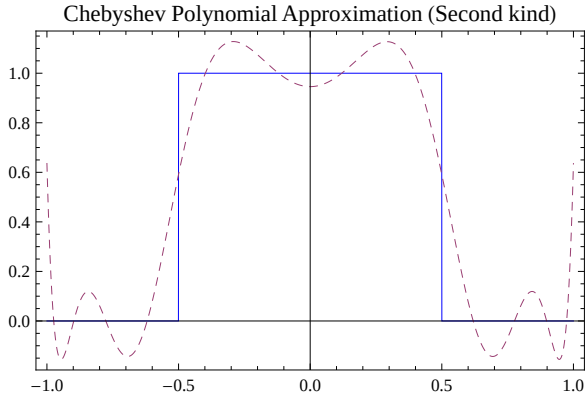

Figure 4.224: Uniform Chebyshev polynomial (second kind) approximation for $n = 12$ and ten million particles.

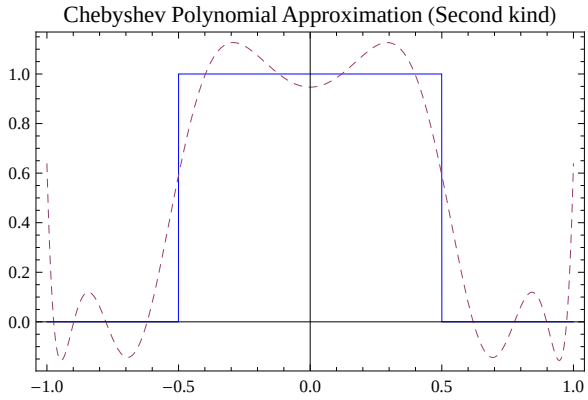

Figure 4.225: Uniform Chebyshev polynomial (second kind) approximation for $n = 12$ and fifteen million particles.

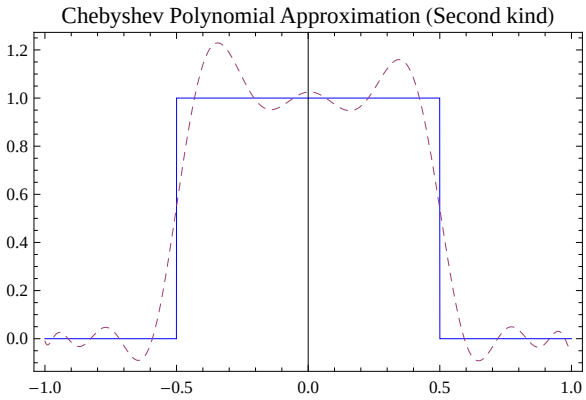

Figure 4.226: Uniform Chebyshev polynomial (second kind) approximation for $n = 16$ and ten thousand particles.

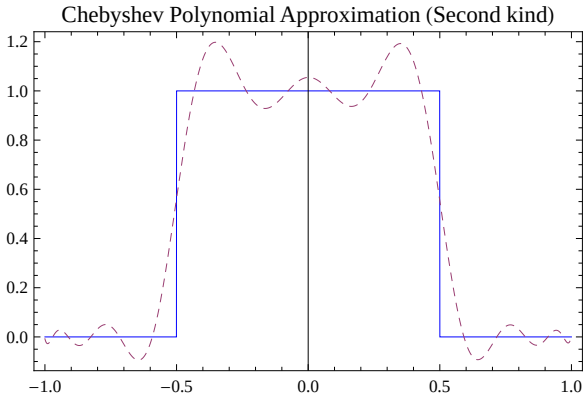

Figure 4.227: Uniform Chebyshev polynomial (second kind) approximation for $n = 16$ and one hundred thousand particles.

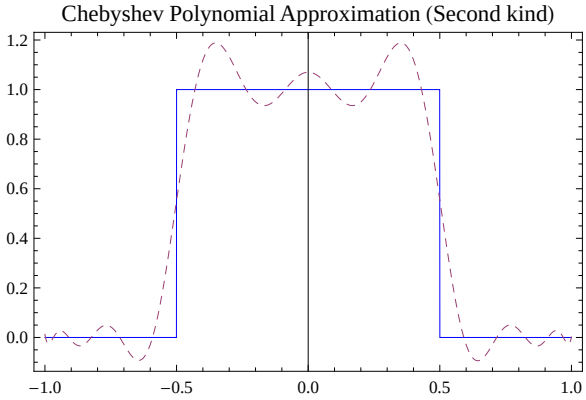

Figure 4.228: Uniform Chebyshev polynomial (second kind) approximation for $n = 16$ and one million particles.

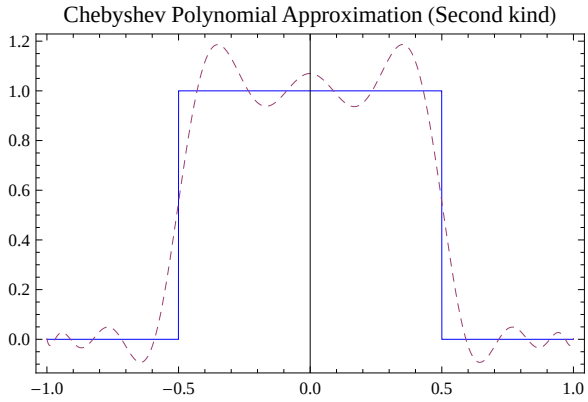

Figure 4.229: Uniform Chebyshev polynomial (second kind) approximation for $n = 16$ and five million particles.

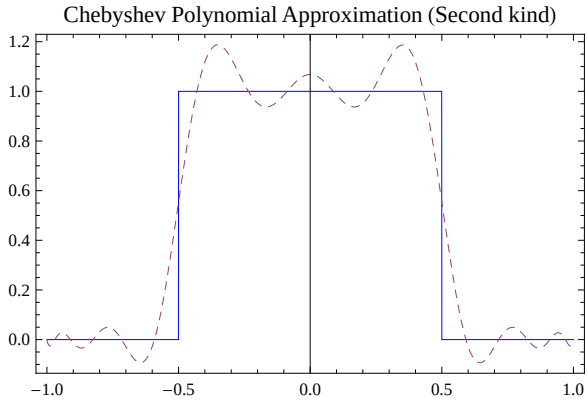

Figure 4.230: Uniform Chebyshev polynomial (second kind) approximation for $n = 16$ and ten million particles.

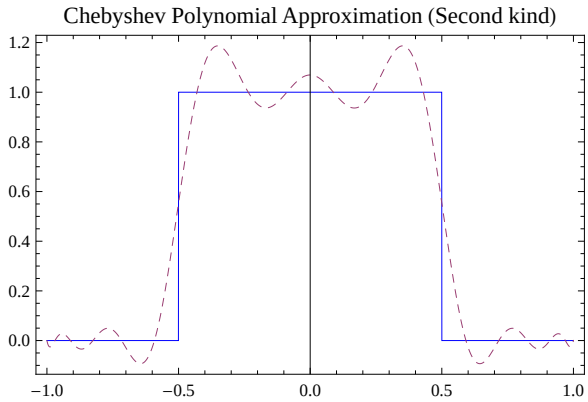

Figure 4.231: Uniform Chebyshev polynomial (second kind) approximation for $n = 16$ and fifteen million particles.

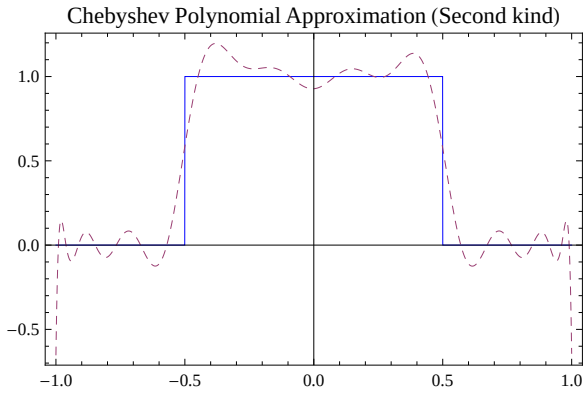

Figure 4.232: Uniform Chebyshev polynomial (second kind) approximation for $n = 20$ and ten thousand particles.

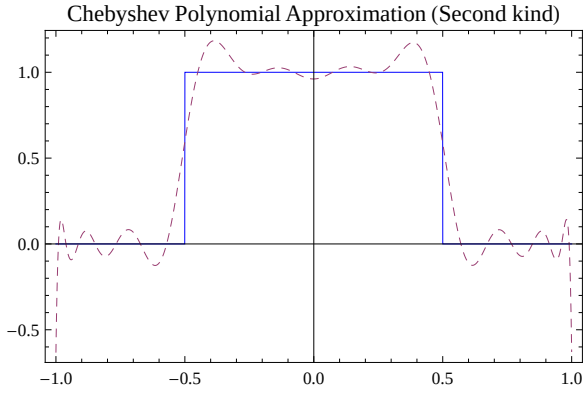

Figure 4.233: Uniform Chebyshev polynomial (second kind) approximation for $n = 20$ and one hundred thousand particles.

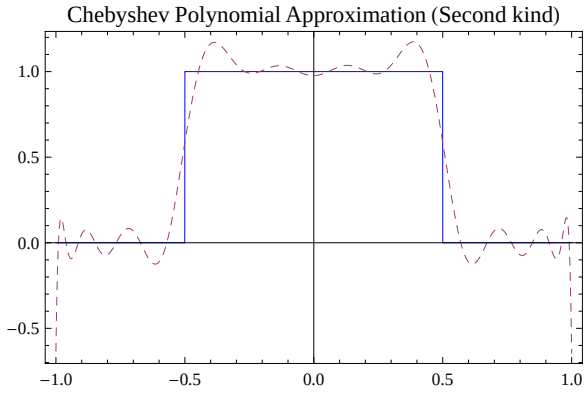

Figure 4.234: Uniform Chebyshev polynomial (second kind) approximation for $n = 20$ and one million particles.

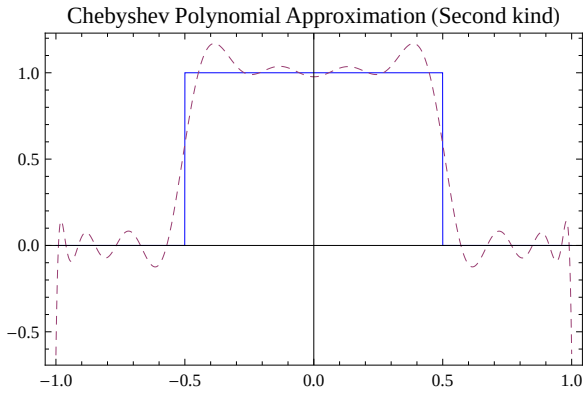

Figure 4.235: Uniform Chebyshev polynomial (second kind) approximation for $n = 20$ and five million particles.

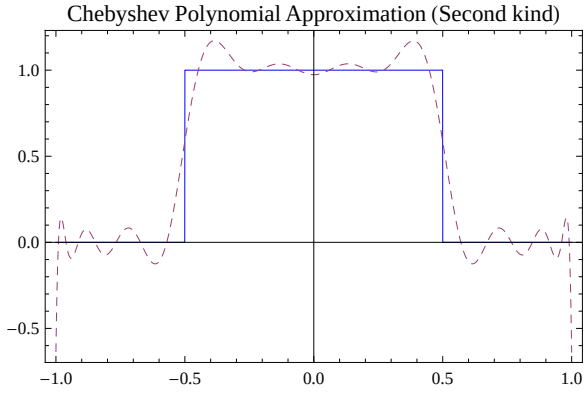

Figure 4.236: Uniform Chebyshev polynomial (second kind) approximation for $n = 20$ and ten million particles.

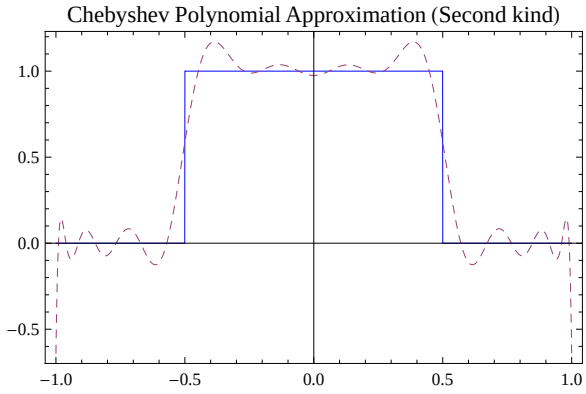

Figure 4.237: Uniform Chebyshev polynomial (second kind) approximation for $n = 20$ and fifteen million particles.

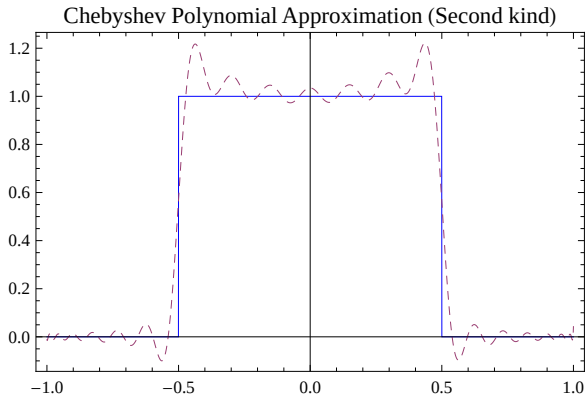

Figure 4.238: Uniform Chebyshev polynomial (second kind) approximation for $n = 40$ and fifteen million particles.

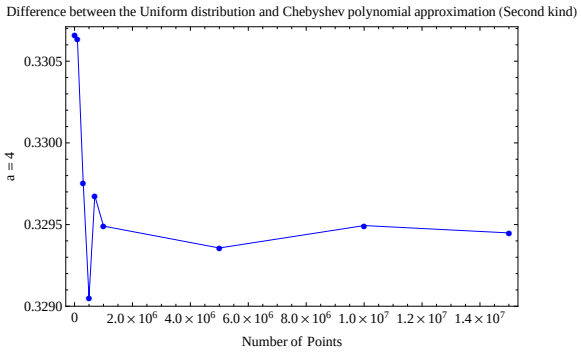

Figure 4.239: Difference between the Uniform distribution and the Chebyshev polynomial (second kind) approximation for $n = 4$.

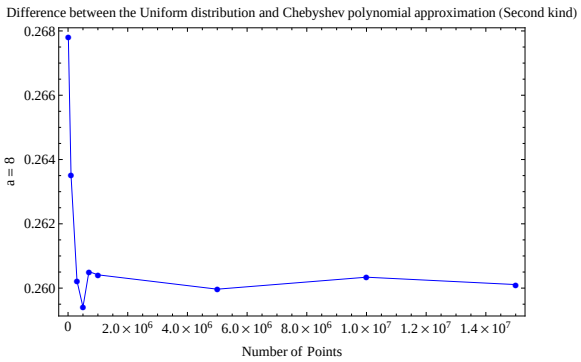

Figure 4.240: Difference between the Uniform distribution and the Chebyshev polynomial (second kind) approximation for $n = 8$.

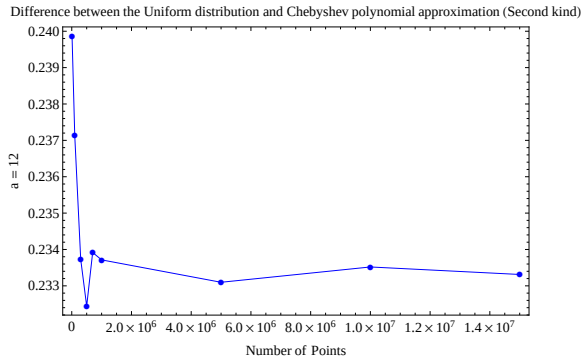

Figure 4.241: Difference between the Uniform distribution and the Chebyshev polynomial (second kind) approximation for $n = 12$.

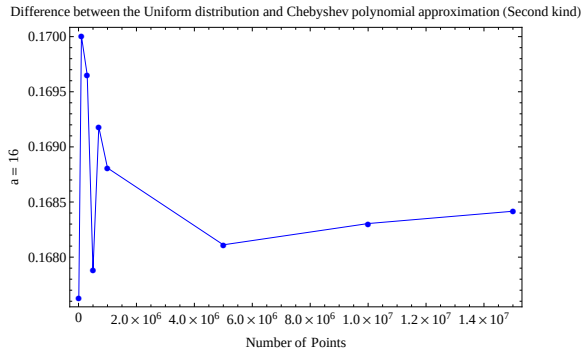

Figure 4.242: Difference between the Uniform distribution and the Chebyshev polynomial (second kind) approximation for $n = 16$.

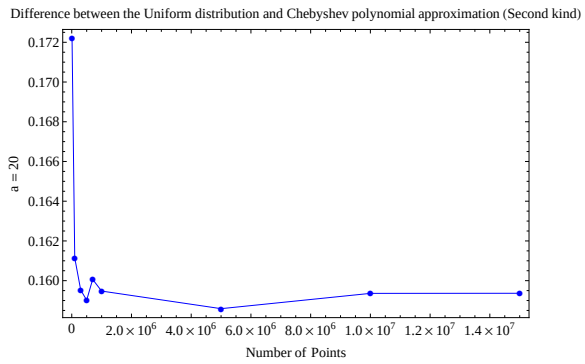

Figure 4.243: Difference between the Uniform distribution and the Chebyshev polynomial (second kind) approximation for $n = 20$.

4.3 Double One-Dimensional Gaussian Distribution

A set of different Double One-Dimensional Gaussian distributions was also used for approximating the charge density. In general, this curve is defined as the sum of two individual Gaussians with specific means and variances, as given in (4.10).

$$g(x) = e^{\frac{-(x-\mu_1)^2}{\sigma_1^2}} + \quad e^{\frac{-(x+\mu_2)^2}{\sigma_2^2}} \tag{4.10}$$

The first approximation of this type of distribution sets $\mu_1 = \mu_2 = 0.4$ and $\sigma_1 = \sigma_2 = 0.3$, allowing for a symmetric curve. The same procedure was followed as for the single Gaussian and Uniform distributions. The coefficients for the charge distribution approximation were calculated up to order $n = 20$ and one hundred thousand particles, followed by the difference of the distribution and approximations.

4.3.1 Legendre Polynomials

Figures 4.244 to 4.248 show the convergence of the coefficients from the Legendre approximation of different orders.

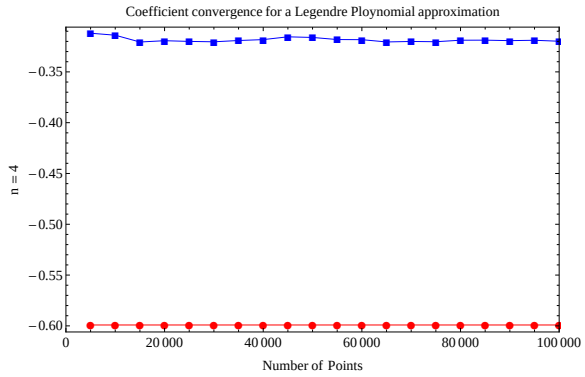

Figure 4.244: Convergence for a double Gaussian Legendre polynomial approximation for $n = 4$.

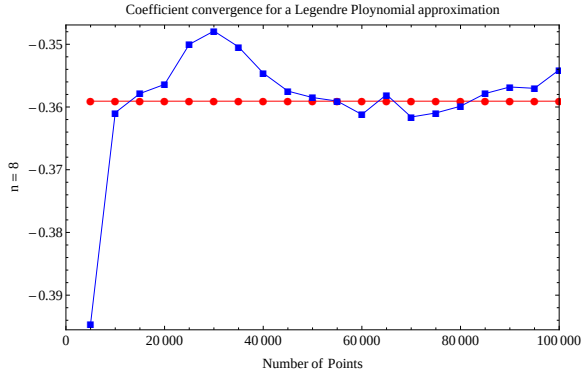

Figure 4.245: Convergence for a double Gaussian Legendre polynomial approximation for $n = 8$.

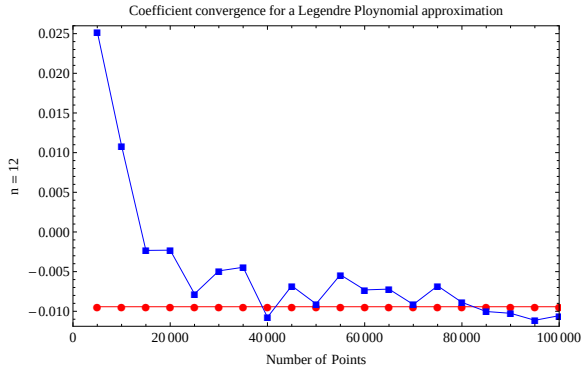

Figure 4.246: Convergence for a double Gaussian Legendre polynomial approximation for $n = 12$.

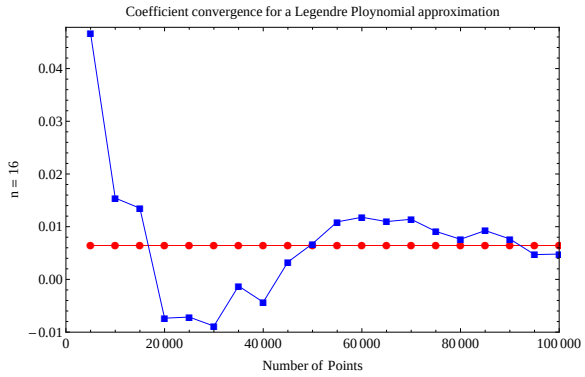

Figure 4.247: Convergence for a double Gaussian Legendre polynomial approximation for $n = 16$.

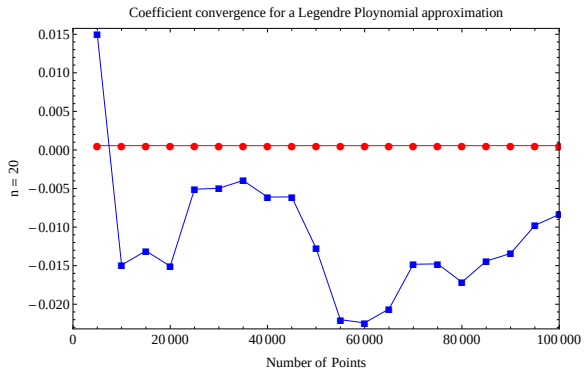

Figure 4.248: Convergence for a double Gaussian Legendre polynomial approximation for $n = 20$.

A visual representation of the approximation is given from figures (4.249) to (4.263) that also serves as a comparison to the actual distribution.

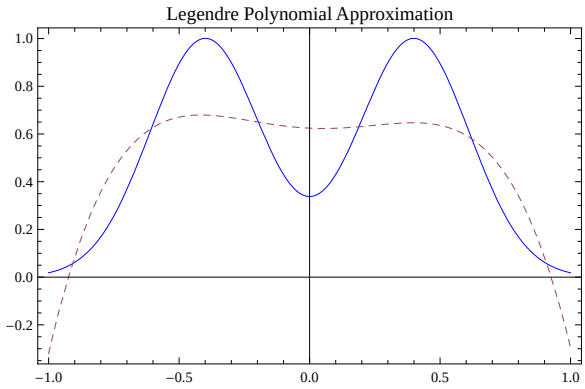

Figure 4.249: Legendre polynomial approximation of a double Gaussian for $n = 4$ and twenty thousand particles.

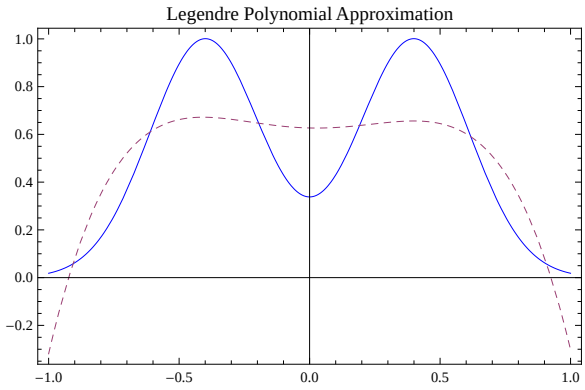

Figure 4.250: Legendre polynomial approximation of a double Gaussian for $n = 4$ and sixty thousand particles.

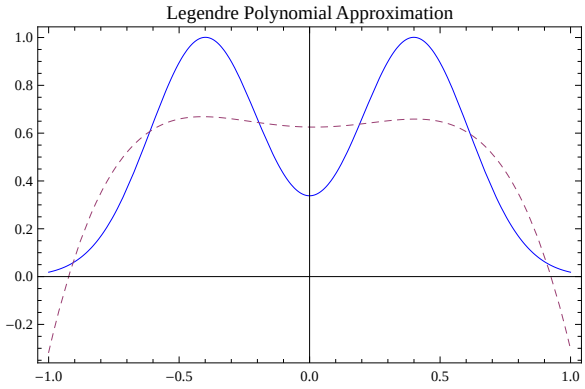

Figure 4.251: Legendre polynomial approximation of a double Gaussian for $n = 4$ and one hundred thousand particles.

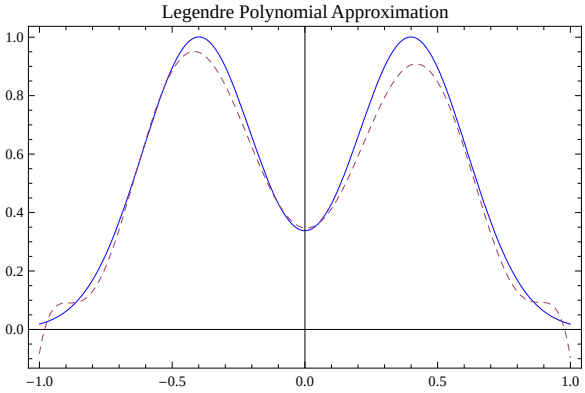

Figure 4.252: Legendre polynomial approximation of a double Gaussian for $n = 8$ and twenty thousand particles.

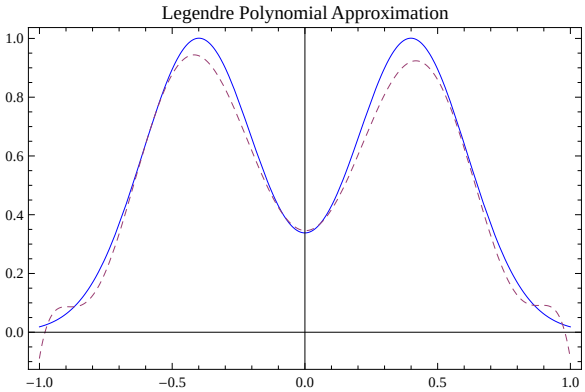

Figure 4.253: Legendre polynomial approximation of a double Gaussian for $n = 8$ and sixty thousand particles.

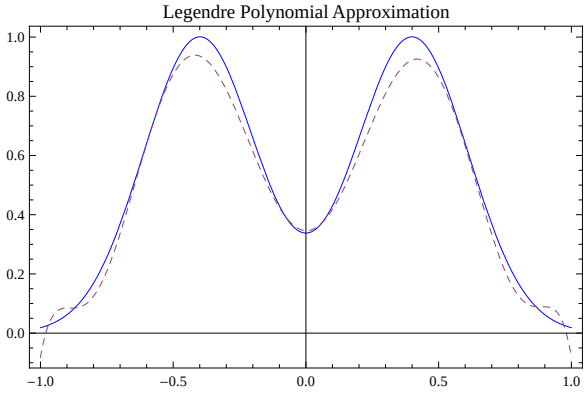

Figure 4.254: Legendre polynomial approximation of a double Gaussian for $n = 8$ and one hundred thousand particles.

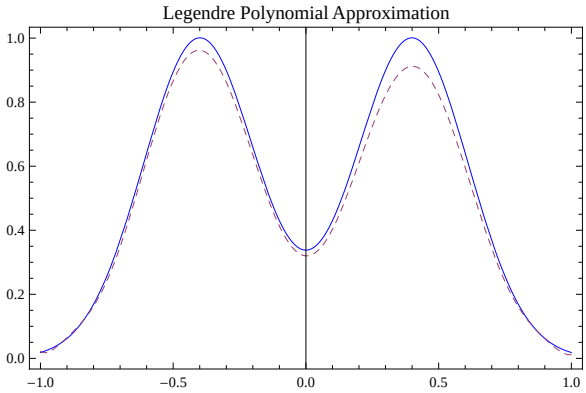

Figure 4.255: Legendre polynomial approximation of a double Gaussian for $n = 12$ and twenty thousand particles.

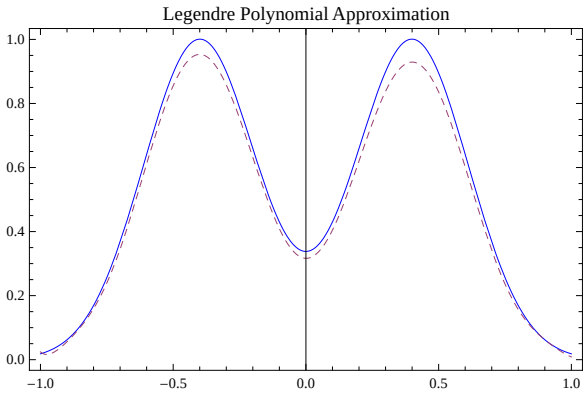

Figure 4.256: Legendre polynomial approximation of a double Gaussian for $n = 12$ and sixty thousand particles.

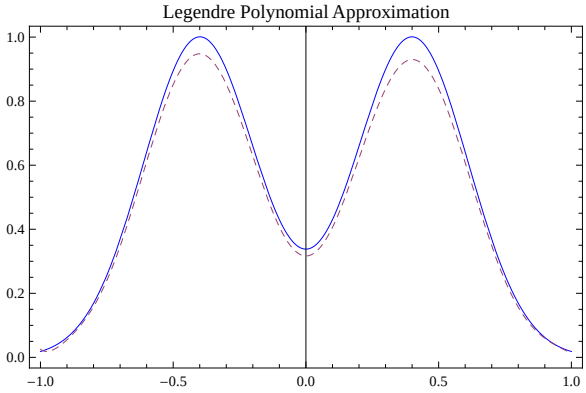

Figure 4.257: Legendre polynomial approximation of a double Gaussian for $n = 12$ and one hundred thousand particles.

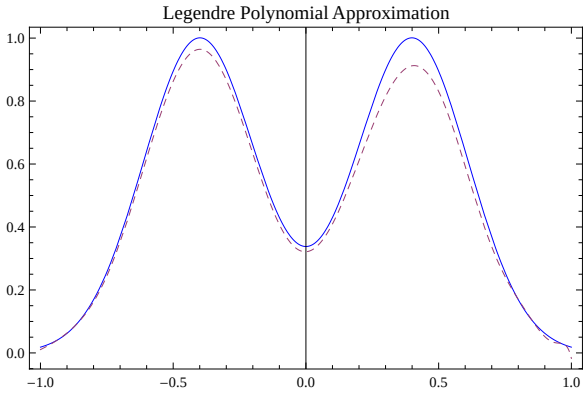

Figure 4.258: Legendre polynomial approximation of a double Gaussian for $n = 16$ and twenty thousand particles.

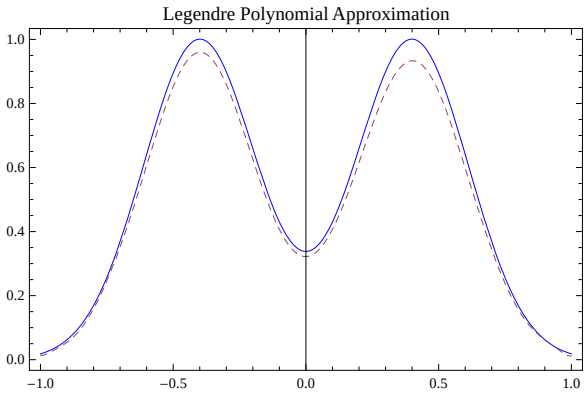

Figure 4.259: Legendre polynomial approximation of a double Gaussian for $n = 16$ and sixty thousand particles.

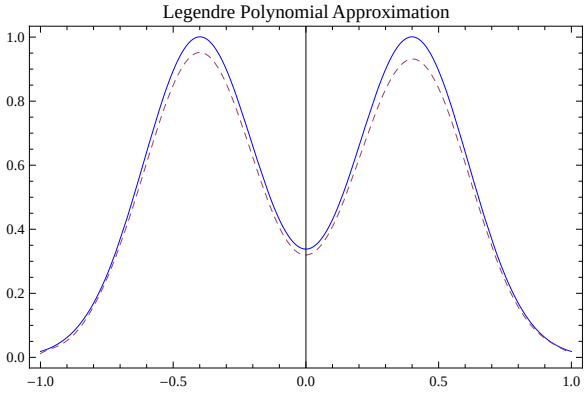

Figure 4.260: Legendre polynomial approximation of a double Gaussian for $n = 16$ and one hundred thousand particles.

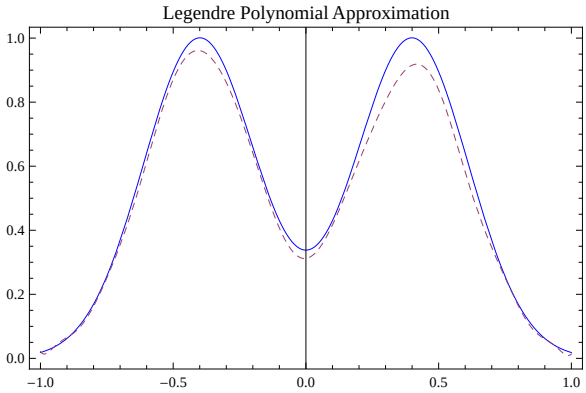

Figure 4.261: Legendre polynomial approximation of a double Gaussian for $n = 20$ and twenty thousand particles.

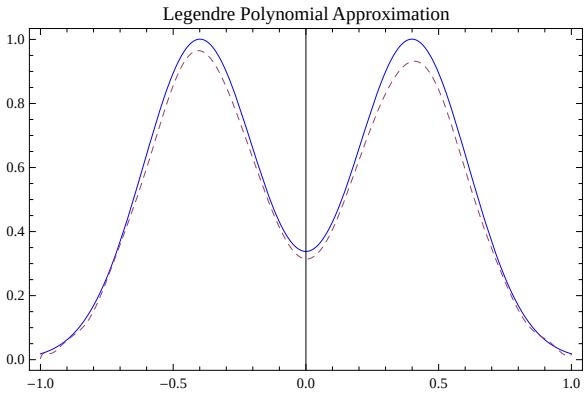

Figure 4.262: Legendre polynomial approximation of a double Gaussian for $n = 20$ and sixty thousand particles.

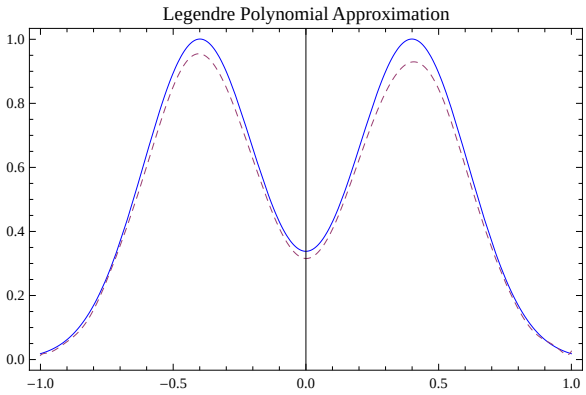

Figure 4.263: Legendre polynomial approximation of a double Gaussian for $n = 20$ and one hundred thousand particles.

Once the approximations have been done, the error is calculated and plotted in order to differentiate between graphs that may look identical. (See Figures 4.264 to 4.268.)

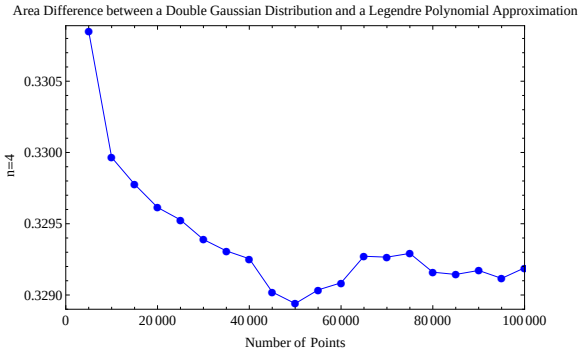

Figure 4.264: Difference for a double Gaussian Legendre polynomial approximation for $n = 4$.

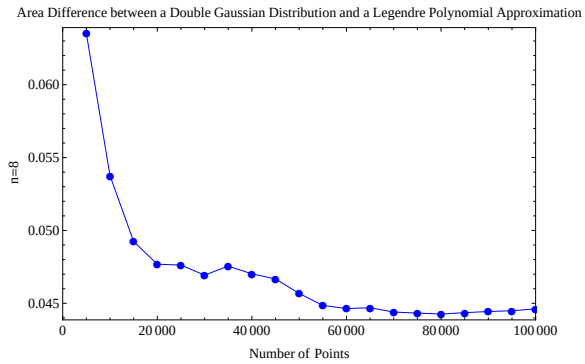

Figure 4.265: Difference for a double Gaussian Legendre polynomial approximation for $n = 8$.

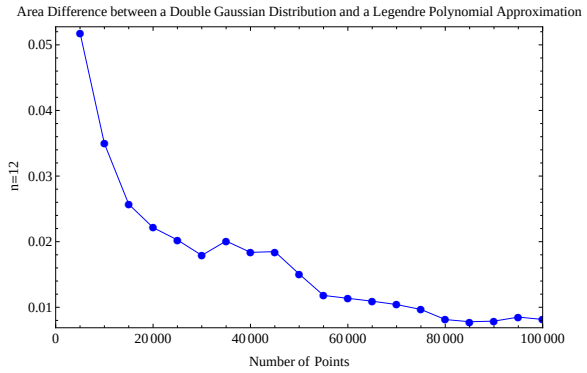

Figure 4.266: Difference for a double Gaussian Legendre polynomial approximation for $n = 12$.

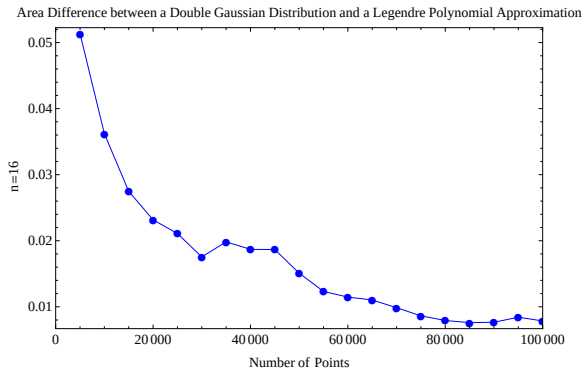

Figure 4.267: Difference for a double Gaussian Legendre polynomial approximation for $n = 16$.

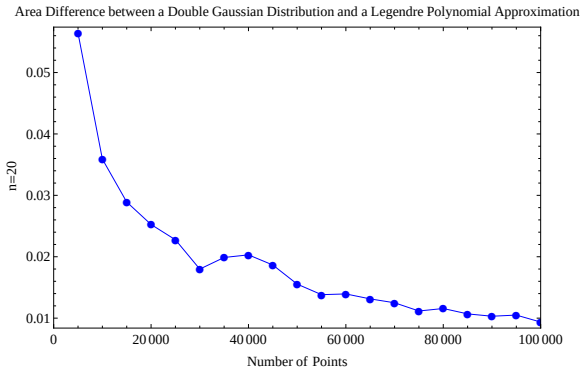

Figure 4.268: Difference for a double Gaussian Legendre polynomial approximation for $n = 20$.

4.3.2 Chebyshev Polynomials of the first kind

To illustrate the change of the coefficients, Figures 4.269 through 4.273 show the coefficient convergence for the first kind Chebyshev approximation.

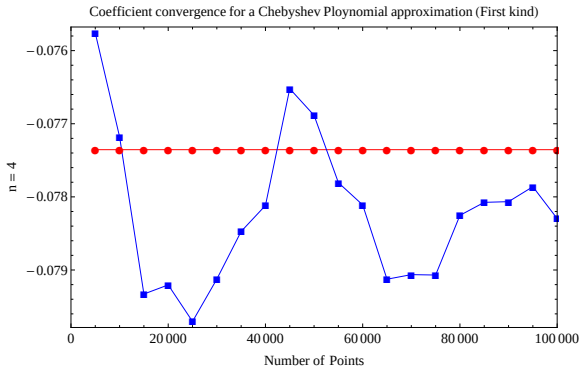

Figure 4.269: Convergence for a double Gaussian Chebyshev polynomial (first kind) approximation for $n = 4$.

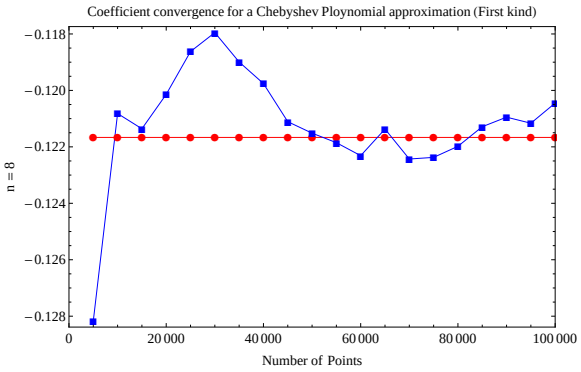

Figure 4.270: Convergence for a double Gaussian Chebyshev polynomial (first kind) approximation for $n = 8$.

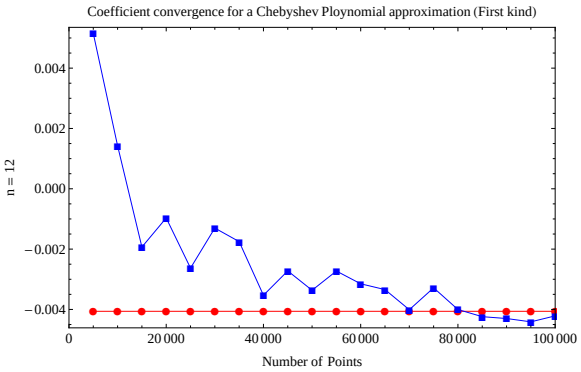

Figure 4.271: Convergence for a double Gaussian Chebyshev polynomial (first kind) approximation for $n = 12$.

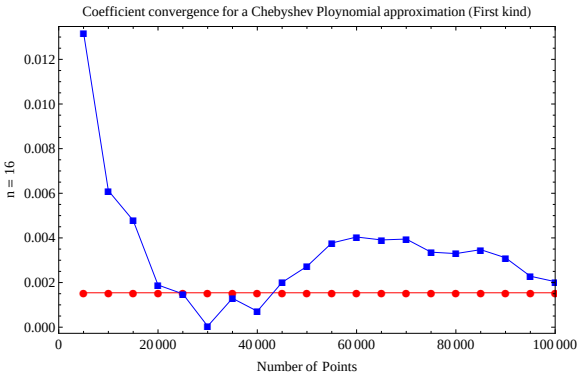

Figure 4.272: Convergence for a double Gaussian Chebyshev polynomial (first kind) approximation for $n = 16$.

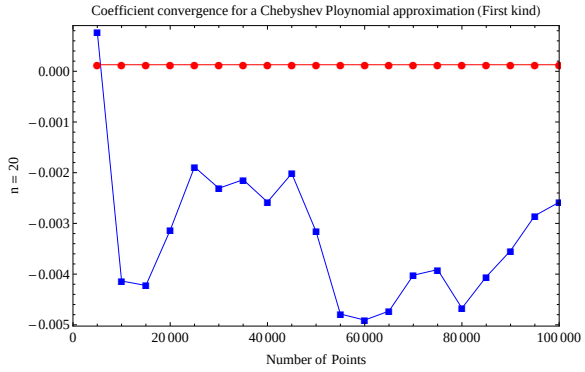

Figure 4.273: Convergence for a double Gaussian Chebyshev polynomial (first kind) approximation for $n = 20$.

A visual representation of the approximation is given from Figures 4.274 to 4.288 that also serves as a comparison to the actual distribution.

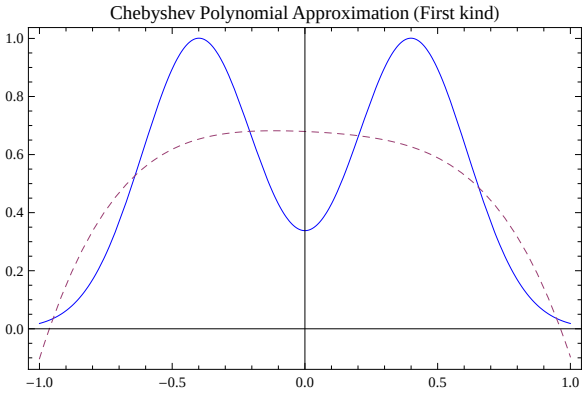

Figure 4.274: Chebyshev polynomial (first kind) approximation of a double Gaussian for $n = 4$ and twenty thousand particles.

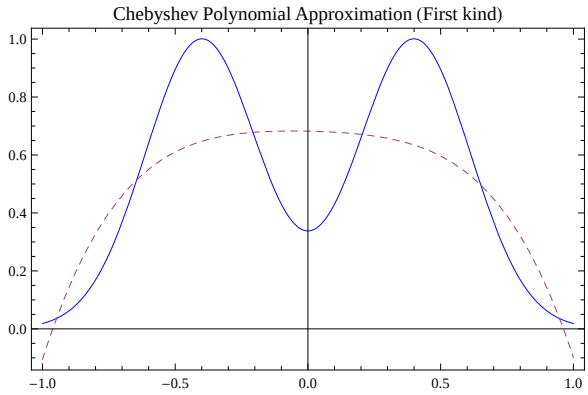

Figure 4.275: Chebyshev polynomial (first kind) approximation of a double Gaussian for $n = 4$ and sixty thousand particles.

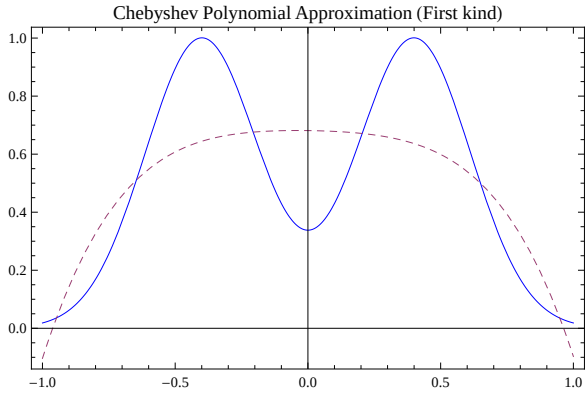

Figure 4.276: Chebyshev polynomial (first kind) approximation of a double Gaussian for $n = 4$ and one hundred thousand particles.

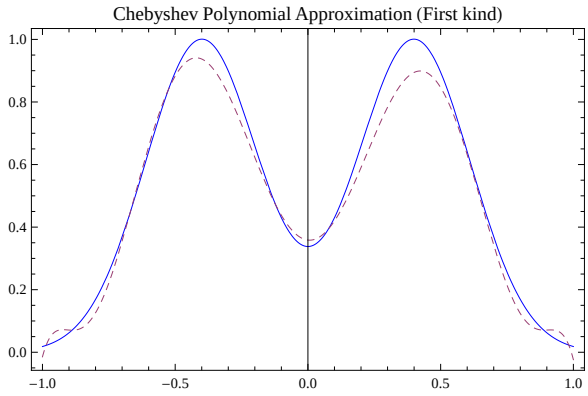

Figure 4.277: Chebyshev polynomial (first kind) approximation of a double Gaussian for $n = 8$ and twenty thousand particles.

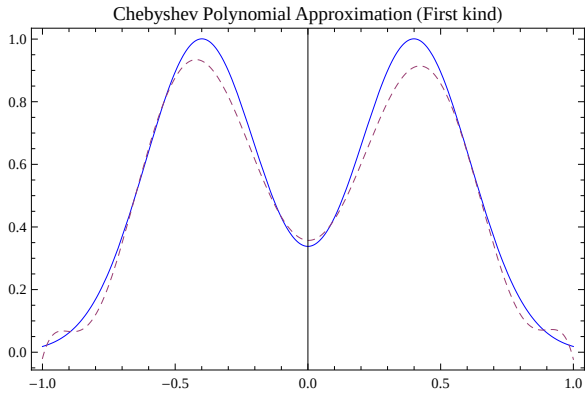

Figure 4.278: Chebyshev polynomial (first kind) approximation of a double Gaussian for $n = 8$ and sixty thousand particles.

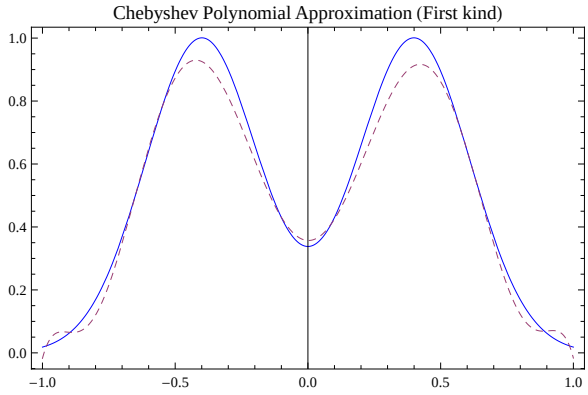

Figure 4.279: Chebyshev polynomial (first kind) approximation of a double Gaussian for $n = 8$ and one hundred thousand particles.

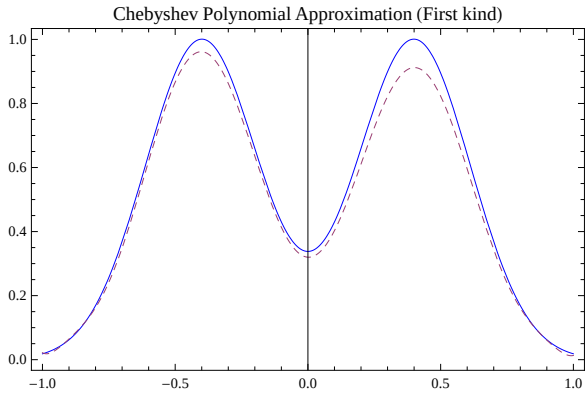

Figure 4.280: Chebyshev polynomial (first kind) approximation of a double Gaussian for $n = 12$ and twenty thousand particles.

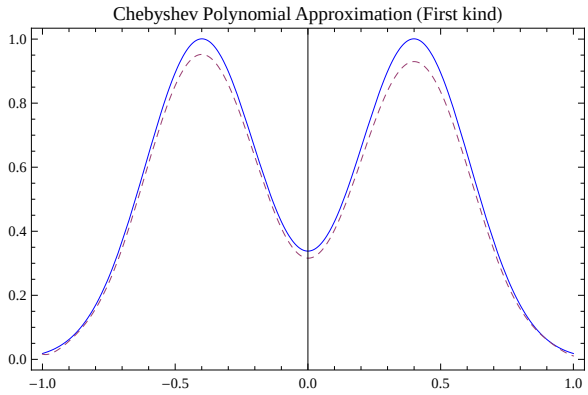

Figure 4.281: Chebyshev polynomial (first kind) approximation of a double Gaussian for $n = 12$ and sixty thousand particles.

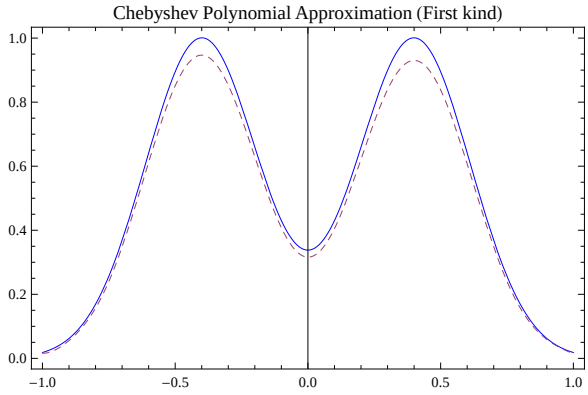

Figure 4.282: Chebyshev polynomial (first kind) approximation of a double Gaussian for $n = 12$ and one hundred thousand particles.

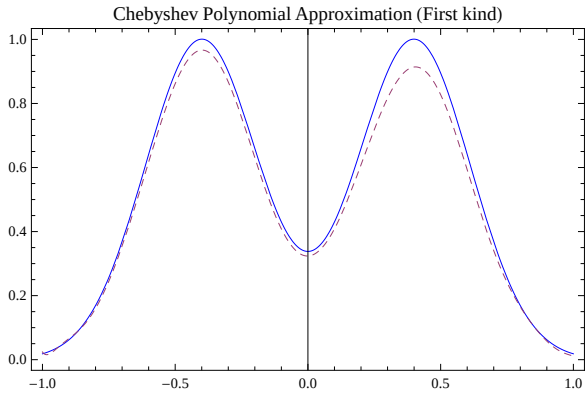

Figure 4.283: Chebyshev polynomial (first kind) approximation of a double Gaussian for $n = 16$ and twenty thousand particles.

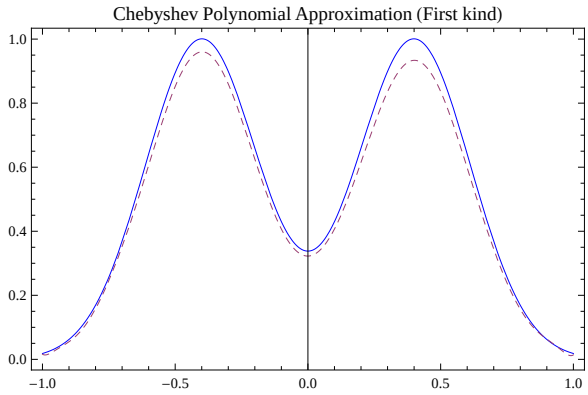

Figure 4.284: Chebyshev polynomial (first kind) approximation of a double Gaussian for $n = 16$ and sixty thousand particles.

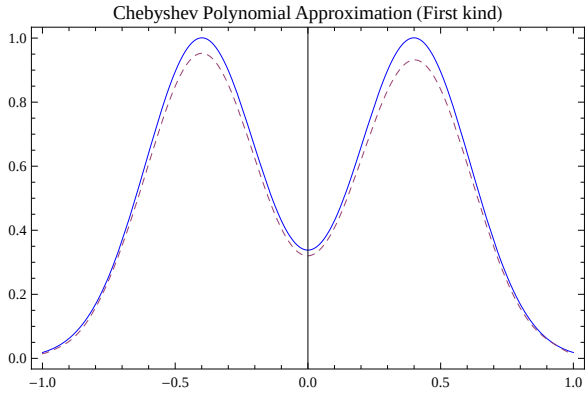

Figure 4.285: Chebyshev polynomial (first kind) approximation of a double Gaussian for $n = 16$ and one hundred thousand particles.

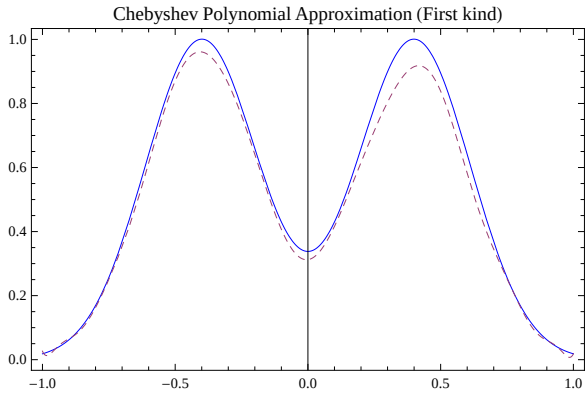

Figure 4.286: Chebyshev polynomial (first kind) approximation of a double Gaussian for $n = 20$ and twenty thousand particles.

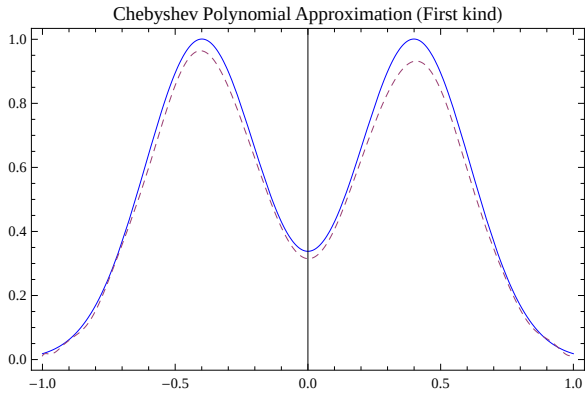

Figure 4.287: Chebyshev polynomial (first kind) approximation of a double Gaussian for $n = 20$ and sixty thousand particles.

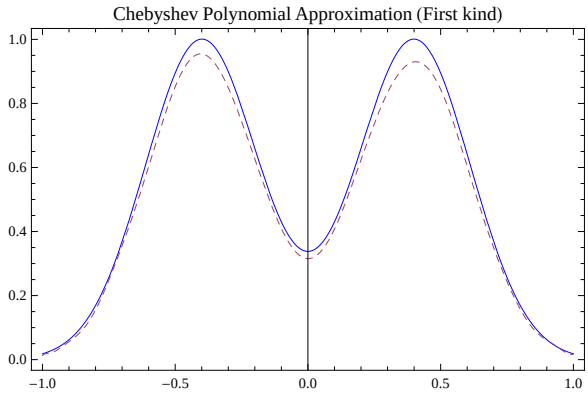

Figure 4.288: Chebyshev polynomial (first kind) approximation of a double Gaussian for $n = 20$ and one hundred thousand particles.

Once the approximations have been done, the error is calculated and plotted in order to differentiate between graphs that may look identical. (See Figures 4.289 to 4.293.)

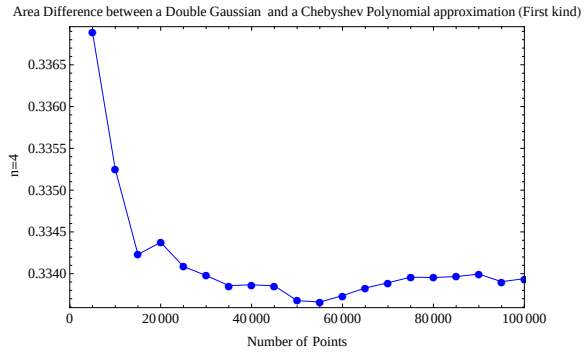

Figure 4.289: Difference for a double Gaussian Chebyshev polynomial (first kind) approximation for $n = 4$.

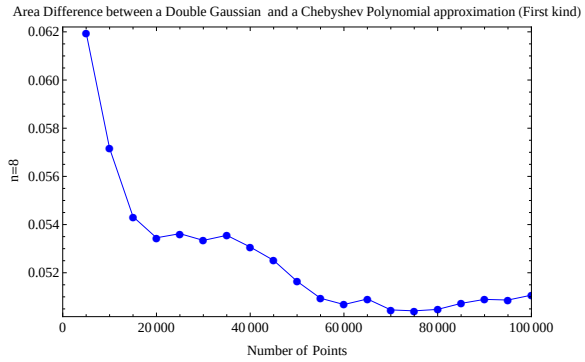

Figure 4.290: Difference for a double Gaussian Chebyshev polynomial (first kind) approximation for $n = 8$.

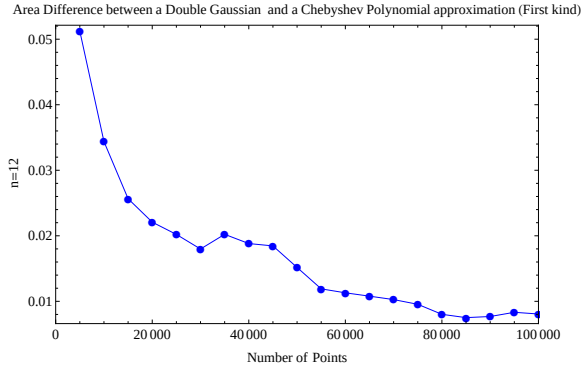

Figure 4.291: Difference for a double Gaussian Chebyshev polynomial (first kind) approximation for $n = 12$.

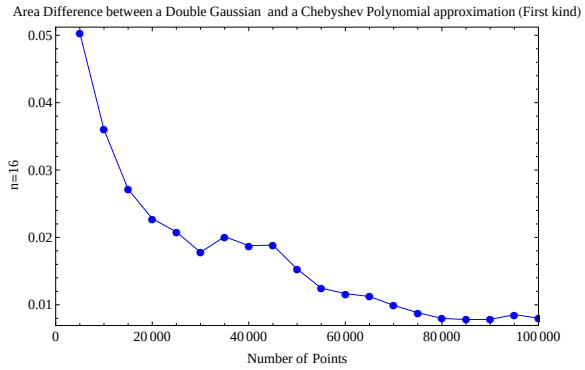

Figure 4.292: Difference for a double Gaussian Chebyshev polynomial (first kind) approximation for $n = 16$.

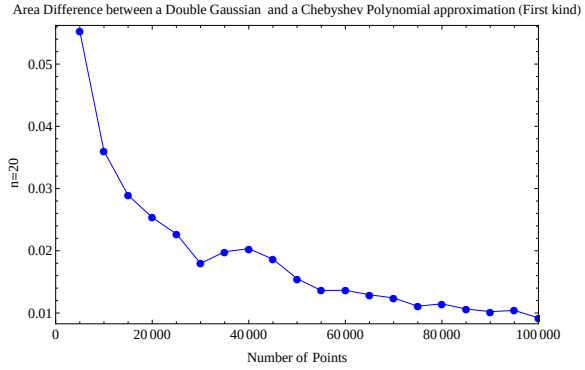

Figure 4.293: Difference for a double Gaussian Chebyshev polynomial (first kind) approximation for $n = 20$.

4.3.3 Chebyshev Polynomials of the second kind

Figures 4.294 to 4.298 show the convergence of the coefficients from the Chebyshev of the first kind approximation of different orders.

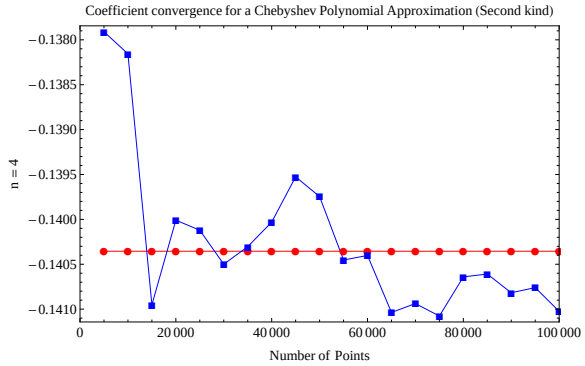

Figure 4.294: Convergence for a double Gaussian Chebyshev polynomial (second kind) approximation for $n = 4$.

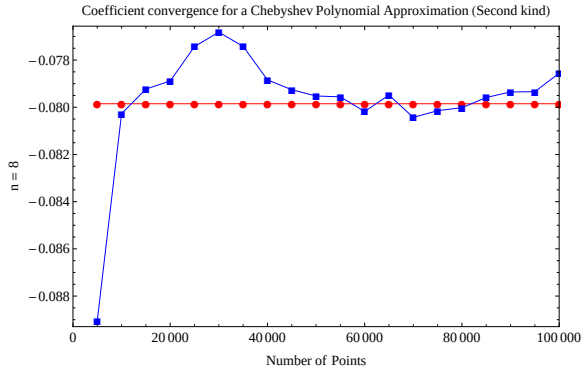

Figure 4.295: Convergence for a double Gaussian Chebyshev polynomial (second kind) approximation for $n = 8$.

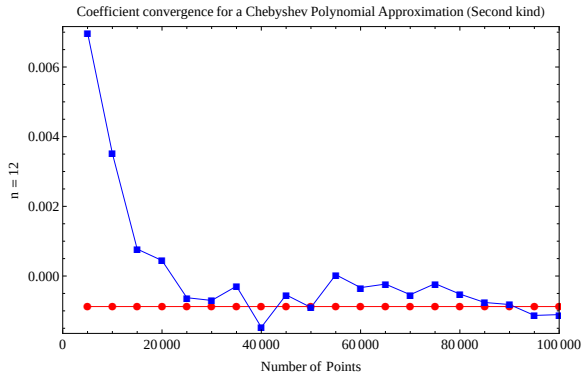

Figure 4.296: Convergence for a double Gaussian Chebyshev polynomial (second kind) approximation for $n = 12$.

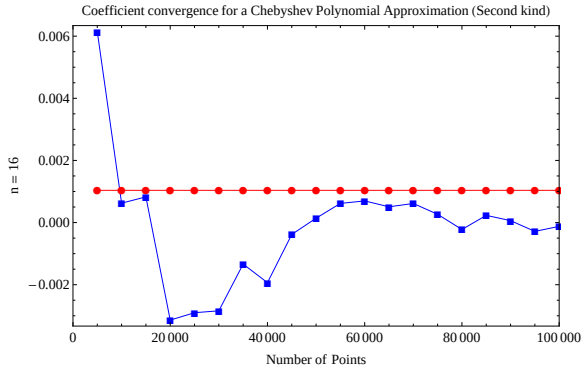

Figure 4.297: Convergence for a double Gaussian Chebyshev polynomial (second kind) approximation for $n = 16$.

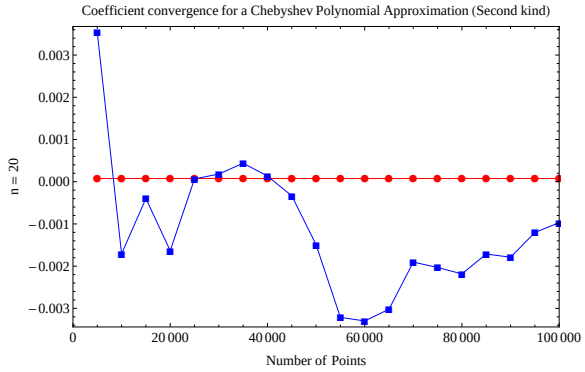

Figure 4.298: Convergence for a double Gaussian Chebyshev polynomial (second kind) approximation for $n = 20$.

A visual representation of the approximation is given from Figures 4.299 to 4.313 that also serves as a comparison to the actual distribution.

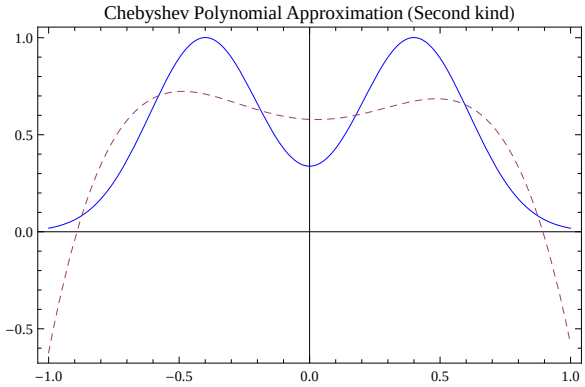

Figure 4.299: Chebyshev polynomial (second kind) approximation of a double Gaussian for $n = 4$ and twenty thousand particles.

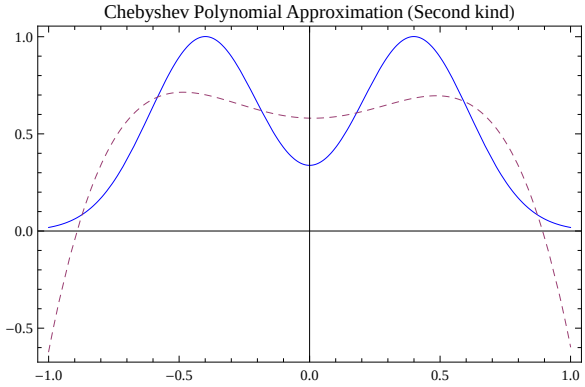

Figure 4.300: Chebyshev polynomial (second kind) approximation of a double Gaussian for $n = 4$ and sixty thousand particles.

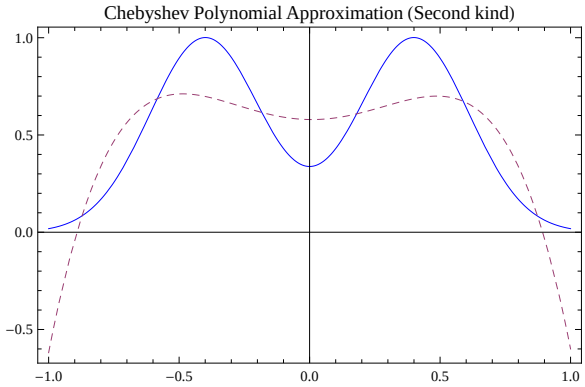

Figure 4.301: Chebyshev polynomial (second kind) approximation of a double Gaussian for $n = 4$ and one hundred thousand particles.

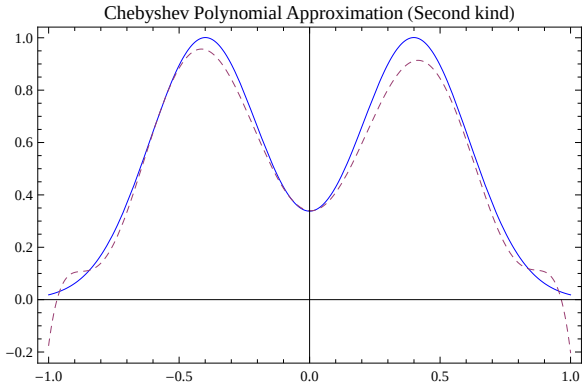

Figure 4.302: Chebyshev polynomial (second kind) approximation of a double Gaussian for $n = 8$ and twenty thousand particles.

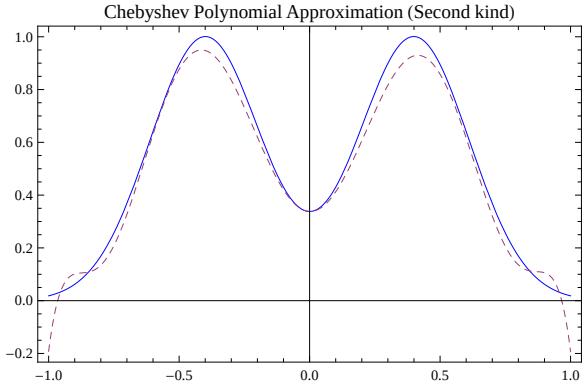

Figure 4.303: Chebyshev polynomial (second kind) approximation of a double Gaussian for $n = 8$ and sixty thousand particles.

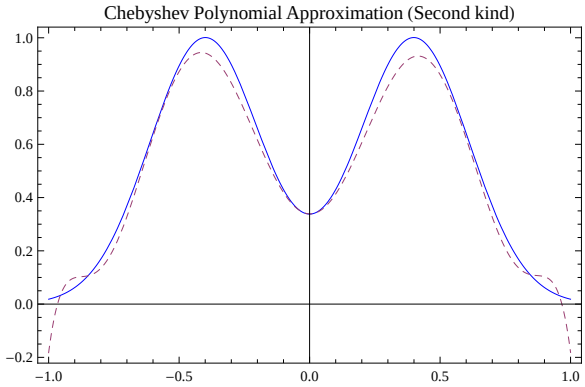

Figure 4.304: Chebyshev polynomial (second kind) approximation of a double Gaussian for $n = 8$ and one hundred thousand particles.

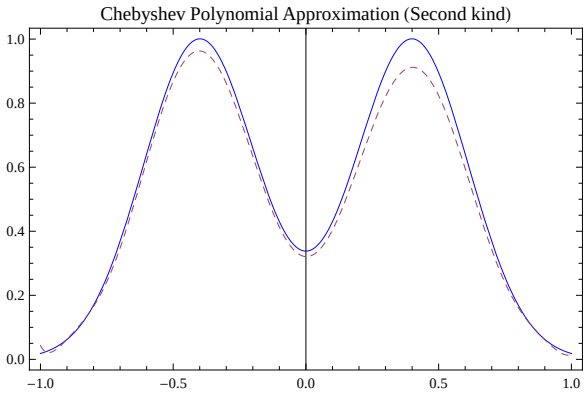

Figure 4.305: Chebyshev polynomial (second kind) approximation of a double Gaussian for $n = 12$ and twenty thousand particles.

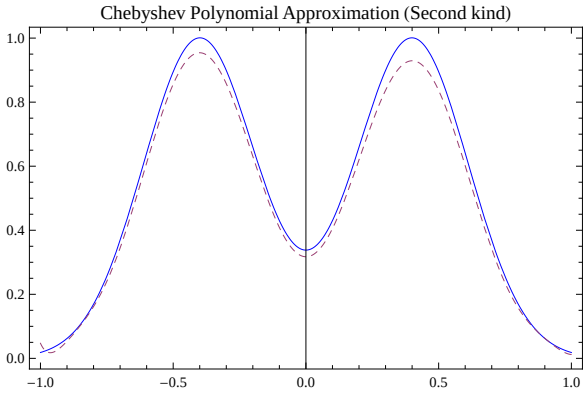

Figure 4.306: Chebyshev polynomial (second kind) approximation of a double Gaussian for $n = 12$ and sixty thousand particles.

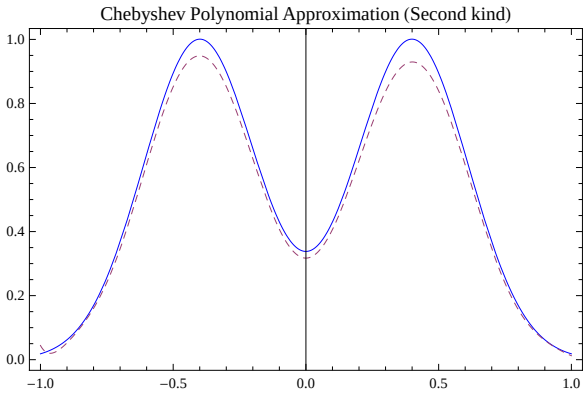

Figure 4.307: Chebyshev polynomial (second kind) approximation of a double Gaussian for $n = 12$ and one hundred thousand particles.

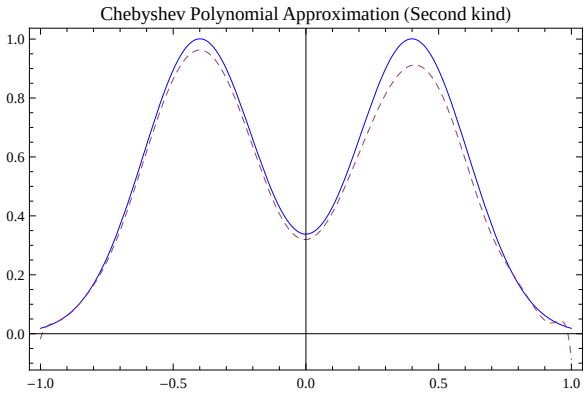

Figure 4.308: Chebyshev polynomial (second kind) approximation of a double Gaussian for $n = 16$ and twenty thousand particles.

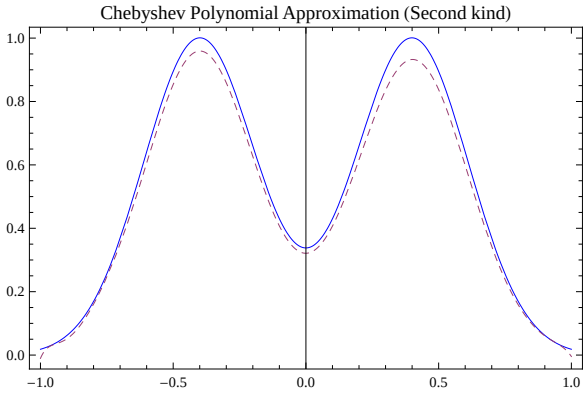

Figure 4.309: Chebyshev polynomial (second kind) approximation of a double Gaussian for $n = 16$ and sixty thousand particles.

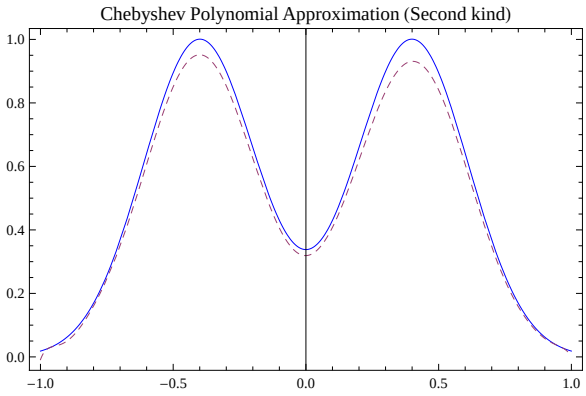

Figure 4.310: Chebyshev polynomial (second kind) approximation of a double Gaussian for $n = 16$ and one hundred thousand particles.

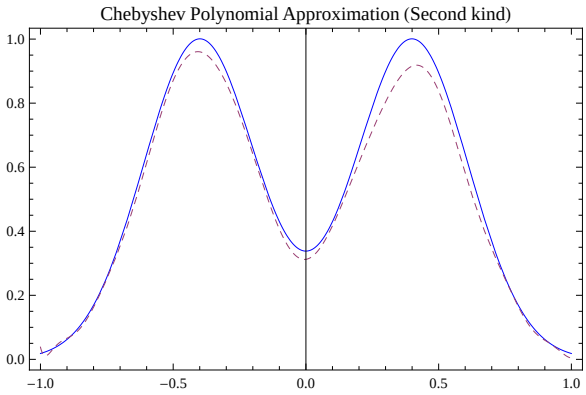

Figure 4.311: Chebyshev polynomial (second kind) approximation of a double Gaussian for $n = 20$ and twenty thousand particles.

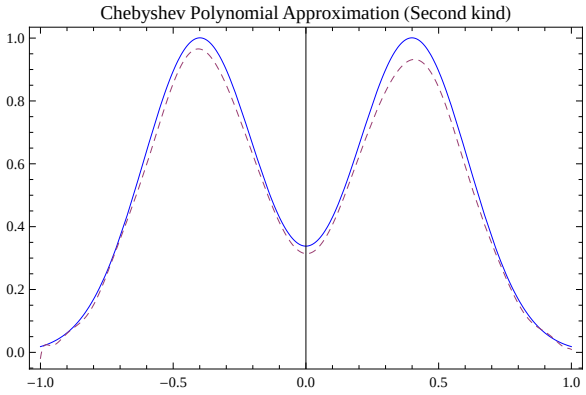

Figure 4.312: Chebyshev polynomial (second kind) approximation of a double Gaussian for $n = 20$ and sixty thousand particles.

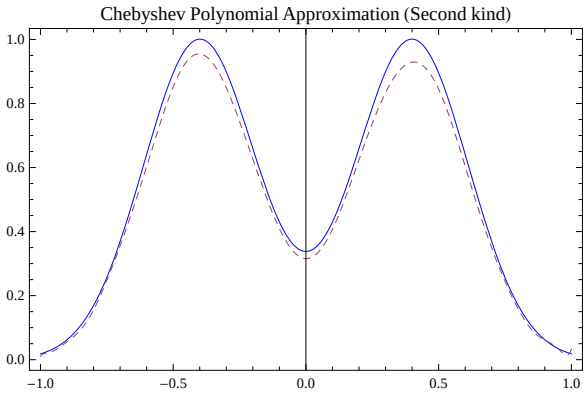

Figure 4.313: Chebyshev polynomial (second kind) approximation of a double Gaussian for $n = 20$ and one hundred thousand particles.

Once the approximations have been done, the error is calculated and plotted in order to differentiate between graphs that may look identical. (See Figures 4.314 to 4.318.)

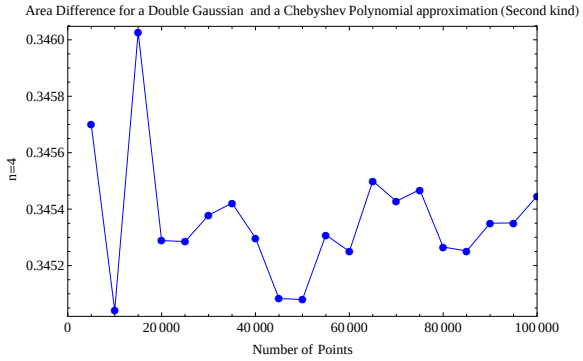

Figure 4.314: Difference for a double Gaussian Chebyshev polynomial (second kind) approximation for $n = 4$.

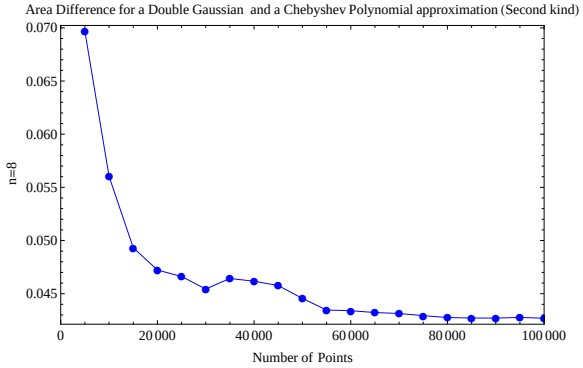

Figure 4.315: Difference for a double Gaussian Chebyshev polynomial (second kind) approximation for $n = 8$.

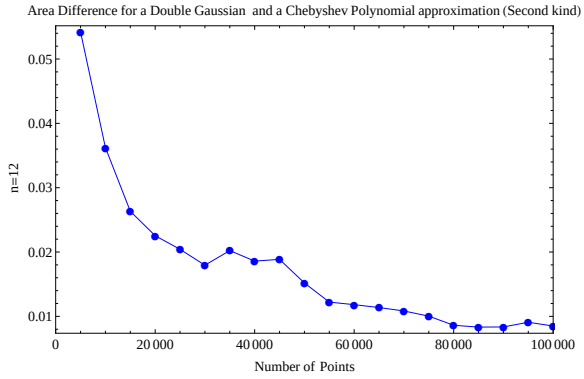

Figure 4.316: Difference for a double Gaussian Chebyshev polynomial (second kind) approximation for $n = 12$.

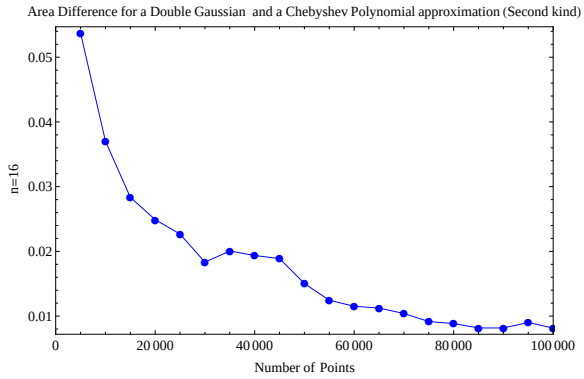

Figure 4.317: Difference for a double Gaussian Chebyshev polynomial (second kind) approximation for $n = 16$.

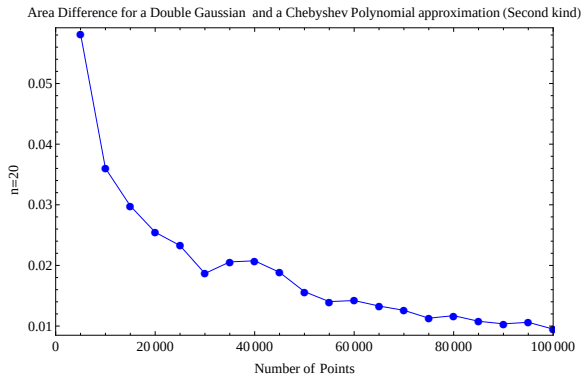

Figure 4.318: Difference for a double Gaussian Chebyshev polynomial (second kind) approximation for $n = 20$.

A second approximation of this type of distribution sets $\mu_1 = 0.6$ and $\mu_2 = 0.3$ and $\sigma_1 = 0.1$ and $\sigma_2 = 0.25$, allowing for an unsymmetrical curve. The parameters were changed to find out whether the approximation would work for a non-symmetric case and to identify any causes of heavy oscillations. (See Figures 4.319 to 4.321.)

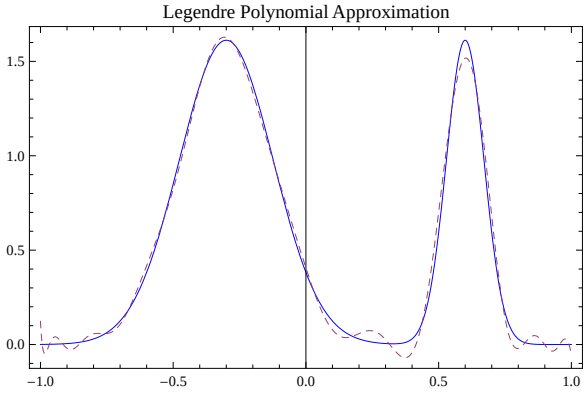

Figure 4.319: Legendre approximation of a double Gaussian for $n = 20$ and one hundred thousand particles.

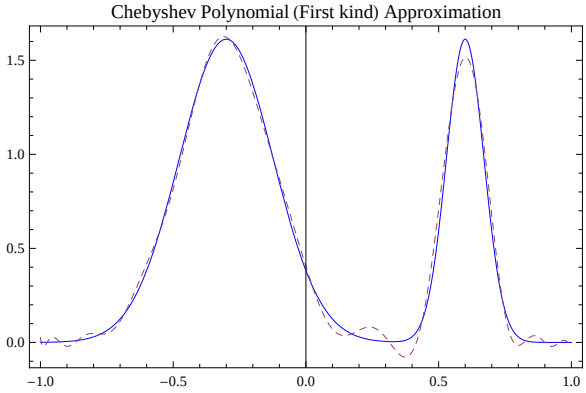

Figure 4.320: Chebyshev polynomial (first kind) approximation of a double Gaussian for $n = 20$ and one hundred thousand particles.

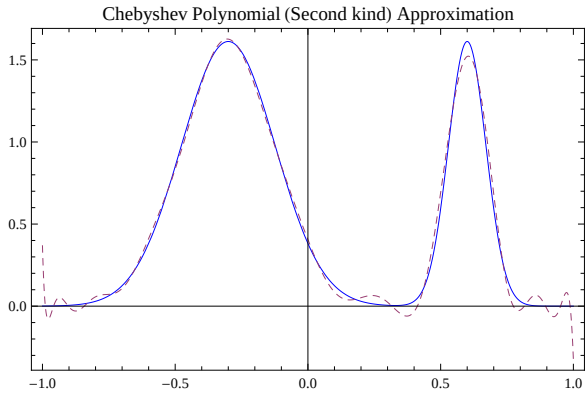

Figure 4.321: Chebyshev polynomial (second kind) approximation of a double Gaussian for $n = 20$ and one hundred thousand particles.

Based on all the double Gaussian figures, the polynomials work very well on approximating the distributions. The small oscillations only seem to occur when the function is far from the boundary and when there is a drastic curve on the function, like the region between the two Gaussian peaks.

4.4 Two-Dimensional Single Gaussian

In addition to approximating singles and double Gaussian, a 2D single normal distribution curve, defined by (4.11) and in Mathematica by $MultinormalDistribution[\mu, \Sigma]$ [20], was also approximated in order to test whether or not the approximation method could be expanded to more dimensions.

$$g(x) = \frac{18e^{-18x^2-18y^2}}{\pi} \tag{4.11}$$

The approximation was set to $\sigma = \frac{1}{6}$ and maximum orders $n = 20$ and $m = 20$, just like the one-dimensional case, but limited the number of particles to one hundred

thousand. Figures 4.322 to 4.325 show how the approximated distributions compare to the actual curve.

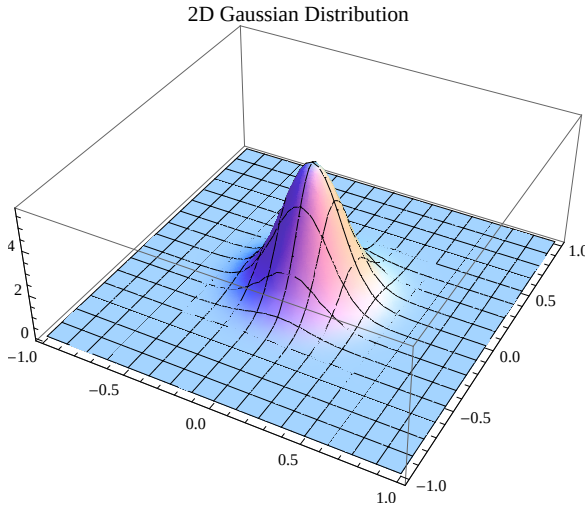

Figure 4.322: 2D Gaussian distribution centered at zero with $\sigma = \frac{1}{6}$.

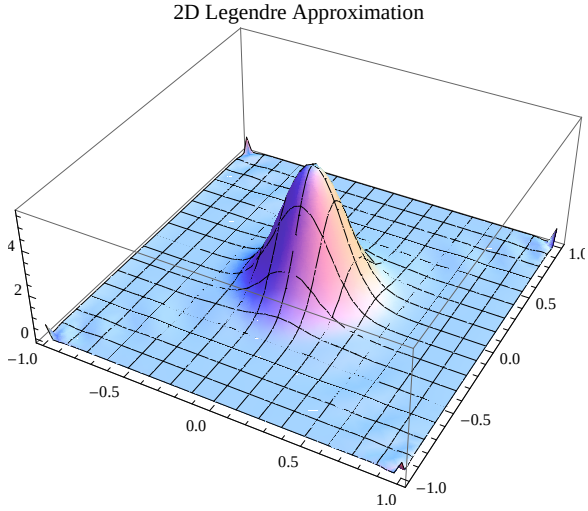

Figure 4.323: Legendre polynomial approximation of a 2D Gaussian for $n = 20$ and one hundred thousand particles.

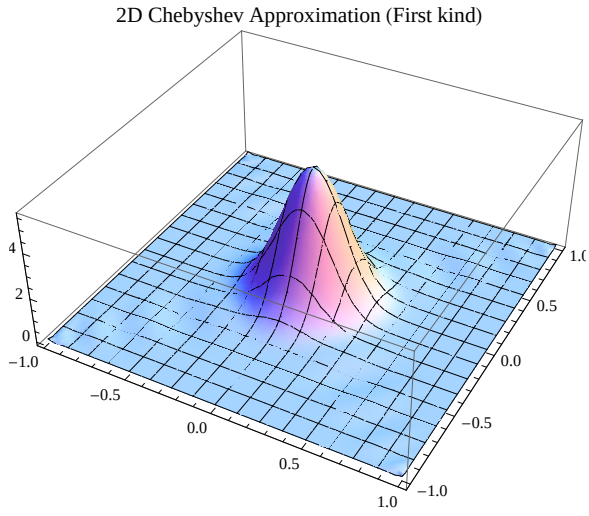

Figure 4.324: Chebyshev polynomial (first kind) approximation of a 2D Gaussian for $n = 20$ and one hundred thousand particles.

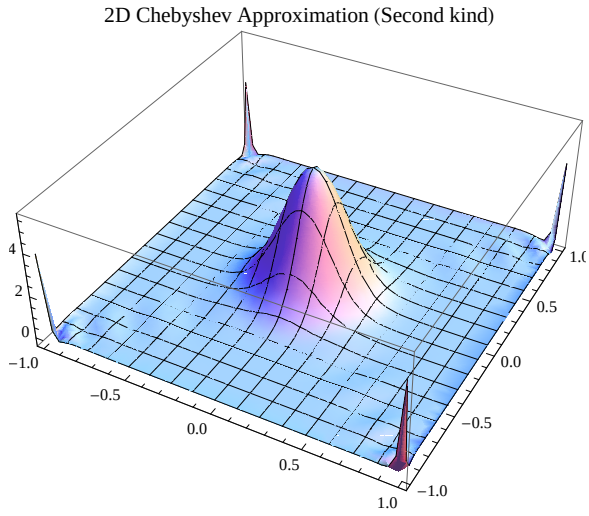

Figure 4.325: Chebyshev polynomial (second kind) approximation of a 2D Gaussian for $n = 20$ and one hundred thousand particles.

4.5 Moment-Based Coefficients

In addition to approximating the charge density by the traditional method described at the beginning of the chapter, we can also use the moment-based polynomials described in Chapter 2 to do the approximation.

Unlike in the traditional method, the moment-based approximation starts by using the measures μ_n determined by a weight $W(x)$, given by (2.44) [13]. Once the measures and the normalized polynomials $P_n(x)$ with $n \in 0, 1, 2, ..., m$ where

$$P_n(x) = \beta_n p_n(x) \tag{4.12}$$

with $p_n(x)$ given by (2.45) and

$$\frac{1}{{\beta_n}^2} = \int_a^b |p_n(x)|^2 d\mu(x) \tag{4.13}$$

After normalizing the moment polynomials, we calculate α_n, a set of measure integrals of the fuction to be approximated, $g(x)$ and given by

$$\alpha_n = \int_a^b x^n g(x) d\mu(x) \tag{4.14}$$

These coefficients only need to be calculated once and from $i = 0$ to $i = n$. Now calculating the charge density coefficients is a simple matter of computing a determinant. The coefficients a_n in the polynomial series $\sum_n^m a_i P_i(x)$ with domain $[a, b]$ approximating the function g(x) are given by modifing (4.7) for orthonormal polynomials, becoming

$$a_n = \int_a^b g(x) P_n(x) d\mu(x) \tag{4.15}$$

Now using Chapter 2, we can solve for a_n by sustituting $P_n(x)$. The special case of (4.17) is $a_0 = \beta_0\alpha_0$.

$$a_n = \beta_n \int_a^b g(x) \det \begin{pmatrix} \mu_0 & \mu_1 & \dots & \mu_n \\ \vdots & \vdots & \ddots & \vdots \\ \mu_{n-1} & \mu_n & \dots & \mu_{2n-1} \\ 1 & x & \dots & x^n \end{pmatrix} \mathrm{d}\mu(x) \tag{4.16}$$

$$a_n = \beta_n \det \begin{pmatrix} \mu_0 & \mu_1 & \dots & \mu_n \\ \vdots & \vdots & \ddots & \vdots \\ \mu_{n-1} & \mu_n & \dots & \mu_{2n-1} \\ \int_a^b g(x)d\mu(x) & \int_a^b xg(x)d\mu(x) & \dots & \int_a^b x^n g(x)d\mu(x) \end{pmatrix} \tag{4.17}$$

$$a_n = \beta_n \det \begin{pmatrix} \mu_0 & \mu_1 & \dots & \mu_n \\ \vdots & \vdots & \ddots & \vdots \\ \mu_{n-1} & \mu_n & \dots & \mu_{2n-1} \\ \alpha_0 & \alpha_1 & \dots & \alpha_n \end{pmatrix} \tag{4.18}$$

This method allows for a faster calculation of the coefficients, since most of the integrals disappear. Once the normalized polynomials have been calculated for a weight function, they can be stored, instead of calculating them every time. In theory, it would be a much faster and efficient way of performing the approximations, but our results were not examples of good approximations. The ideal weight function for a good approximation requires further study of the moment method.

CHAPTER 5

SUMMARY AND CONCLUSION

Three different orthogonal polynomials were used to approximate charged distributions based on a series of functions, including one- and two-dimensional Gaussians, as well as Uniform. In addition to the traditional approximation method, the use of moment-based polynomials was also explored with the one- and two-dimensional Gaussians.

Although all three polynomials are similar, each yields different results in regards to the approximated function. By looking at the overlapped plots for the approximations, an increase in order always lead to a better approximation, but the increase in particles requires a look at the distributions' differences.

5.1 One-dimensional Gaussian Distribution

Based on Table 5.1, with the Legendre polynomials, $n = 20$ does the best job in the approximation. In addition, it is also noticeable that, after five million particles, there is not that much of a difference in how good the approximation is. In Table 5.2, Chebysbev polynomials of the first kind have a very similar result to the Legendre polynomials. Order $n = 20$ gave the best result for the approximation and very little change is seen after five million particles. The table for Chebyshev of the second kind, 5.3, once again shows similar results for the approximation. With $n = 20$ the curve was the best with no significant change after five million particles.

Table 5.1: Difference between the Single Gaussian Distribution and Legendre polynomial approximation for select orders and particle numbers.

Order	10,000	100,000	1,000,000	5,000,000	10,000,000	15,000,000
4	0.673312198	0.673264076	0.673343637	0.673434088	0.673450785	0.673390266
8	0.246080522	0.245836831	0.245835071	0.245927254	0.246015022	0.245912512
12	0.063762041	0.062552471	0.062222366	0.062265653	0.062339133	0.062270572
16	0.022876965	0.014159529	0.011297076	0.011314259	0.011309431	0.011285057
20	0.023624278	0.008629923	0.002056601	0.001669998	0.001564721	0.001600216

Table 5.2: Difference between the Single Gaussian Distribution and Chebyshev polynomial approximation of the first kind for select orders and particle numbers.

Order	10,000	100,000	1,000,000	5,000,000	10,000,000	15,000,000
4	0.670394907	0.670686612	0.670663695	0.670689492	0.670697819	0.670720855
8	0.250016494	0.250574537	0.250566378	0.250613776	0.250634222	0.250682235
12	0.064725213	0.064893636	0.064693183	0.064679982	0.064695263	0.064722195
16	0.015545551	0.014330973	0.012177441	0.011924992	0.011930436	0.011933069
20	0.011362198	0.009703577	0.003183312	0.001882564	0.001718973	0.001737186

Table 5.3: Difference between the Single Gaussian Distribution and Chebyshev polynomial approximation of the second kind for select orders and particle numbers.

Order	10,000	100,000	1,000,000	5,000,000	10,000,000	15,000,000
4	0.719580139	0.718212004	0.718061029	0.717984492	0.718124153	0.718130777
8	0.260351901	0.258907272	0.257904656	0.257799866	0.257906484	0.257925697
12	0.065932441	0.065873049	0.064436297	0.064331578	0.064334585	0.064313296
16	0.016588087	0.014109671	0.011749535	0.011525488	0.011468213	0.011445279
20	0.012924613	0.006971633	0.002652175	0.001684812	0.001571712	0.001683641

Also from Tables 5.1 to 5.3 we can see that the approximation gets better as the order number increases. In addition, the Chebyshev polynomials of the first give a better result approximation the single Gaussian at low order, followed by Legendre and Chebyshev of the second kind. At about $n = 8$, it switches to Legendre polynomials giving the best approximation, followed by Chebyshev polynomials of the second and first kinds.

The single Gaussian was modified expanded to 2D to determine if the approximation would work just as well. However, we can tell by Figures 4.322 to 4.325 that

all three polynomials did very well, with an error between 1.8% and 2.7% for one hundred thousand particles at order twenty.

5.2 Uniform Distribution

Contrary to a single one-dimensional Gaussian distribution, the Uniform distribution is much more difficult to approximate because of the sharp corners particular to this curve. Afer taking the order up to $n = 20$, the error difference between the distributions is around 13% and 16% at order 20 respectively, which can be seen in Tables 5.4 to 5.6. Even after increasing the order of the approximation to order 40, the approximation is still far from perfect with an error between 6.3% and 8.1%.

Table 5.4: Difference between the Uniform Distribution and Legendre polynomial approximation for select orders and particle numbers.

Order	10,000	100,000	1,000,000	5,000,000	10,000,000	15,000,000
4	0.314519162	0.315048257	0.314470619	0.314480176	0.314472774	0.314451233
8	0.225953858	0.226572790	0.225416788	0.225445268	0.225381385	0.225440464
12	0.201434607	0.200145721	0.200866090	0.200928700	0.200719510	0.201086750
16	0.144121730	0.146832734	0.147864826	0.148499669	0.148763085	0.148422937
20	0.130602233	0.127072985	0.126722894	0.127172312	0.127353292	0.127106943

Table 5.5: Difference between the Uniform Distribution and Chebyshev polynomial approximation of the first kind for select orders and particle numbers.

Order	10,000	100,000	1,000,000	5,000,000	10,000,000	15,000,000
4	0.315206491	0.315226641	0.315542861	0.315316211	0.315364161	0.315372191
8	0.228600047	0.228785652	0.230566681	0.229363893	0.229588304	0.229637599
12	0.202600179	0.198886932	0.198592673	0.198775300	0.198800266	0.198770433
16	0.145212020	0.151123457	0.147847075	0.148693125	0.148646678	0.148660693
20	0.133724356	0.127667375	0.123569408	0.124212667	0.124295031	0.124347389

Table 5.6: Difference between the Uniform Distribution and Chebyshev polynomial approximation of the second kind for select orders and particle numbers.

Order	10,000	100,000	1,000,000	5,000,000	10,000,000	15,000,000
4	0.330657667	0.330633943	0.329490701	0.329356789	0.329493920	0.329449017
8	0.267818808	0.263511494	0.260413232	0.259966752	0.260339254	0.260110138
12	0.239872152	0.237139939	0.233713918	0.233098157	0.233519017	0.233312732
16	0.167628179	0.170005329	0.168808707	0.168111750	0.168304648	0.168416267
20	0.172195374	0.161147409	0.159476163	0.158590435	0.159359822	0.159364880

5.3 One-Dimensional Double Gaussian

For the symmetric one-dimensional double Gaussian, Legendre and the first kind of Chebyshev polynomials perform fairly well on the approximation. Because a final convergence has not been reached yet at one hundred thousand particles, it is impossible to tell how the number might change with an increase in the number of particles. (See Tables 5.7 to 5.9.)

Table 5.7: Difference between the Double Gaussian Distribution and Legendre polynomial approximation for select orders and particle numbers.

Order	20,000	40,000	60,000	80,000	100,000
4	0.329614	0.329254	0.329085	0.329160	0.329190
8	0.047685	0.047023	0.044639	0.044264	0.044619
12	0.022152	0.018370	0.011366	0.008132	0.008149
16	0.023169	0.018699	0.011470	0.007925	0.007857
20	0.025253	0.020307	0.013943	0.011570	0.009362

Table 5.8: Difference between the Double Gaussian Distribution and Chebyshev polynomial approximation of the first kind for select orders and particle numbers.

Order	20,000	40,000	60,000	80,000	100,000
4	0.334376	0.333867	0.333737	0.333954	0.333940
8	0.053452	0.053070	0.050681	0.050479	0.051070
12	0.022085	0.018817	0.011299	0.008019	0.008067
16	0.022784	0.018778	0.011651	0.007984	0.008020
20	0.025363	0.020337	0.013654	0.011475	0.009225

Table 5.9: Difference between the Double Gaussian Distribution and Chebyshev polynomial approximation of the second kind for select orders and particle numbers.

Order	20,000	40,000	60,000	80,000	100,000
4	0.345289	0.345297	0.345250	0.345266	0.345446
8	0.047228	0.046174	0.043399	0.042760	0.042692
12	0.022538	0.018590	0.011819	0.008616	0.008496
16	0.024907	0.019362	0.011519	0.008841	0.008145
20	0.025474	0.020762	0.014210	0.011713	0.009499

5.4 Conclusion

To approximate the charge distribution of a beam, we explored various distributions. We performed studies of one- and two-dimensional distributions. In 1D, we looked at smooth distributions such as single and double symmetric and asymmetric Gaussians. At the other end of the spectrum of typically used distributions we considered the uniform distribution. In 2D we restricted ourselves to multinormal distributions. For these cases, we developed two different methods of generating the orthogonal polynomials, the classic method and the moment-based method. We obtained fairly good results for the Gaussians and the traditional method, especially using Legendre polynomials. Generally speaking, whether or not one of the polynomials performs better than another might be most likely specific to the function being approximated. However, the differences are expected to be small among the

three types of polynomials utilized. The best combination seems to be, as expected, a high number of particles and order number. For example, the 1D single Gaussian returned errors below 0.16% at the highest order with $n = 20$ and ten to fifteen million particles. For the 2D Gaussians, the method also gives the expansion and approximation the density straightforwardly. In fact, it works very nicely with an error below 3% for one hundred thousand particles and $n = 20$, but the major increase of the number of coefficients needed for the approximation lengthens the time of calculation considerably. Non-smooth functions with sharper edges, like the uniform distribution, require even higher numbers and may still not be as good as those of the smoother functions. If the number of particles must be kept low, increasing the order number will still improve the approximation. Ideally, for best results it is necessary to have a few million particles and a truncation order of at least $n = 16$. This constitutes a reasonable practical advice for production runs that combines good efficiency with acceptable accuracy. The moment-based orthogonal polynomials allow the calculations to be done more efficiently, but it is still an open question as to how to choose an optimal weight function that will generate the appropriate orthogonal polynomials to be used for the estimation of the densities that minimize the error in the scalar potentials that are the solutions of the Poisson equation. This topic will be the subject of future work.

REFERENCES

[1] J. B. Rosenzweig. *Fundamentals of Beam Physics*. Oxford University Press Inc., New York, 2003.

[2] M. Young. *Stone-Weierstrass Theorem*. `http://www.mast.queensu.ca/~speicher/Section14.pdf`.

[3] P. L. Clark. *Stone-Weierstrass Theorem*. `http://math.uga.edu/~pete/243functions4.pdf`.

[4] E. W. Nissen. *Differential algebraic methods for space charge modeling and applications to the University of Maryland Electron Ring*. Ph.D. dissertation, Northern Illinois University, 2011, Dekalb, Illinois.

[5] C. J. Bocchetta. *Intra-Beam Scattering*. `http://cas.web.cern.ch/cas/BRUNNEN/Presentations/PDF/Bocchetta/IBS.pdf`.

[6] K. Schindl. *Space Charge*. `http://cas.web.cern.ch/cas/Loutraki-Proc/PDF-files/I-Schindl/paper1.pdf`.

[7] K. Y. Batygin, *Conservation of space-charge-dominated beam emittance in a strong nonlinear focusing field. Phys. Rev. E.* **53***, 5358 (1996).*

[8] M. L. Boas. *Mathematical Methods in the Physical Sciences*. John Wiley & Sons, Inc., 1983.

[9] P. Beckmann. *Orthogonal Polynomials for Engineers and Physicists*. The Golem Press, Boulder, Colorado, 1973.

[10] T. J. Rivlin. *Chebyshev Polynomials: From Approximation Theory to Alegebra and Number Theory*. John Wiley & Sons, Inc., 1990.

[11] *Sigma-Algebras*. `https://www.math.lsu.edu/~sengupta/7312s02/sigmaalg.pdf`.

[12] S. B. Provost, *The Mathematica Journal* ***9****, 4 (2005).*

[13] W. Gautschi. *Orthogonal Polynomials: Computation and Approximation*. Oxford University Press Inc., New York, 2003.

[14] C. F. Dunkl and Y. Xu. *Orthogonal Polynomials of Several Variables*. Cambridge University Press., Cambridge, 2001.

[15] *NCSSM Statistics Leadership Institute Notes: Introduction to The Central Limit Theorem*. `http://courses.ncssm.edu/math/Stat_Inst/PDFS/SEC_4_f.pdf`.

[16] M. Reisner. *Theory and design of charged particle beams*. John Wiley & Sons, Inc., 1994.

[17] C. Prior. *Dynamics of Non-Linear Beams with Space-Charge*. `http://cas.web.cern.ch/cas/Bilbao-2011/Lectures/PriorbeamDynamics2.pdf`.

[18] *Normal Distribution*. Wolfram Research Inc., 2012. `http://reference.wolfram.com/mathematica/ref/NormalDistribution.html`.

[19] *Uniform Distribution*. Wolfram Research Inc., 2012. `http://reference.wolfram.com/mathematica/ref/UniformDistribution.html`.

[20] *Multinormal Distribution*. Wolfram Research Inc., 2012. `http://reference.wolfram.com/mathematica/ref/MultinormalDistribution.html`.

APPENDIX

MATHEMATICA PROGRAMS

The following are sample Mathematica programs used to perform all the calculations: the generation of points, coefficient calculations, plots of the approximations, error calculations, etc. For functions that are built into Mathematica, like the 1D and 2D Gaussians, as well as the Uniform distributions, the process of generating points from the curves is more straightforward than for the double Gaussian.

A.1 Standard Mathematica Functions

This section contains a generalization of the code used to approximate both the 1D Gaussian and Uniform distributions. The variable $g(x)$ is defined as the chosen function as well as $W(x)$, the weight function for the polynomial used. Mathematica defines Legendre as $LegendreP[n, x]$ and the Chebyshev polynomials as $ChebyshevT[n, x]$ and $ChebyshevU[n, x]$ respectively. The first part of the code will calculate the coefficients from the distribution itself, followed by the approximated coefficients, plots of the curves and error calculations.

A.1.1 Charge density approximation using a Gaussian Distribution and Legendre Polynomials

This section of the code calculates the approximated coefficients based on a desired number of particles as well as the coefficients based on the actual function. In this case, the code loops to calculate the approximated coefficients over several numbers of particles and order number. It also prints and stores the coefficients in an array for later use. Once the coefficients have been calculated, these can be

stored in a program like Excel for later use. The file only needs to be imported in the appropriate format for the use.

```
gauss[x]:=(1/((1/6) * Sqrt[2 * Pi]))E^(-(x^2)/(2/36));

a[n_]:=Integrate[gauss[x]LegendreP[n, x], {x, -1, 1}]/Integrate[LegendreP[n, x]^2, {x, -1, 1}];

For[i = 0, i <= 20, i++, Print["a[", i, "] = ", N[a[i]]]]
 empty[x_, y_]:=0;
ResultsArray = Array[empty, {21, 100}];
minpoints = 10000;
maxpoints = 1000000;
interval = 10000;

Do[{
points = Table[RandomReal[NormalDistribution[0, 1/6]], {numberofpoints}],
b[n_]:=Sum[LegendreP[n, points[[i]]], {i, 1, Length[points]}]/Integrate[LegendreP[n, x]^2, {x, -1, 1}],
Print["Number of points = ", numberofpoints],
For[i = 0, i <= 20, i++,
{result = N[b[i]/numberofpoints],
Print["b[", i, "] = ", result],
row = i + 1, column = numberofpoints/interval,
ResultsArray[[row, column]] = result
}]}, {numberofpoints, minpoints, maxpoints, interval}]

For[i = 0, i <= 20, i++,
{Print["b[", i, "]"],
Print[ResultsArray[[i + 1]]]
}]
```

A.2 User-defined Mathematica functions

When the function used to approximate the density function is not defined in Mathematica, the code shown above needs to be modified to manually generate the particle positions that will later be used to approximate the coefficients.

A.2.1 Charge density approximation using an Asymmetric Gaussian Distribution and Legendre Polynomials

The first section generates and prints the points that will be used on the approximation, based on the desired function and interval. After the points are generated, they can be used in the approximation by selecting the appropriate point in the calculation. The rest of the code is just like the first described.

```
min = −1;
max = 1;
findrootstart = 0;
numofpoints = 100000;
probdist[x_]:=E^(−(x − 0.6)^2/0.1^2) + E^(−(x + 0.3)^2/0.25^2)
intprobdist = Integrate[probdist[x], {x, min, max}];
normdist[x_]:=probdist[x]/intprobdist
distarea[x_]:=Integrate[normdist[t], {t, min, x}]
mypoints = {};
Timing[Do[
{a = RandomReal[1];
rawsolution = FindRoot[a == distarea[x], {x, findrootstart}];
solution = DeleteCases[rawsolution, {x → z_Complex}];
```

```
result = x/.solution[[1]],
mypoints = Append[mypoints, result]}
, {numofpoints}]]
Histogram[mypoints, 20]

Print[mypoints]

empty[x_, y_]:=0;
ResultsArray = Array[empty, {21, 20}];
minpoints = 5000;
maxpoints = 100000;
interval = 5000;

Do[{
b[n_]:=Sum[LegendreP[n, mypoints[[i, 1]]]
{i,1,numberofpoints}]/Integrate[LegendreP[n, x]^2, {x, -1, 1}],
Print["Number of points = ", numberofpoints],
For[i = 0, i ≤ 20, i++,
{result = N[b[i]/(numberofpoints)],
Print["b[", i, "] = ", result],
row = i + 1, column = numberofpoints/interval,
ResultsArray[[row, column]] = result
}]}, {numberofpoints, minpoints, maxpoints, interval}]
```